Universidade do Minho
Escola de Ciências

Diana Margarida da Costa Ribeiro

Optimization of transient expression procedures in *Catharanthus roseus* and *Arabidopsis thaliana* for subcellular localization studies

Outubro de 2010

Optimization of transient expression procedures in *Catharanthus roseus* and *Arabidopsis thaliana* for subcellular localization studies

Diana Margarida da Costa Ribeiro

UMinho | 2010

Universidade do Minho
Escola de Ciências

Diana Margarida da Costa Ribeiro

Optimization of transient expression procedures in *Catharanthus roseus* and *Arabidopsis thaliana* for subcellular localization studies

IBMC
INSTITUTO DE BIOLOGIA MOLECULAR E CELULAR
INSTITUTE FOR MOLECULAR AND CELL BIOLOGY

Dissertação de Mestrado
Mestrado em BioTecnologia e Bio-Empreendedorismo em Plantas Aromáticas e Medicinais

Trabalho efectuado sob a orientação do
Professora Doutora Mariana Sottomayor (IBMC, Porto)

Co-Orientadore
Doutora Patrícia Duarte (IBMC, Porto)

Supervisor na instituição
Professor Doutor Manuel Ferreira (Uminho)

Outubro de 2010

Agradecimentos

Olhando para trás, muitos foram os que contribuíram para que o último ano fosse especial e inesquecível, na maioria dos casos palavras não chegam para expressar a minha gratidão.

Gostaria de começar por agradecer a toda a família por tudo o que me têm vindo a ensinar, por me fazer sentir capaz de tudo e claro por todos os momentos extraordinários, barulhentos e cheios de risos que passamos juntos!

Às minhas Biomininas e Biomininos que foram o meu refúgio sempre que precisei de motivação, animo, paciência e ajuda para prosseguir. Estiveram sempre presentes nos momentos especiais e acima de tudo durante dificuldades inesperadas, e que nunca me deixaram desanimar! Ao grupinho do comboio que me ajudaram a alegrar as inúmeras e muito chatas viagens de comboio! E em especial, tenho que agradecer à Cheila por todos os bons conselhos!

Gostaria igualmente de agradecer às meninas das peroxidases e menino, claro, por me terem recebido tão bem no grupo, por me terem ajudado sempre no lab, pela boa disposição, e por terem contribuírem para o meu bem-estar durante esta pequena estadia na Invicta.

Muito muito obrigado à minha chefinha, Patrícia, que me ensinou tudo o que hoje sei fazer num laboratório, agradeço toda a paciência, dedicação, orientação, disponibilidade, todos os ensinamentos e todos fins-de-semana que passou a trabalhar em conjunto para esta tese.

À Doutora Mariana agradeço a confiança que depositou em mim mesmo sem me conhecer, e a excelente orientação. Foi uma honra trabalhar com um grupo tão dinâmico!

Para o meu tio...

Optimization of transient expression procedures in *Catharanthus roseus* and *Arabidopsis thaliana* for subcellular localization studies.

Abstract

Nowadays, the availability of much gene sequence information demands the development of tools for their fast characterization at the protein level, where function actually resides. Here, the interest in the characterization of certain of the known *Arabidopsis* class III peroxidase (Prx) genes, as well as the interest in the characterization of candidate genes implicated in the metabolism of the anticancer terpenoid indole alkaloids of *Catharanthus roseus*, has led to the need of establishing transient expression procedures for these two species.

Therefore, the main goal of this work was the development and optimization of simple/fast, efficient and reproducible transient expression protocols for subsequent subcellular localization studies of proteins coded by Prx genes, and for characterization of candidate genes provided from omic approaches, namely implicated in the regulation, biosynthesis or transport of the valuable alkaloids from *C. roseus*. A complementary goal was to investigate the subcellular localization and sorting determinants of Prxs, namely the vacuolar sorting capacity of a C-terminal amino acid sequence extension (CTE) present in vacuolar Prxs, using as examples the well characterized and most abundant vacuolar Prx from *C. roseus* leaves, CrPrx1, and the most abundant Prx in the leaves of *Arabidopsis*, AtPrx34. For this, already available CrPrx1-GFP fusions and newly generated AtPrx34-GFP fusions were used in the transient expression assays.

The successful establishment of protocols for PEG-mediated transformation of both *Arabidopsis* and *C. roseus* mesophyll protoplasts was achieved and validated as excellent transient expression systems. Transient expression by *Agrobacterium* infiltration of *Arabidopsis* and *C. roseus* leaves was also attempted, but it was only successful with in vitro *C. roseus* plants. However, promising insights were made into the development of this technique.

Expression of CrPrx1-GFP fusions in *Arabidopsis* and *C. roseus* protoplasts using the established protocols confirmed the vacuolar localization of this Prx. Additionally the CrPrx1 signal peptide (SP) and CTE were confirmed as sorting determinants that target GFP to the ER and vacuole, respectively. The characterization of the subcellular

localization and sorting determinants of AtPrx34 was not elucidated, possibly due to malfunctioning of the vector plasmid used for protoplast infiltration. In fact, upon agroinfiltration of in vitro *C. roseus* plants, it was possible to observe sorting to the ER of an $SP_{AtPrx34}$-GFP fusion coded by a construct harboured in a binary vector plasmid, different from the one used for protoplast transformation. Thus, a resolution of the subcellular sorting of AtPrx34 should be possible in the near future.

The transient expression assays described in the present study were highly reproducible, resulted in very satisfactory transformation efficiencies, and constitute a reliable and inexpensive methods that can be performed in most labs, and that are suitable test-systems to characterize genes of unknown function. This is also the the first time a transient expression system for *C. roseus* protoplasts is reported, using a PEG-mediated transformation protocol.

Keywords: *Catharanthus roseus*, *Arabidopsis*, protoplasts, PEG-mediated transformation, agroinfiltration, GFP fusions, subcellular localization, secretory pathway, sorting signals, vacuole, confocal microscopy.

Optimização de procedimentos de expressão transiente em *Catharanthus roseus* e *Arabidopsis thaliana* para estudos de localização subcelular.

Resumo

Actualmente, a disponibilidade de inúmeras sequências genómicas exige o desenvolvimento de ferramentas para uma rápida caracterização ao nível protéico, onde de facto reside a função. Neste trabalho a caracterização de determinados genes de Peroxidases de Classe III (Prx) de *Arabidopsis*, assim como o interesse na caracterização de possíveis genes envolvidos no metabolismo de alcalóides indólicos terpenóides anticancerígenos de *Catharanthus roseus*, impulsionou a necessidade de estabelecer procedimentos de expressão transiente para estas duas espécies.

Consequentemente, o objectivo principal deste trabalho foi o desenvolvimento e optimização de protocolos de expressão transiente simples/rápidos, eficientes e reproduzíveis para estudos de localização subcelular de proteínas codificados por genes Prx, e para a caracterização de possíveis genes obtidos de abordagens omicas, nomeadamente implicados na regulação, biossíntese ou transporte de alcalóides relevantes de *C. roseus*. Como objectivo complementar investigar a localização subcelular e sinais de direccionamento de Prxs, designadamente a capacidade de direccionamento vacuolar da extensão C-terminal aminoacídica (CTE) presente em Prxs vacuolares, utilizando como exemplos a Prx vacuolar mais abundante e estudada presente nas folhas de *C. roseus*, Crprx1, e a Prx mais abundante nas folhas de *Arabidopsis*, AtPrx34. Para tal, fusões CrPr1-GFP já disponíveis e fusões AtPrx34-GFP recém geradas foram utilizadas em procedimentos de expressão transiente.

O estabelecimento com sucesso de protocolos de transformação mediada por PEG para protoplastos de mesófilo de *Arabidopsis* e *C. roseus* foi alcançado e validado como um excelente sistema de transformação transiente. Transformação transiente por infiltração com *Agrobacterium* de folhas de *Arabidopsis* e *C. roseus* foi abordado, mas apenas foram obtidos resultados positivos com plantas de *C. roseus in vitro*. Todavia progressos promissores foram realizados para o desenvolvimento desta técnica.

Expressão de fusões CrPrx1-GFP em protoplastos de *Arabidopsis* e *C. roseus* utilizando os protocolos estabelecidos confirmaram a localização vacuolar desta Prx. Adicionalmente o péptido sinal (SP) e a extensão C-terminal (CTE) de CrPrx1 foram

confirmados com sinais determinantes que direccionam a GFP para o RE e o vacúolo, respectivamente. A caracterização da localização subcelular e sinais de direccionamento de AtPrx34 não foram elucidados, possivelmente devido a uma irregularidade funcional do vector plasmídeal utilizado na transformação de protoplastos. De facto, após agroinfiltraçao de plantas *C. roseus in vitro*, foi possível observar o direccionamento para o RE da fusão $SP_{AtPrx34}$-GFP codificada por um constructo incluído em vector binário, diferente do vector utilizado na transformação de protoplastos. Portanto, a caracterização do direccionamento subcelular da AtPrx34 poderá ser possível num futuro próximo.

Os procedimentos de expressão transiente descritos no presente estudo manifestaram-se bastante reproduzíveis, resultando em níveis satisfatórios de eficiência de transformação, e constituem métodos fidedignos e de baixo custo que podem ser realizados na maioria dos laboratórios, e são sistemas-teste convenientes para caracterizar genes de função desconhecida. Foi também reportado pela primeira vez um sistema de transformação transiente em protoplastos de *C. roseus*, utilizando um protocolo de transformação mediada por PEG.

Palavras-chave: *Catharanthus roseus*, *Arabidopsis*, transformação mediada por PEG, Agroinfiltração, fusões-sGFP, localização subcelular, via secretora, sinais de direccionamento, vacúolo, microscopia confocal.

Table of contents

List of abbreviations

35S - Cauliflower Mosaic virus promoter

4-MN - 4-methoxy-α-naphthol

aa – Amino acid

Acc/dec - Acceleration/deceleration

AtPrx34 - *Arabidopsis thaliana* Peroxidase 34

AVLBS - Anhydrovinblastine synthase

BAP - 6-Benzylaminopurine

Bdd - Bi-distilled deionized

BiP – Binding protein

BN - pTH2-BN

BP-80 - Binding-protein of 80 kDa

cDNA - Complementary DNA

CCV - Clathrin coated vesicles

CDS – Coding sequence

COPI - Coat protein complex I

COPII - Coat protein complex II

CrPrx1 - *Catharanthus roseus* Peroxidase 1

CrPrx2b - *Catharanthus roseus* Peroxidase 2b

CTE or CE - C-Terminal Extension

ctVSD - C-terminal Vacuolar Sorting Domain

cv. - Cultivar

DMAPP - Dimethylallyl diphosphate

DNA - Deoxyribonucleic acid

dNTPs - Deoxyribonucleotide triphosphate: Purine (Adenine, Guanine), Pyrimidine (Uracil, Thymine, Cytosine)

DV - Dense vesicles

EDTA - Ethylenediaminetetraacetic acid

e.g. - For example

ER - Endoplasmic Reticulum

ERES - Endoplasmic Reticulum Export Sites

FP - Fluorescent Protein

FW - Fresh Weight

g - Gram

G10H - Geraniol 10-hydroxylase

GFP - Green Fluorescent Protein (originally isolated from *Aequorea victoria*)

GPP - Geranyl diphosphate

HDS - Hydroxymethylbutenyl 4-diphosphate synthase

HRPC - Horseradish peroxidase isoenzyme *C*

IPP - Isopentenyl diphosphate

L – Liter

LB - Luria Bertrani

LV - Lytic vacuole

MEP - 2-C-methyl-D-erythritol4-phosphate

MES - 2-(*N*-morpholino)ethanesulfonic acid

mL – Milliliter

mM - Millimolar

mRNA - messenger Ribonucleic acid

MS - Murashige & Skoog

MVB - Multivesicular body

Nos ter - NOS terminator (*nopaline synthase)* from *A.tumefaciens*

OD - Optical density

ON - Overnight

PAC - Precursor-accumulating vesicle

pDNA – plasmid DNA

PEG 4000 - Polyethylene glycol with a molecular weight of 4000

Prx - Class III peroxidase

Primer fwd - Primer forward

Primer rev - Primer reverse

psVSD - Physical structure Vacuolar Sorting Domain

PSV - Protein-storage vacuole

PVC - Prevacuolar compartment

RFP - Red Fluorescent Protein (originally isolated from *Acropora millepora*)

RMR - luminal Receptor homology domain trans Membrane domain and RING-H2 motif in the cytoplasmic tail protein

RT - Room temperature

ROS - Reactive oxygen species

rpm - Revolutions per minute

SAV - Senescence-associated vacuole

SP - Signal peptide

ssVSD - sequence-specific Vacuolar Sorting Domain

SGD - strictosidine β-D-glucosidade

STR - Strictosidine synthase

TDC - Tryptophan decarboxylase

TGE - Transient gene expression

TIA - Terpenoid indole alkaloid

TIP - Tonoplast intrinsic protein

Tm - Melting temperature

Vir - Virulence genes

v/v – volume/volume

VSD - Vacuolar Sorting Domain

YEB - Yeast Extract Broth

w/v – weight/volume

ºC - Degree Celsius

µg - microgram

µL – microliter

µM – microMolar

- Amino Acid terminology, abbreviation terms and single letter for each amino acid:

Amino Acid	Abbreviation	Single letter
Lysine	LYS	K
Asparagine	ASN	N
Threonine	THR	T
Arginine	ARG	R
Methionine	MET	M
Isoleucine	ILE	I
Glutamine	GLN	Q
Histidine	HIS	H
Proline	PRO	P
Glutamic acid	GLU	E
Aspartic acid	ASP	D
Alanine	ALA	A
Glycine	GLY	G
Valine	VAL	V
Tyrosine	TYR	Y
Serine	SER	S
Tryptophan	TRP	W
Cysteine	CYS	C
Leucine	LEU	L
Phenylalanine	PHE	F

List of figures

List of tables

Short *Curriculum vitae*

Diana M. da Costa Ribeiro was born in 1987 in Braga, Portugal. She presently lives in Braga and works, as a researcher, in the 3B's Research Group (Biomaterials, Biodegradables and Biomimetics), under the supervision of Nuno Neves.

Her background includes a three-year graduation in Applied Biology, by the School of Sciences, University of Minho. She has just submitted her M.Sc thesis on Biotechnology and Bio-Entrepreneurship in Aromatic and Medicinal Plants to the University of Minho, which was fully developed in the Institute for Molecular and Cell Biology (IBMC), Porto, Portugal.

During the last two months of her graduation, Diana M. da Costa Ribeiro worked in the vegetal biology field, under the supervision of Manuel Ferreira. Her work focusing on the *in vitro* cultures from primary explants and regeneration of *Mentha* sp., *Mentha* x *piperita* var. *piperita* L., *Mentha spicata* var. *'Crispa'* L., *Mentha pulegium* L. and *Mentha aquatica* L. As well as the chemical characterization of essential oils, isolated by hydrodistillation, from *in vivo* plants and *in vitro* cultures of the same *Mentha* sp., analyzed by Gas Chromatography (GC) and Gas Chromatography-Mass Spectrometry (GC-MS) techniques.

During the three-year graduation she was involved in several scientific events organized by the Applied Biology students, and attended the most important national meetings organized by biology students, National Meeting of Biology Students, and in 2008 she was part of the commission of biology students that organized the XII National Meeting of Biology Students, in Braga, Portugal.

In 2009 she joined the research group of Plant Peroxidases and Secondary Metabolism (IBMC, Porto) to develop her master thesis, where she worked for a year on the development of new transient expression procedures in *Catharanthus roseus* and *Arabidopsis thaliana* for subcellular localization studies, under the supervision of Mariana Sottomayor. This work had involved the design and production of the appropriate fluorescent proteins fusions, and the use of transient transformation protocols, PEG-mediated transformation of protoplasts and Agroinfiltration of leaves.

As a result of her master research work a paper is being prepared, and is expected to be submit very soon.

Introduction

1. Introduction

1.1. *Catharanthus roseus:* the plant and its clinical uses

Catharanthus roseus is a perennial semi-shrub known as the Madagascar periwinkle, highly appreciated as an ornamental plant. Linnaeus first published *C. roseus* as *Vinca rosea*, in his "Systema Naturae" in 1759. This species was later published as *Catharanthus* by George Don in his "General System of Gardening and Botany" (1835) (Figure 1).

Currently, *C. roseus* has a pantropical distribution, being naturalized in Africa, America's, Asia, Australia and Southern Europe, and on some islands in the Pacific Ocean (Van Der Heijden et al. 2004).

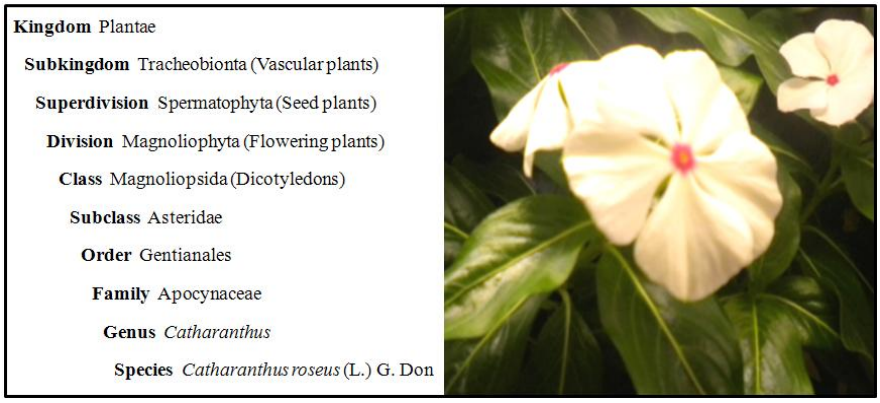

Figure 1. Flowering plant of *Catharanthus roseus* (L.) G. Don cv. Little Bright Eyes and respective taxonomic classification. Adapted from The PLANTS Database (http://plants.usda.gov).

C. roseus has long been used in traditional medicine as an oral hypoglycemic agent in the treatment of diabetes (Singh et al. 2001), and investigation of this activity ultimately led to the discovery of two anticancer alkaloids present in the leaves of this plant, vinblastine and vincristine (Noble 1990).

The presence of the two anti-tumour alkaloids, vinblastine and vincristine, found in the leaves, together with the accumulation of one alkaloid with anti-hypertensive properties, ajmalicine, found in the roots, justify the extensive investigation performed on this species. Alkaloids are low molecular-weight, nitrogen-containing compounds

derived mostly from amino acids, usually with basic properties and very often particularly pharmacologically active (Facchini 2001; Ziegler & Facchini 2008).

Vinblastine and vincristine form the so-called Vinca alkaloids together with a few semisynthetic derivatives (Figure 2), and they are mitotic inhibitors that became the first natural anticancer agents to be clinically used, being still an indispensable part of most curative regimens used nowadays in cancer chemotherapy (Van Der Heijden et al. 2004; Sottomayor & Ros Barceló 2006; Loyola-Vargas et al. 2007).

Chemically, vinblastine and vincristine are dimeric terpenoid indole alkaloids differing only in that vincristine has a formyl group at a position where vinblastine has a methyl group (Figure 2). Despite the minor difference in structure between vinblastine and vincristine, a significant difference exists in the spectrum of human cancers that respond to the drugs. Vinblastine is used mainly in the treatment of Hodgkin's disease (a type of lymphoma). Vincristine has superior anti-tumour activity compared to vinblastine but is more neurotoxic. It is especially useful in the treatment of leukaemia, and other cancer conditions, including non-Hodgkin's lymphomas and breast cancers. *C. roseus* also synthesises anti-hypertensive agents such as ajmalicine and serpentine, which are used to combat heart arrhythmias and to improve the blood circulation in the brain (Sottomayor & Ros Barceló 2006).

Regarding the Vinca alkaloids, these are known to inhibit cell mitosis acting by binding to tubulin, thus preventing polymerization into microtubules and the organization of the mitotic spindle. This mode of action is shared with other natural agents such as colchicine (Dewick 2002; Van Der Heijden et al. 2004; Sottomayor & Ros Barceló 2006; Loyola-Vargas et al. 2007).

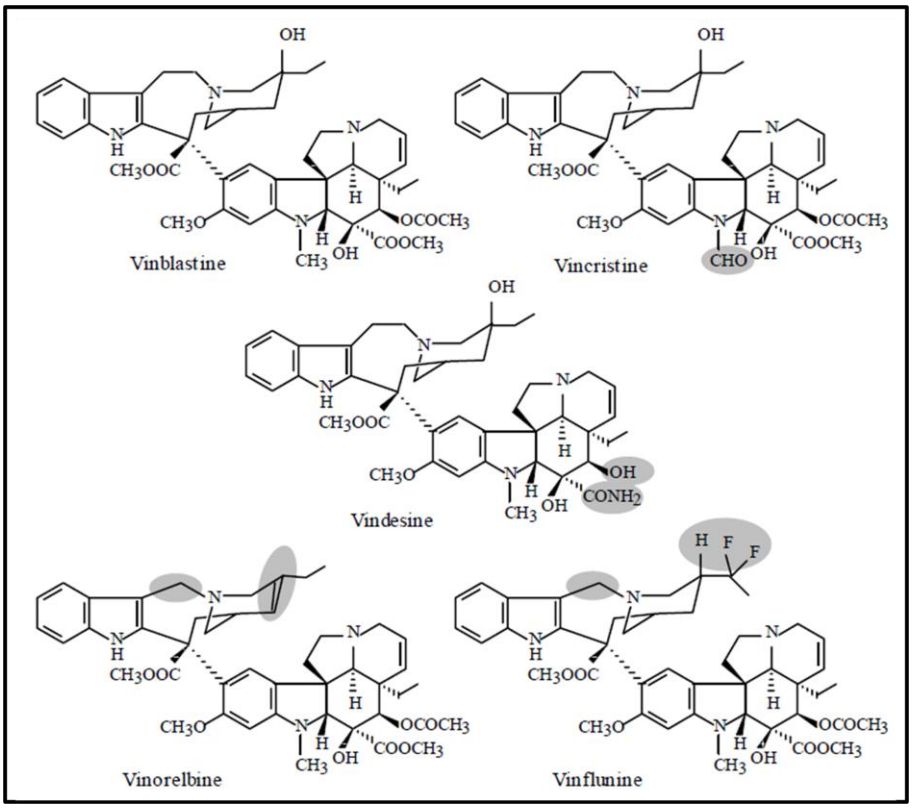

Figure 2. Structure of natural and semi synthetic Vinca alkaloids. Shaded areas indicate the structural differences from vinblastine. *In* Sottomayor & Alfonso Ros Barceló 2006.

A major problem associated with the clinical use of vinblastine and vincristine is that only very small amounts of these desirable alkaloids are present in the plant. Although the total alkaloid content of the leaf can reach 1% or more, over 500 kg of dried Catharanthus leaves are needed to yield 1 g of vincristine. Due to this low yield, the extraction is both costly and tedious, requiring large quantities of raw material and extensive use of chromatographic fractionations (Van Der Heijden et al. 2004; Sottomayor & Ros Barceló 2006). Moreover, the greater importance of vincristine over vinblastine as a drug, is not reflected in the plant, which produces a much higher proportion of vinblastine. Those facts stimulated intense investigation in alternative methods for the production of vinblastine and vincristine, like the semi-synthesis of the dimeric alkaloids from the monomers catharanthine and vindoline - produced in *C. roseus* at much larger amounts, as well as investigation in the modification of the molecules aiming a higher specificity (lower toxicity), a higher activity and a different pharmacological profile (Dewick 2002; Van Der Heijden et al. 2004; Sottomayor & Ros Barceló 2006; Loyola-Vargas et al. 2007). The pharmaceutical company Eli Lilly developed several series of derivatives with modifications in the vindoline part of the dimeric structure, producing vindesine (Figure 2). In 1975, Potier and collaborators

proposed that, *in planta*, the dimeric vinblastine type alkaloids resulted from the coupling of catharanthine and vindoline and, in light of this hypothesis, they reported for the first time the chemical synthesis of α-3',4'-anhydrovinblastine, later proved to be the first dimeric biosynthetic precursor of vinblastine in the plant (Potier et al. 1975). The group of Potier investigated possible modifications of anhydrovinblastine and produced vinorelbine (Figure 2). Vindesine is a semi-synthetic derivative of vinblastine and has a vincristine-like spectrum of activity, and vinorelbine has a broader anticancer activity with lower neurotoxic side-effects than either vinblastine or vincristine (Dewick 2002; Van Der Heijden et al. 2004; Sottomayor & Ros Barceló 2006). Recently, the pharmaceutical company Pierre Fabre Medicaments developed the highly promising derivative vinflunine which has just been approved for chemotherapy in 2009 (Sottomayor & Ros Barceló 2006; Pierre Fabre SA 2009).

1.2. Biosynthesis of the Vinca alkaloids in *C. roseus*

Plant cells are considered to be excellent producers of a broad variety of chemical compounds. Many of these compounds are of high economic value such as various drugs, flavours, fragrances and insecticides. These compounds usually play a role in the interaction of the plant with its environment, e.g. as toxins to defend the plant against microorganisms or various predators, as messengers, attractants, repellents. They are called secondary metabolites because they are not directly involved in the normal growth, development, or reproduction of organisms (Facchini 2001; Ziegler & Facchini 2008).

Alkaloids are one of the most diverse groups of secondary metabolites found in living organisms, especially in plants. A great number of alkaloids have been used in medicine and many of them are prominent components of modern drugs organisms (Facchini 2001; Ziegler & Facchini 2008). The alkaloids of *C. roseus* are terpenoid indole alkaloids (TIAs), which are almost restricted to four plant families of Dicotyledones: Apocynaceae – where *C. roseus* is included, Loganiaceae, Rubiaceae and Nyssaceae.

C. roseus accumulates more than 100 TIAs (El-sayed & Verpoorte 2007) and the TIA biosynthetic pathway has been extensively studied. It has been shown to involve at least 30 enzymes from primary precursors to vinblastine, from which 12 steps have been characterized at the enzyme and/or gene level (Verpoorte et al. 2007).

The TIA biosynthetic pathway of *C. roseus* is extremely intricate, complex and highly compartmentalized inside the cell. A number of enzymes involved in this pathway were shown to be localized in different subcellular compartments. The compartmentalization / localization involved in this metabolic pathway can be considered a regulatory mechanism that plants develop to accomplish the final function of their secondary metabolism, since this location might require the transport of different metabolites from one point to another for its biosynthesis to be completed (St-Pierre et al. 1999). The early stages of the TIA pathway involve the formation of secologanin derived from the terpenoid biosynthesis and its condensation with tryptamine to produce the central intermediate strictosidine [Figure 3; (Facchini 2001; Van Der Heijden et al. 2004; El-sayed & Verpoorte 2007; Roytrakul & Verpoorte 2007; Ziegler & Facchini 2008)].

The enzyme condensing secologanin and tryptamine is strictosidine synthase (STR), and its subcellular localization was determined to be the vacuole (Sottomayor & Ros Barceló 2006; El-sayed & Verpoorte 2007; Roytrakul & Verpoorte 2007; Loyola-Vargas et al. 2007).

Strictosidine is the general precursor of several divergent pathways leading to the multitude of TIAs accumulated by *C. roseus* (Sottomayor & Ros Barceló 2006). Somewhere, downstream of strictosidine formation, the pathway of TIAs suffers several ramifications mostly uncharacterized. The less characterized branches are the ones leading to catharanthine and vindoline, the monomeric precursors of the Vinca alkaloids, and the ones that will be the discussed here.

The information on catharanthine biosynthesis is very limited. Enzymes and genes involved in the catharanthine pathway have not been isolated or cloned yet, and almost nothing is known about the nature of the enzymes involved in the conversion of cathenamine to catharanthine and tabersonine (Figure 3). On another hand it has been established that tabersonine is transformed into vindoline by a sequence of six steps which are well characterized. These steps include: aromatic hydroxylation, O-methylation, hydration of the 2,3-double bond, N(1)-methylation, hydroxylation at position 4 and 4-O-acetylation (Figure 3). The data reported suggest that the route of vindoline biosynthesis is regulated by development and is restricted to the aerial parts of the adult plant, mainly in young leaves and cotyledons. This activity diminishes with age and organ type, and is already low in adult leaves, floral stems, roots and tips

(Sottomayor & Ros Barceló 2006; El-sayed & Verpoorte 2007; Roytrakul & Verpoorte 2007; Loyola-Vargas et al. 2007; Oudin et al. 2007) .

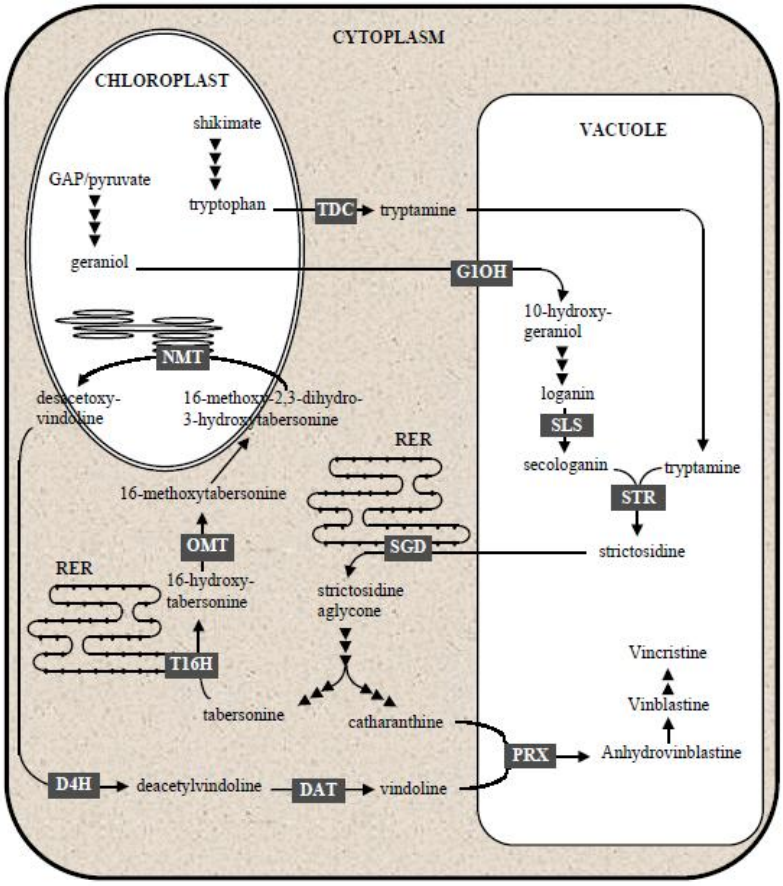

Figure 3. Compartmentalization of the biosynthetic pathway of terpenoid indole alkaloids in *C. roseus* cells. G10H: geraniol 10-hydroxylase; SLS: secologanin synthase; TDC: tryptophan decarboxylase; STR: strictosidine synthase; SGD: strictosidine β-D-glucosidade; T16H: tabersonine 16-hydroxylase; OMT: S-adenosyl - L-methionine : 16-hydroxytabersonine - 16-O-methyltransferase; NMT: S-adenosyl - L-methionine : 16-methoxy - 2,3-dihydro-3-hydroxytabersonine - N-methyltransferase; D4H: desacetoxy vindoline 4-hydroxylase; DAT: acetylcoenzyme A : 4-O-deacetylvindoline 4-O-acetyltransferase; PRX: peroxidase. *In* Sottomayor & Alfonso Ros Barceló 2006.

The product resulting from the coupling of the monomeric TIAs catharanthine and vindoline is the dimeric α-3',4'-anhydrovinblastine, which is converted into vinblastine (further converted into vincristine), leurosine and Catharine (Figure 4). The coupling process is thought to be catalysed by a class III peroxidase with anhydrovinblastine synthase activity, CrPrx1 (Sottomayor et al. 1998; Sottomayor & Ros Barceló 2003; Sottomayor et al. 2004; El-sayed & Verpoorte 2007; Loyola-Vargas et al. 2007) .

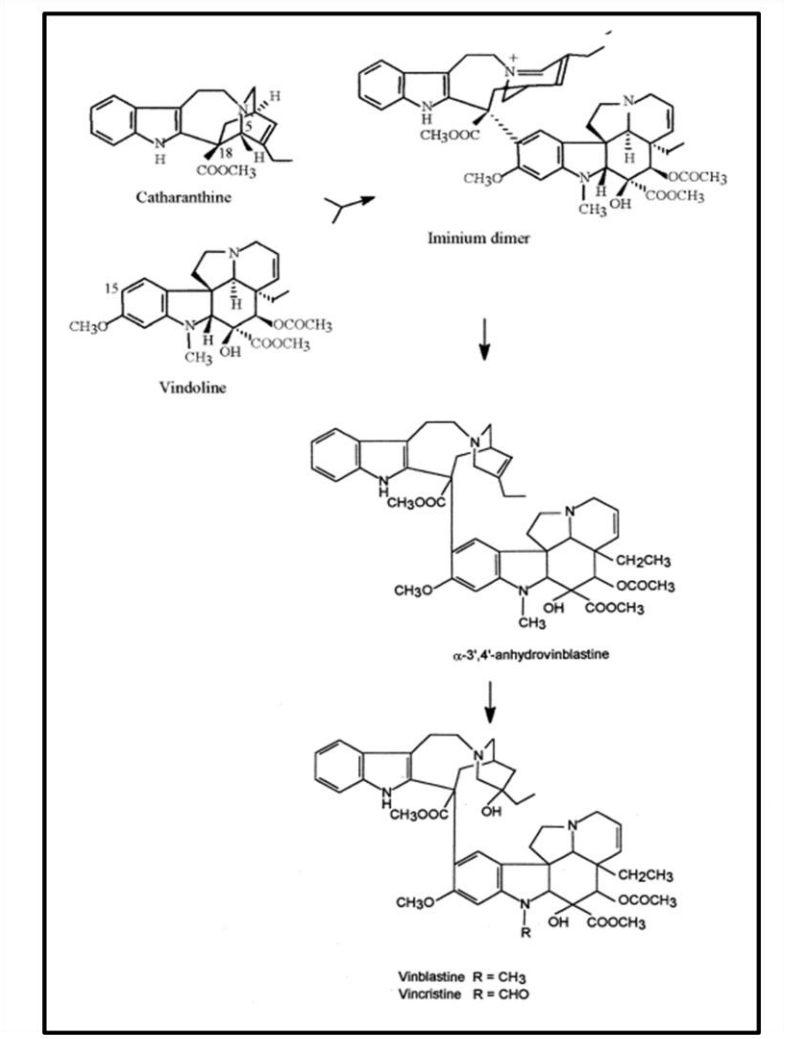

Figure 4. Structures of vinblastine and vincristine and their precursors. The coupling of catharanthine and vindoline originates an unstable iminium cation that is reduced to yield *α*-3',4'-anhydrovinblastine. Adapted from Sottomayor et al. 1998.

The laboratory where this thesis was developed described the purification, cloning and characterization of CrPrx1, the only enzyme detected so far with α-3',4'-anhydrovinblastine synthase activity(see section 1.3), and showed that this was the most likely *in vivo* responsible for the synthesis of anhydrovinblastine (Sottomayor et al. 1998; M. M. R. Costa et al. 2008). This conclusion was based on the confirmation of the same subcellular localization of both CrPrx1, substrates and product of the dimerization reaction - the vacuole. CrPrx1 was shown to belong to the plant branch of the peroxidase superfamily (class III peroxidises), given the visible spectrum of the protein, with maxima at 404, 501 and 633 nm indicative of a high spin ferric heme protein, and its ability to oxidize a range of common phenolic substrate at the expense of hydrogen peroxide (H_2O_2) (Sottomayor & Ros Barceló 2003; Sottomayor et al. 2004;

El-sayed & Verpoorte 2007; Loyola-Vargas et al. 2007). Therefore, the laboratory developed a general interest in.

1.3. Class III peroxidases

Peroxidases are multifunctional enzymes capable of catalyzing the oxidation of different low molecular weight substrates reactions at the expense of H_2O_2. Peroxidases are found in animals, plants and microorganisms, and they are divided into three superfamilies based on their structural and catalytic properties [Table 1; (Welinder 1992; Hiraga et al. 2001; Tognolli et al. 2002; Welinder et al. 2002; Cosio & Dunand 2008)].

Table 1. Classification of peroxidases. *In* Welinder 1992.

Superfamily	Class	Members	Origin
Animal peroxidases		Myeloperoxidase, glutathione peroxidase, lactoperoxidase, etc.	Animal
Catalase		Catalase	Animal, plant and fungus
Plant, fungal and bacterial peroxidases	I	Cytochrome *c* peroxidase, catalase-peroxidase, ascorbate peroxidase	Bacterium, fungus and plant
	II	Manganese-dependent peroxidase, ligninase	Fungus
	III	**Peroxidase**	**Plant**

Class III peroxidases (Prxs; EC 1.11.1.7), which are exclusive of plants, present a low specificity, being able to oxidise a broad range of substrates including aromatic phenols, amines, indoles, alkaloids, and sulfonates (Sottomayor et al. 2004). Prxs show also a remarkable diversity, with the presence of a high number of isoenzymes in a single plant, being present as large multigene families – 73 Prx genes were identified in *Arabidopsis* genome and 138 in rice (Tognolli et al. 2002; Welinder et al. 2002; Passardi et al. 2004).

The structural elements of Prxs are illustrated in Figure 5. Prxs are heme-containing glycoproteins that have highly conserved domains: a distal heme-binding domain, a central heme-binding domain and a proximal heme-binding domain. Both the

position and the arrangement of these domains are strictly conserved among Prxs (Hiraga et al. 2001). Two stabilizing Ca^{2+} ions are present in the structures of all active Prxs, and each Ca^{2+} site has two negatively charged aspartates and one or two hydroxy side chains as ligands (Welinder et al. 2002).

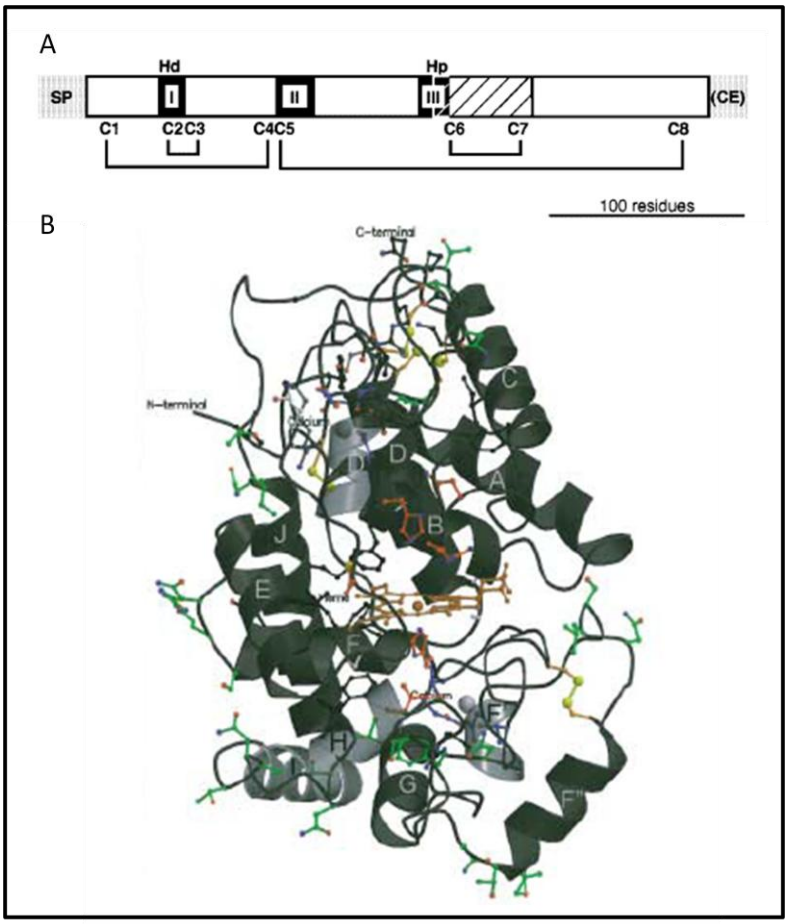

Figure 5. Prx features according with the structure of horseradish peroxidase isoenzyme C (HRPC). A. Structural representation of HRPC. N-terminal signal peptide (SP) and C-terminal extension (CE) are indicated by gray boxes. Filed boxes represent a conserved catalytic and distal heme-binding domain (I), a central heme-binding domain (II) and a proximal heme-binding domain (III) of unknown functions. A region presumed to be important for determining the specific function is indicated by a hatched box. Invariable distal histidine (Hd), proximal histidine (Hp) and eight cysteine residues (C1 to C8), which form a disulfide bond network are shown above and below the boxes, respectively (*in* Hiraga *et al.*, 2001). B. Three-dimensional structure of HRPC. The central heme group is sandwiched between the two protein domains (orange). Helices A-J are marked; active site residues are in red; side chain ligands to the distal and proximal Ca^{2+} ions are in blue; cysteine residues involved in disulfide bridges showed in yellow; an invariant ion-pair motif are on a grey background; and putative N-glycosylated triplets are in green. N-terminal and C-terminal extensions are indicated. *In* Welinder et al. 2002.

N-linked glycans were predicted for all putative Prxs, and the eight N-linked glycans of HRPC have been experimentally verified (Welinder 1979). The majority of

Prxs carry one or two putative glycans, therefore the high number of glycans found in HRPC is unusual among Prxs. Since glycans are large, those close to substrate-binding residues (near Pro139) are likely to affect substrate access and reaction dynamics (K. L. Nielsen et al. 2001).

Regarding subcellular localization, Prs are secretory enzymes localized in the cell wall or in the vacuole(s) of plant cells. These enzymes possess a signal peptide necessary for the routing of the protein to the endoplasmic reticulum (ER), and some also present a C-terminal extension (CTE) which seems to be responsible for the vacuolar targeting of these proteins (M. M. R. Costa et al. 2008).

Studies that compare Prx primary sequences indicate that these enzymes are highly variable within a single plant species (homologies lower than 35%). However, when comparing Prxs from different plant species, one realizes that nearly 90% of the residues are identical among taxa, suggesting the horizontal existence of a basic common set of Prxs with similar characteristics (Hiraga et al. 2001).

The diversity of the processes catalysed by Prxs, together with the high number of genes encoding these enzymes, suggests the existence of functional specialization of the members of this protein family. The fact that all plant peroxidase sequences contain both conserved regions and variable parts further supports this hypothesis (Cosio & Dunand 2008).

Prxs can be engaged in two catalytic cycles: (i) the classic peroxidative cycle that can oxidize various substrates at the expense of H_2O_2 and (ii) the hydroxylic cycle that can regulate the H_2O_2 level and release ROS (Passardi et al. 2005). Since purified Prx preparations generally catalyze the oxidation of a broad range of reductants *in vitro*, it would not be reasonable to consider the functions of individual Prxs on the basis of merely *in vitro* catalytic properties. Therefore a combination of characteristic (e.g. *in vitro* properties, localization and gene expression profiles) defines the specific functions of a respective Prx (Hiraga et al. 2001).

Prxs have been implicated in a broad range of physiological processes throughout the plant life cycle, specially related with the arquitecture and properties of the cell wall, including lignification and suberization, and cross-linking of cell wall structural proteins, but also in auxin catabolism, defence against pathogens, salt tolerance, senescence, etc. Through their hydroxylic cycle Prxs are also thought to generate highly reactive ROS which can possess an intrinsic activity during different environmental

responses and developmental processes, including the oxidative burst, or cell elongation. Alternatively, ROS can also act as part of signal transduction pathways during specific mechanisms, including biotic and abiotic stress responses, allelopathic plant-plant interactions, cell division/elongation, and programmed cell death (Passardi et al. 2005; Almagro et al. 2009). The task of defining specific functions for individual Prxs is hardened by the presence of many isoenzymes and low substrate specificity *in vitro* (Hiraga et al. 2001).

In contrast with the high number of studies on the functions of cell wall Prxs, much less is known about vacuolar Prxs (Welinder et al. 2002; M. M. R. Costa et al. 2008). *In vitro* studies have shown the capacity of plant Prxs to accept a number of vacuolar metabolites as substrates, such as phenols, flavonoids and alkaloids, and it has been suggested that, *in vivo*, Prxs assume specific functions related to the metabolism of these compounds (Sottomayor et al. 2004; Takahama 2004).

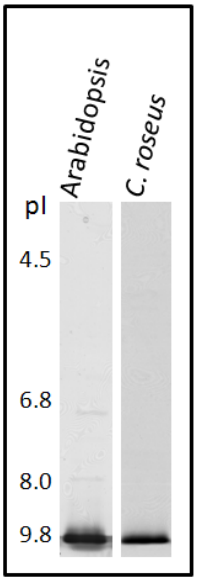

Figure 6. *In gel* Prx activity of *Arabidopsis* and *C. roseus* leaf extracts. Isoelectric focusing (IEF) gel showing that the main Prx activity observed in leaf protein extracts of these two species is due to the presence of a basic isoenzyme, identified as AtPrx34 and CrPrx1, for *Arabidopsis* and *C. roseus*, respectively. Unpublished data.

As stated above, the research group in which the present work was developed has previously reported the cloning, characterization and vacuolar localization of an enzyme with anhydrovinblastine synthase activity identified as the major class III peroxidase present in *C. roseus* leaves and named CrPrx1 – *Catharanthus roseus* peroxidase 1 [Figure 6; (Sottomayor et al. 1998; Sottomayor & Ros Barceló 2003; M. M. R. Costa et al. 2008)]. This team has also investigated the determination of the vacuolar sorting of CrPrx1 using GFP fusions, and have shown that the C-terminal extension present in

CrPrx1 was necessary and sufficient for the vacuolar sorting of this protein (M. M. R. Costa et al. 2008). The sorting of the different CrPrx1-GFP fusions was assayed using both *C. roseus* (homologous system) and *Arabidopsis* (heterologous system) mesophyll protoplasts. Subsequently, the research group became interested in the vacuolar sorting determination of other Prxs, namely of CrPrx03, also cloned in the group, and of leaf *Arabidopsis* Prxs. The main Prx of *Arabidopsis* leaves was purified and identified as being AtPrx34 [Figure 6, (Carqueijeiro 2008)], which presents a C-terminal extension similarly to CrPrx1 and therefore is putatively vacuolar.

In silico analysis of the expression of the whole *Arabidopsis* Prx family using the microarray database Genevestigator (Zimmermann et al. 2004) has shown that the main Prx genes expressed in the leaves of this plant are AtPrx42 and AtPrx34 (Figure 7).

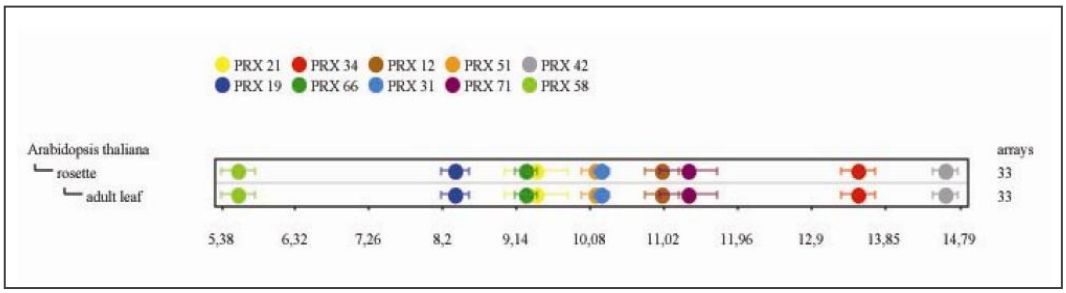

Figure 7. *In silico* analysis of Prx gene expression in *Arabidopsis* adult leaves, using the GENEVESTIGATOR microarray database (https://www.genevestigator.ethz.ch/). In this figure are represented the levels of expression of the ten most expressed AtPrx genes.

According to Genevestigator data and previous reports, AtPrx42 is, by far, the Prx gene with higher expression not only in leaves, but also in most organs of the plant and at all developmental stages (Tognolli et al. 2002; Welinder et al. 2002; Carter et al. 2004). However, results obtained in our lab using *Arabidopsis* leaf extracts tested for Prx activity revealed that the only band detected corresponds to AtPrx34 (Figure 6; (Carqueijeiro 2008). Since AtPrx34 is predicted to be vacuolar due to the presence of a C-terminal extension, contrary to AtPrx42, and because it is the most abundant Prx activity detected in *Arabidopsis* leaves, it was decided to study its sorting through the plant secretory pathway.

1.4. The plant secretory pathway

In the mid to late 1960s, the discovery that e proteins secreted by eukaryotic cells are first segregated in the lumen of the ER and then travel within membranous structures to

reach the cell surface, placed the ER at the start point of a newly recognized metabolic pathway, now known as the secretory pathway (Palade 1975). With the exception of proteins synthesized in mitochondria and plant plastids, protein synthesis initiates in the cytosol, and then secretory proteins are first inserted co-translationally into the ER, followed by traffic to their final destination using either vesicles or direct connections between compartments (Vitale & Hinz 2005; Foresti et al. 2008).

The translocation of secretory proteins to the ER depends on the presence of an N-terminal signal peptide (SP) (Vitale & Denecke 1999; Vitale & Hinz 2005; Foresti et al. 2008). When the beginning of the SP emerges from the ribosome, the whole translation complex is targeted to the ER translocation channel and the SP is removed co-translationally, while the nascent polypeptide is emerging into the ER lumen. Removal of the SP is performed by a signal peptidase, an enzyme located on the luminal surface of the ER membrane (Vitale et al. 1993; Vitale & Denecke 1999). Secretory proteins are then either secreted from the cell by default or delivered to one of the compartments of the endomembrane system, which includes the ER, the Golgi complex, and hydrolytic compartments (vacuoles), if further sorting signals are present in the protein (Vitale & Denecke 1999; Vitale & Hinz 2005; Foresti et al. 2008).

The ER is classically divided into three subdomains: the rough ER, smooth ER, and perinuclear ER (Okita 1996), and all three compartments contain soluble ER resident proteins, including the lumenal chaperone family of binding proteins (BiP). The chaperones facilitate proper folding and assembly of newly synthesized polypeptides in the lumen, and also act as a quality control monitor in binding and retaining unassembled or misfolded proteins in the ER (Vitale & Denecke 1999; Kleizen & Braakman 2004; Pimpl et al. 2006; Foresti et al. 2008). Secretory proteins often undergo post-translational modifications that in many cases are necessary for their activity and stability. Examples are the formation of disulfide bonds between cysteine residues, N-glycosylation and specific proteolytic maturation steps (Helenius & Aebi 2001; Seidah & Prat 2002; Tu & Weissman 2004; Faye et al. 2005).

The first step in the transport of proteins through the secretory pathway is generally the transfer from the ER to the Golgi apparatus (Figure 8). This occurs by means of a coat protein complex II (COPII)-mediated mechanism at specialized areas known as ER export sites (ERES), from which anterograde transport to the Golgi apparatus is thought to occur (Sanderfoot & Raikhel 1999; Matheson et al. 2006). The

nature of the transport intermediates that carry cargo from the ER to the Golgi is unknown. However, there is speculation surrounding the existence of closed compartments, such as vesicles or tubules, and the possibility that export occurs via a direct connection. In fact, it is suggested that the Golgi apparatus in plants not only may be physically linked to the ER but also may be a specialized subcompartment of the ER formed through continuous membrane flow (Dupree & Sherrier 1998; Sanderfoot & Raikhel 1999; Hawes & Satiat-Jeunemaitre 2005).

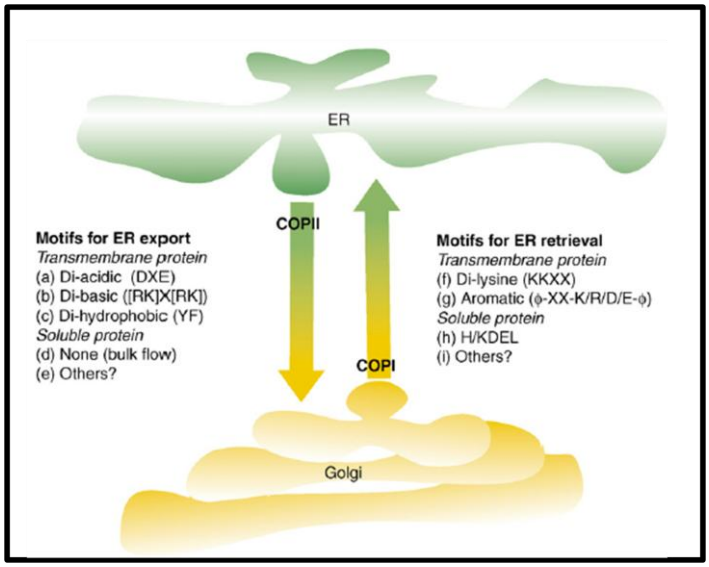

Figure 8. Anterograde and retrograde transport between ER and Golgi in plant cells. Protein motifs that are important for anterograde and retrograde cargo recognition are indicated. *In* Matheson et al., 2006.

Proteins also move from the Golgi to the ER via retrograde transport, in this case by means of a coat protein complex I (COPI)-mediated mechanism, as a way to balance the biosynthetic traffic by running in the opposite direction. This process allows endocytosis of extracellular molecules as well as recycling of membranes and proteins to maintain the integrity of the different compartments (Sanderfoot & Raikhel 1999; Vitale & Denecke 1999; Matheson et al. 2006).

For most secretory proteins, the ER is a compartment of transit. In opposition to the ER of animal cells, the ER of plant cells can tolerate an unusually high accumulation of protein without compromising plant development and reproduction, and the mechanisms through which naturally occurring resident proteins are retained within plant ER have been exploited. In all eukaryotes, proteins that remain acummulated in the ER have a C-terminal tetrapeptide, usually KDEL or HDEL, which is recognized by a receptor localized in the Golgi complex. Upon binding, the receptor

retrieves those C-terminal tagged proteins back into the ER. The mechanism is therefore retrieval, rather than a true retention system, but it is very efficient (Pelham 1990).

A central function has been attributed to the Golgi apparatus in the plant secretory pathway: directing traffic to and from such diverse organelles as the endoplasmic reticulum (ER), lytic and storage vacuoles, and the plasma membrane. More recently, the Golgi apparatus has been implicated in the transport of proteins to 'non-conventional' secretory organelles, such as peroxisomes and chloroplasts (Dupree & Sherrier 1998; Gutensohn et al. 2006; Matheson et al. 2006).

One of the purposes of this work is to study protein transport to vacuoles. Vacuoles are multifunctional organelles that can be regarded as one of the defining features of plant cells, and they can constitute up to 90% of the total cell volume. The principal function of vacuoles is the maintenance of cell turgour, but they are also involved in the turnover of macromolecules, ion homeostasis, and the sequestration of toxic compounds and secondary metabolites. Vacuoles also participate in programmed cell death and can accumulate and protect proteins against undesired proteolysis (Wink 1993; Jolliffe et al. 2005; Vitale & Hinz 2005; Zouhar & Rojo 2009).

The fact that this array of seemingly contrasting functions can be performed by the same organelle can be explained by the finding that plant cells have different types of vacuoles, and these can coexist in a single cell, or alternatively, that one vacuole may contain separate compartments separated by membranes (Hunter et al. 2007). Vacuoles generally can be divided into two main categories: (i) lytic vacuoles (LVs) that are acidic compartments, rich in hydrolases and can be regarded as the equivalent of mammalian lysosomes; and (ii) protein-storage vacuoles (PSVs), found in storage organs, mainly seeds, and that can store large amounts of proteins that will be used as a source of nitrogen during seed germination (Jolliffe et al. 2005; Zouhar & Rojo 2009). However, the distinctions between the different types of vacuoles may not be as clear as their names indicate.

Studies of vacuole function and biogenesis led to the discovery of tonoplast integral membrane proteins, called tonoplast intrinsic proteins (TIPs). TIPs belong to a family of proteins that function as aquaporins, channels to transport water, therefore essential to maintain vacuole function (Neuhaus & Rogers 1998). In experiments using labeled vacuoles for specific TIP antibodies, it was hypothesized that a specific TIP isoform is required for, and defines, the specific structure and function of a vacuole.

These leaded to the identification of α-TIP, recognized as specifically present in PSV, and γ-TIP specifically present in LV. In some cases, vacuoles labeled with both antibodies were identified; they are thought to represented cells where the two separate vacuolar compartments had been merged, presumably to expose storage proteins to an environment where their degradation could proceed (Paris et al. 1996; Neuhaus & Rogers 1998). This data demonstrates that multiple types of vacuoles occur not only in a single plant species but also in a single cell. Nevertheless, the biological functions of the multiple types of vacuoles in different cell types are not fully understood. Also, the relationship between the different types of vacuoles and the biogenesis and distribution of these organelles in the cell remain elusive. The highly dynamic nature of the vacuole in terms of biological functions makes often difficult to define their exact cellular roles in the cell (M. Park et al. 2004).

In addition to PSVs and LVs, other case of co-existing vacuoles has been reported in *Arabidopsis*. During leaf senescence the senescence-associated vacuoles (SAVs) are formed *de novo*. SAVs are characterized by a higher cysteine-protease activity and a lower pH than the LVs (Otegui et al. 2005). They are smaller in size and lack a γ-TIP tonoplast aquaporin, which is highly abundant in the membrane of the LVs from the same cells. How SAVs are formed is unknown. They contain aggregates that resemble partially degraded cytosolic material, but their size is smaller than regular autophagosomes, suggesting that they are not originated directly by autophagy.

According to the current working model for protein transport to vacuoles (Vitale & Hinz 2005), proteins are initially translocated into the ER and then travel through the Golgi complex where they can enter two possible pathways to two different destinations (Figure 9): (i) a route to the LV via clahtrin coated vesicles and a prevacuolar compartment/multivesicular body (PVC/MVB) , which is mediated by the sorting receptor "binding protein of 80 kDa" (BP-80),; and (ii) a less well-characterized route to the PSV that employs non-coated 'dense vesicles' (DV), possibly mediated by luminal Receptor homology domain trans Membrane domain and RING-H2 motif in the cytoplasmic tail protein (RMR proteins). These are transmembrane proteins that have characteristics of a protein receptor and travel through the Golgi complex and PSVs (Sanderfoot & Raikhel 1999; Vitale & Denecke 1999; Vitale & Galili 2001; M. Park et al. 2004; Vitale & Hinz 2005; Robinson et al. 2005; J. H. Park et al. 2007).

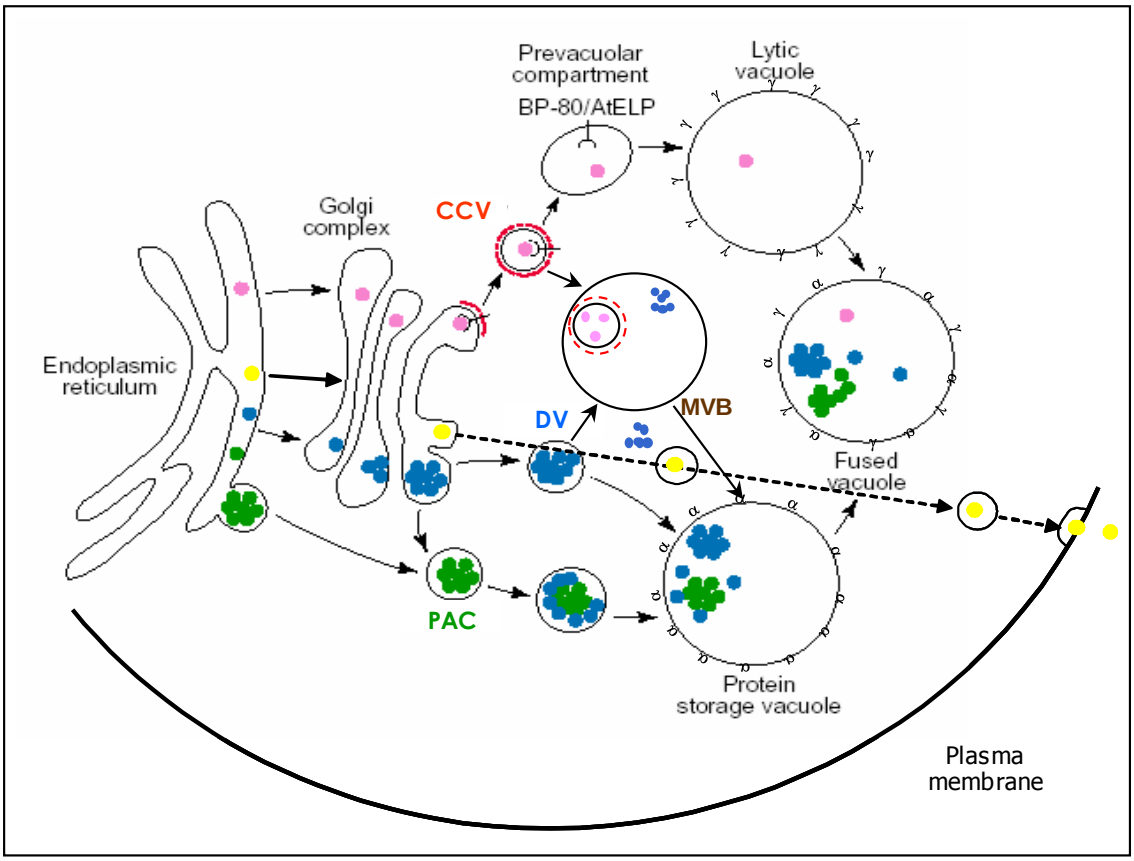

Figure 9. A working model for soluble protein traffic to the different vacuoles and cell wall. All proteins are translocated into the ER lumen. Cargo proteins (pink dots) destined to the lytic vacuoles (LVs) bind the sorting receptor BP-80, and enter clathrin coated vesicles (CCVs). They are then released into the prevacuolar compartment/multivesicular body (PVC/MVB), from where BP-80 is recycled, and are eventually delivered to LV. The broken red line represents the clathrin coat. Most storage proteins (blue dots) are concentrated throughout the Golgi stack and packaged into dense vesicles (DVs), which eventually fuse with the protein storage vacuole (PSV). Green dots indicate a pathway where proteins are directed to PSVs following a Golgi-independent route. MVBs might be a last intermediate station before PSVs. The fused vacuole represents the situation in many mature cells, where the LVs and PSVs merge into a single compartment capable of receiving both lytic and storage proteins. Yellow dots represent proteins that follow the default pathway to the cell wall. The Greek letters indicate specific vacuole types identified because they carry a specific TIP in their tonoplast: α for α-TIP on PSV, γ for γ-TIP on LV. The recycling pathways are not shown. Adapted from Vitale and Raikhel, 1999.

One major difference between RMR and BP-80 is that the former has been detected in the PSV crystalloid, whereas neither the lytic nor the storage vacuole tonoplast contains BP-80. Thus, an effective recycling machinery seems to recycle BP-80 but not RMR to the Golgi complex, so if stoichiometric interactions of receptor and ligand are always required for vacuolar protein sorting in the plant secretory pathway, it is difficult to understand how a non-recycling protein could function efficiently as a receptor (Vitale & Galili 2001; J. H. Park et al. 2007). At any case, M. Park et al. (2005)

reported an *A. thaliana* RMR protein (AtRMR1) that acted as a sorting receptor of phaseolin for its trafficking to the PSV.

In vegetative cells, the two pathways, to the LV and to the PSV, coexist and the separate vacuoles might ultimately merge to form the large central vacuole (Vitale & Raikhel 1999; Hunter et al. 2007). A third, alternative transport pathway has also been described involving large precursor-accumulating (PAC) vesicles that bypass the Golgi and fuse directly with PSV (Jolliffe et al. 2005). Thus, the mechanisms of protein trafficking to the storage vacuole may be either Golgi-dependent or Golgi independent.

Initial work on vacuolar protein trafficking was focused on identifying the sorting signals that marked cargo for the vacuolar sorting route. Three main types of vacuolar sorting determinants (VSDs) have been found: (i) sequence-specific VSDs (ssVSDs); (ii) C-terminal VSDs (ctVSDs) and (iii) physical structure VSDs (psVSDs). The ssVSDs show sequence conservation (usually NPIR,and always containing a crucial Ile/Leu residue), they are ususally N-terminal, but they are fucntional at any position within the precursor proteins. The ctVSDs lack any obvious sequence conservation but they have in common their strict localization at the C-terminus of the protein and the over representation of hydrophobic amino acids. It was postulated that ss proteins with VSDs where recognized by BP-80 and trafficked in clathrin coated vesicles (CCVs) to the LV, whereas proteins with ctVSDs and internal determinants were trafficked in dense vesicles (DV) to the PSV, possibly through RMR mediated recognition (Neuhaus & Rogers 1998; Vitale & Hinz 2005; J. H. Park et al. 2007). psVSD may be determinants of aggregation and mediate transport to vacuoles by means of dense vesicles, but this is yet to be proved (Matsuoka & Neuhaus 1999; Jolliffe et al. 2005; Vitale & Hinz 2005; J. H. Park et al. 2007).

It is noteworthy that the vacuolar sorting scenario is more complicated than the traditional picture portrayed above. Some reports describe ctVSS determining sorting to LVs, while others describe ssVSS that determine sorting to PSVs (Miller & Anderson 1999a; Miller & Anderson 1999b; Matsuoka 2000). In fact, vacuolar Prxs, such as CrPrx1 and AtPrx34, don't also fit the general sorting model, since they contain a putative C-terminal signal but accumulate in the central vacuole of plant cells, usually considered to be lytic in nature. To complicate matters further, some proteins even combine ssVSDs and ctVSDs. It is important to note that relatively few VSDs have been characterized and maybe new types still remain to be discovered. Moreover,

although *Arabidopsis* is now established as the primary model for intracellular trafficking studies, only a few endogenous vacuolar cargo have been studied and even fewer VSDs have been characterized in this plant (Zouhar & Rojo 2009).

1.5. Transient gene expression systems

The technology for gene transfer has developed to the stage whereby almost any plant of choice can be transformed, although there are still some practical limitations (Newell 2000). Currently, numerous transformation methods are available. They can be divided into two main groups: (i) indirect and (ii) direct.

The indirect methods of plant transformation are based on the introduction of a plasmid-carried T-DNA bearing the gene construct into the target cell by means of bacteria: *Agrobacterium tumefaciens* or *Agrobacterium rhizogenes*.

The direct methods cause physical or chemical modifications on the cell wall or the plasma membrane, therefore allowing the introduction of the exogenous DNA into the cell. These methods avoid the complex interaction between bacterium and plant tissue, with the result that the DNA to be introduced does not require the sequences necessary for T-DNA replication and transfer (Rao et al. 2009).

Transfer of DNA into plant cells can lead to transient or stable expression of the introduced DNA. Transient gene expression (TGE) assays offer two advantages over analysis of stable transformants. The major advantage is undoubtedly that gene activity can be measured within hours or days after DNA introduction. By comparison, it takes several weeks or months before stably transformed lines are available for detailed studyFurthermore, because the vast majority of transferred DNA remains extrachromosomal during the time course of a TGE assay, the analysis is not confounded by influences exerted by chromosomal sequences adjacent to the sites of integrated genes (Newell 2000; Ueki et al. 2009). Conversely, as a result of stable transformation, the introduced DNA is integrated into the host cell DNA, may suffer such influences, but will be passed on to succeeding generations.

Transient gene expression is therefore a powerful tool to provide invaluable insights into many protein functions, such as subcellular localization and trafficking, protein-protein interactions, protein stability and degradation, and protein activity (e.g.,

transcriptional activation), as well as into cellular processes induced by the transcription of the expressed gene, e.g., RNA silencing (Newell 2000; Ueki et al. 2009).

An ideal transient gene transfer system combines high efficiency of transformation with low cost and straightforward execution. Table 2 summarizes the main advantages and disadvantages of several TGE assays, two of which were used in this work.

Table 2. Main advantages and disadvantages of different TGE techniques.

	Agrobacterium*	**PEG**	**Biolistic**	**Electroporation**	**Microinjection**
Advantages	- easy - non invasive - inexpensive supplies and equipments	- species independent - inexpensive supplies and equipments	- species independent - applicable to cells and tissues	- applicable to cells and tissues	- species independent - applicable to cells and tissues
Disadvantages	- host range limitations	- care-intensive - time-consuming - PEG can injure cells	- expensive instrument - large sample variations	- formation of temporary pores can affect cell survival	- not routinely - expensive instrument needed - large amounts of effort may be expended for no return
Refs	(Di Fiore et al. 2004; Wydro et al. 2006; Zottini et al. 2008)	(Mathur & Koncz 1998; Mi Jeon et al. 2007; Yoo et al. 2007)	(Ueki et al. 2009; Guirimand et al. 2009; Rao et al. 2009)	(Fromm 1985; Chowrira et al. 1995; Newell 2000)	(Morikawa & Yamada 1985; Crossway et al. 1986; Rao et al. 2009)

* Only the transformation of leaves was considered.

1.5.1.*Agrobacterium*-mediated transformation

As a genus, *Agrobacterium* can transfer DNA to a remarkably broad group of organisms from different kingdoms like Plantae and Fungi (Gelvin 2003). In plants the members of this genus cause the neoplastic diseases crown gall (*Agrobacterium tumefaciens* and *Agrobacterium vitis*), hairy root (*Agrobacterium rhizogenes*), and cane gall (*Agrobacterium rubi*) on numerous plant species (Gelvin 2009).

Genetic experiments indicated that a particular class of plasmids, the tumour-inducing (Ti), and later the rhizogenic (Ri) plasmids, were responsible for the tumorigenesis induced by Agorbacterium, and that a portion of these plasmids, the transferred DNA (T-DNA), is transferred to plant cells and incorporated into the plant

genome. It was thus obvious to propose that Ti plasmids be used as a vector to introduce foreign genes into plant cells (Gelvin 2003; Tzfira & Citovsky 2006; Gelvin 2009). A valuable extension to *Agrobacterium* utility occurred when it was conclusively proven that monocots, such as rice, could indeed be successfully transformed by the bacterium, because initially monocots were thought not to be amenable to transformation in this way (Newell 2000; Gelvin 2003; Gelvin 2009).

The biological process by which *Agrobacterium* transfers and integrates its T-DNA included in the Ti plasmid, into the host plant DNA has been the subject of intensive investigation over the last 20 years (de La Riva et al. 1998; Newell 2000; Gelvin 2003; Gelvin 2009; Rao et al. 2009). The molecular basis of genetic transformation of plant cells by *Agrobacterium* is represented in Figure 10. The DNA is delimited by border sequences with 25 bp in length, highly homologous in sequence, and which flank the T-region in a directionally repeated orientation. These sequences are the target of the VirD1/VirD2 border-specific endonuclease that cuts the T-DNA separating it from the Ti plasmid (de La Riva et al. 1998; Gelvin 2003). Processing of the T-DNA from the Ti plasmid and its subsequent export from the bacterium to the plant cell result in large part from the activity of further virulence (*vir*) genes carried by the Ti plasmid (figure 10).

The final step of T-DNA transfer is its integration into the plant genome. The mechanism involved in the T-DNA integration has not yet been fully characterized. It is considered that the integration occurs by illegitimate recombination (de La Riva et al. 1998).

In nature, the T-DNA carries a set of oncogenes and opine-catabolism genes which, upon expression in plant cells, lead to neoplastic growth of the transformed tissue and the production of opines, amino acid derivatives used by the bacteria as a nitrogen source. Recombinant disarmed *Agrobacterium* strains, in which the T-DNA oncogenes have been replaced with genes of interests, are the most efficient vehicles used today for the introduction of foreign genes into plants and for the production of transgenic plant species (de La Riva et al. 1998; Tzfira & Citovsky 2006).

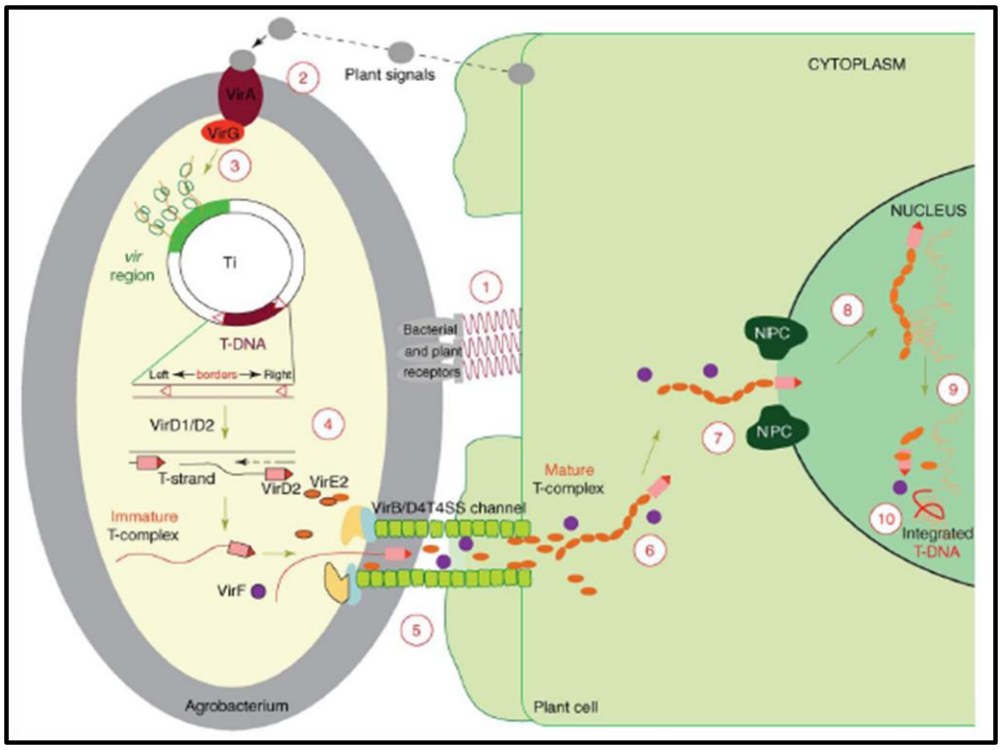

Figure 10. A model for the *Agrobacterium*-mediated genetic transformation. The transformation process comprises 10 major steps and begins with recognition and attachment of the *Agrobacterium* to the host cells (1) and the sensing of specific plant signals by the *Agrobacterium* VirA/VirG two-component signal-transduction system (2). Following activation of the vir gene region (3), a mobile copy of the T-DNA is generated by the VirD1/D2 protein complex (4) and delivered as a VirD2–DNA complex (immature T-complex), together with several other Vir proteins, into the host-cell cytoplasm (5). Following the association of VirE2 with the T-strand, the mature T-complex forms, travels through the host-cell cytoplasm (6) and is actively imported into the host-cell nucleus (7). Once inside the nucleus, the T-DNA is recruited to the point of integration (8), stripped of its escorting proteins (9) and integrated into the host genome (10). *In* Tzfira and Citovsky, 2006.

A strategy described by (Hoekema et al. 1983) and de Framond et al. (1983) involved a separation of the T-region and the *vir* genes into two different replicons. When these replicons were within the same *Agrobacterium* cell, products of the *vir* genes could act in *trans* on the T-region to effect T-DNA processing and transfer to a plant cell. (Hoekema et al. 1983) called this a binary-vector system: the replicon harbouring the T-region constituted the binary vector, whereas the replicon containing the *vir* genes became known as the *vir* helper. The great advantage of the binary system, which is today used almost universally, is that the binary vector plasmids are small and easy to manipulate in both *E. coli* and *Agrobacterium,* and generally contain multiple unique restriction endonuclease sites within the T-region, into which genes of interest can be cloned (Dessaux et al. 1992; Gelvin 2003). Therefore, a number of binary vectors were developed such as the pGreen collection, pPVP and pBIN, and

Agrobacterium strains containing non-oncogenic *vir* helper plasmids have also been developed: LBA4404, GV2260, C58C1, GV3100, GV3101, GV3850, A136, EHA 101, A281, A543, EHA105 and AGL1. *Agrobacterium* can also be used for transient expression assays by infiltration of leaves - agroinfiltration). This is an easy and non-invasive technique that simply requires the infiltration of a suspension of bacteria carrying the plasmid constructs into the plant material. This methodology has been widely used in tobacco (*Nicotiana tabacum*) with high levels of transgene expression, mainly because the size of the leaves of this plant allows to test multiple constructs/combination of constructs in a single leaf (Wydro et al. 2006). However, and up till now, agroinfiltration of *Arabidopsis* and *C. roseus* leaves has not been very successful, especially for subcelular studies (Bent 2000; Zárate & Verpoorte 2007; Rao et al. 2009).

1.5.2. PEG-mediated transformation

Direct DNA delivery systems have been deeply reviewed (Barcelo & Lazzeri 1998). Early work on plant transformation suggested that monocotyledonous species were recalcitrant to infection by *Agrobacterium*, due to host-range restrictions. This led to exploration of other avenues of transformation for such species, and plant protoplasts became an obvious target (Newell 2000).

Protoplasts are cells that have had their cell walls removed. This can be done mechanically, or by enzymatic digestion, resulting in 'naked' cells surrounded only by a plasma membrane. Mesophyll protoplasts present many practical advantages. For example, plant materials are grown from seeds that are genetically stable, leaves represent an inexpensive source of material, and they usually represent active and homogeneous cell populations that are amenable for synchronous pharmacological and biochemical treatments (Sheen 2001; Yoo et al. 2007).

Although a range of species has now been transformed in such a way, two major disadvantages are intimately associated to methods using protoplasts. One is that the regeneration of plants from protoplast cultures can be a complex and time-consuming process - however, this issue is not relevant when transient expression is the goal (Newell 2000). Another is that since protoplast isolation requires enzymatic removal of the cell walls, this may affect the behaviour and viability of the cells. In fact, there may

be the mistaken impression that protoplasts are irreversibly wounded and are dying cells, which is not true. However, these treatments do stress the cells and disrupt the developmental control systems dependent on cell/cell contact or on the position of a cell in an organized structure. Still, when properly isolated and maintained, protoplasts retain most of their original biochemical and cellular activities. In fact, it has been proved that freshly isolated protoplasts can maintain their viability for more than 48h in a simple mannitol solution (Sheen 2001), and that wild-type mesophyll protoplasts maintain most leaf features and responses, which are often lost in undifferentiated suspension culture cells (Yoo et al. 2007).

There are a number of methods for introducing DNA into plant protoplasts, but the most commonly used technique is the polyethylene glycol (PEG) mediated DNA uptake. The PEG-mediated transformation is simple and efficient, allowing a simultaneous processing of many samples with low amounts of protoplasts, and yields a transformed cell population with high survival and division rates (Yoo et al. 2007). How DNA is introduced into the cells is not completely elucidated, perhaps PEG molecules promote the DNA interaction with the cell surface, this being later included by endocytosis (J. J. Finer et al. 1996). On the other hand, PEG may also protect the DNA against nucleases (J. J. Finer et al. 1996). The method utilizes inexpensive supplies and equipments, and helps to overcome a hurdle of host range limitations of *Agrobacterium*-mediated transformation. The PEG-mediated DNA transfer can be readily adapted to a wide range of plant species and tissue sources (J. J. Finer et al. 1996; Mathur & Koncz 1998; Sheen 2001).

In *Arabidopsis thaliana*, several methods of direct gene transfer to protoplasts have been reported, especially using cell suspension cultures (Axelos *et al.*, 1992; Doelling and Pikaard, 1993). However, leaf mesophyll protoplasts may be a preferable material for many gene expression studies, since these are cells derived from normal, differentiated plant tissues, and not from undifferentiated cells. Furthermore, suspension cultures may accumulate changes in ploidy and mutations due to somaclonal variation (Larkin & Scowcroft, 1981).

Fast and simple procedures have been established to obtain homogeneous, active, and responsive mesophyll protoplasts from *Arabidopsis* leaves for transient gene expression analysis (Abel & Theologis 1994; Hoffman et al., 1994; Sheen, 2001) and their PEG mediated transformation has also been performed with success (Yoo et al. 2007).

1.6. Objectives

The main goal of this work was the development and optimization of simple/fast, efficient and reproducible transient expression protocols for subsequent subcellular localization studies of proteins coded by Prx genes, and for characterization of candidate genes provided from omic approaches, namely implicated in the regulation, biosynthesis or transport of the valuable alkaloids from *C. roseus*. For this purpose, two distinct methodologies were selected, to be used with two different sources of plant material: *Agrobacterium*-mediated transformation of leaves (agorinfiltration) and PEG-mediated transformation of protoplasts, using both *Catharanthus roseus* and *Arabidopsis thaliana*. The species *Arabidopsis thaliana* was used not only because of the interest on *Arabidopsis* Prxs, but also because this is the consensual model organism in plant sciences, to which most of the available protocols were developed or optimized, being commonly used as an heterologous system. Fusions of the main vacuolar Prx expressed in *C. roseus* leaves (CrPrx1) with GFP (M. M. R. Costa et al. 2008), already available in our lab, together with two marker fusions, were used to validate the methodologies under development.

Another goal of this work was to investigate the subcellular localization of AtPrx34, the main Prx activity expressed in *Arabidopsis* leaves (Carqueijeiro 2008), in order to confirm its vacuolar localization and sorting determination. In fact, AtPrx34 was previously identified in the *Arabidopsis* leaf vacuolome (Carter et al. 2004), and the presence of a CTE (C-terminal extension) in its sequence also predicts a vacuolar localization. Therefore, a set of constructs corresponding to fusions of GFP with different AtPrx34 regions (SP, CTE and mature protein with and without CTE) were designed and generated, to assess the sorting capacity of the CTE of AtPrx34 and to characterize its precise subcellular localization, by means of transient expression using PEG-mediated transformation of *Arabidopsis* protoplasts. An AtPrx34-GFP fusion construct harboured in a binary vector already available in our lab was also used for agorinfiltration.

Materials and methods

2. Materials and methods

2.1. Biological material

2.1.1. Plant material

Plants of *Catharanthus roseus* (L.) G. Don cv. Little Bright Eye were grown at 25°C in a growth chamber, under a 16 h photoperiod, using white fluorescent light with an intensity of 30-70 μmol m^{-2} s^{-1}. *C. roseus* seeds were acquired from AustraHort (Australia) and voucher specimens are deposited at the Herbarium of the Department of Biology of the Faculty of Sciences of the University of Porto (PO 61912).

C. roseus seeds were germinated on moist filter paper, in plastic boxes covered with cling film (Figure 11A), for two to four weeks, and seedlings (usually presenting two to four leaves) were transferred onto pots with compost (SiroPlant - Universal Potting Substrate, Siro). The pots were initially covered with cling film to start the acclimatization process. *C. roseus* plants were regularly transferred into bigger pots as growth proceeded (Figure 11B-E). Adult *C. roseus* plants, i.e. with fully developed and healthy dark green leaves were used for protoplasts isolation (Figure 11D,E); for agroinfiltration procedures adult plants, seedlings (figure 11C) and in vitro regenerated *C. roseus* plants (figure 11F) were also used.

In vitro regenerated *C. roseus* plants produced previously in the laboratory were also used [Figure 1F, (L. Cardoso 2009)]. These derived from mature zygotic embryos (MZEs) dissected from sterile *C. roseus* seeds, initially plated on Murashige and Skoog medium (MS; Duchefa) supplemented with 3% (w/v) sucrose, 0.7% (w/v) agar and 7.5 μM thidiazuron. MZEs were incubated in the dark at 25ºC to differentiate shoots that were then transferred onto proliferation medium composed of MS supplemented with 3% (w/v) sucrose, 0.7% (w/v) agar and 4.44 μM 6-benzylaminopurine. Rooting of shoots to regenerate complete plants was performed in MS medium supplemented with 2% (w/v) sucrose, 0.7% (w/v) agar and 1.2 μM 3-indole butyric acid.

Figure 11. *Catharanthus roseus* plants at different developmental stages. A. Seeds germinating on filter paper. B. Seedlings recently transferred to soil at the beginning of the acclimatization process. C. Young acclimatized plants in individual pots. D. Non-flowering plant. E. Adult flowering plants. F. Regenerated plants, obtained *in vitro* from mature zygotic embryos, at the beginning of the acclimatization process.

A. thaliana seeds, ecotype Columbia-0 (Col-0), were purchased from the Nottingham *Arabidopsis* Stock Centre (NASC). *Arabidopsis* seeds were scattered onto pots with soil, covered with cling film, and subjected to a two to four-day vernalization period by putting the pots at 4ºC. *Arabidopsis* seeds were germinated in a walk-in chamber at 21°C, under a 12 h photoperiod using white fluorescent light with an intensity of 100 µmol m^{-2} s^{-1}. As soon as the first pair of true leaves emerged, seedlings were transferred into individual pots and covered with cling film for acclimatization (Figure 12A and B).

Plants suitable for protoplast isolation and transformation were obtained six to eight weeks after germination, when the rosette growth was completed, but the inflorescence had still not emerged (Figure 12C and D). This corresponds to the stage 4 of *Arabidopsis* growth as defined by Boyes et al. (2001) and all *Arabidopsis* plants used in this work were at this stage of development.

Occasionally, *Arabidopsis* plants were left to grow further (past the 8th week) in order to generate seeds.

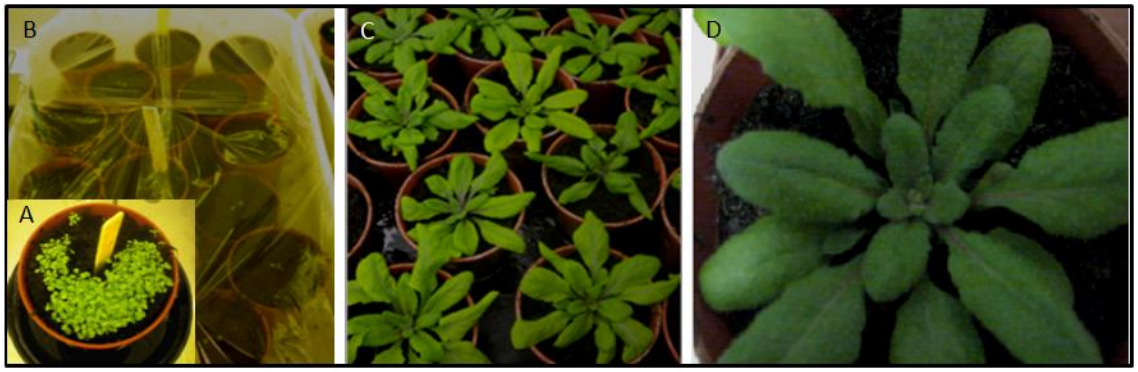

Figure 12. Plants of *Arabidopsis thaliana* at different developmental stages. A. Seedlings at the original pot where seeds were scattered to germinate. B. Seedlings exhibiting the first pair of true leaves after transference into individual pots. Pots were covered with cling film to start acclimatization. C. Plants at the developmental stage 4 defined by Boyes *et al.* (2001). D. Magnification of C.

2.1.1. Bacterial strains and plasmids

The bacterial strains used in this work were *Escherichia coli* DH5α and *Agrobacterium tumefaciens*, disarmed strains EHA105, LBA4404 and GV3101 (Hellens et al. 2000).

E. coli DH5α competent cells were grown in Luria-Bertrani (LB) medium (Difco™; for one litre of LB medium: 10 g of tryptone, 5 g of yeast extract and 10 g of NaCl) supplemented with 150 µg/mL ampicillin (Sigma). Cultures were grown overnight (ON) at 37ºC (Infors HT Multriton Incubator) with vigorous shaking (200 rpm). Aliquots of all cell cultures used in this work were cryopreserved in 10% (v/v) glycerol (Merck) and stored at -80ºC.

Chemically competent *E. coli* DH5α cells were subjected to transformations using the heat shock method. Typically, 50-100 µL of DH5α chemically competent cells were used for transformation either with 1 µL of plasmid DNA (pDNA) or half of the volume of a ligation reaction (5 µL). After an incubation of 30 minon ice, the mixture of competent bacteria and DNA was heat-shocked at 42°C for 2 min and placed back on ice for 2 min. One mL of LB was added to the mixture and the cells were left to recover for 1h at 37ºC. The cell suspension was centrifuged at 4000 rpm for 4 min at room temperature (RT) and 900 µL of supernatant were removed. The cells were resuspended in the remainder volume, were plated onto LB-agar (LB with 1.5% agar; Liofilchem) supplemented with 150 µg/mL of ampicillin, and the plates were incubated ON at 37ºC. Single isolated colonies were picked to inoculate 5 mL of LB medium supplemented

with 150 µg/mL of amplicillin to check for the presence of the correct DNA by boiling (section 2.1.5) or alkaline lysis (Plasmid Miniprep Kit, Fermentas) plasmid mini-preps.

Agrobacterium tumefaciens strains EHA105, LBA4404 and GV3101 harbouring binary vectors encoding the constructs described in Table 1, were grown either in LB or in YEB media [for one litre of YEB: 5 g of beef extract (Difco), 1 g of yeast extract (Difco), 5 g of peptone (Difco), 5 g of sucrose (Merck) and 2 mM $MgSO_4$ (Sigma)]. Whenever used, YEB was supplemented with 10 mM MES (pH 5.6; Carl Roth) and 20 µM acetosyringone (Sigma) in dimethyl sulfoxide (DMSO; Merck). In all cases, appropriated antibiotics were added to the medium and the bacteria were allowed to grow ON at 28ºC with vigorous shaking (200 rpm). Aliquots of all cell cultures used in this work were cryopreserved in 10% (v/v) glycerol (Merck) and stored at -80ºC.

The *Agrobacterium* clones used in this work to try to establish the agroinfiltration techniques and eventually already assess the subcellular localization of AtPrx34 and CrPrx3, were already available in the laboratory and are described in Table 3. CrPrx3 is a root expressed *C. roseus* Prx highly homologous to CrPrx1, also bearing a CTE. These constructs had not been tested before.

Table 3. List of *Agrobacterium* clones and respective GFP/RFP constructs used to study the vacuolar sorting capacity of the CTE of AtPrx34 and CrPrx2. All constructs were under the control of the cauliflower mosaic virus (CaMV) 35S constitutive promoter.

Gene	*Agrobacterium* strain	Binary vector	Helper plasmid	Antibiotic resistance*	Construct	Expected subcellular localisation
AtPrx34	GV3101	pGreen II	pSoup	Km^R, Gm^R	$SP_{AtPrx34}$-GFP	Sec. Pathway / cell wall
CrPrx3	EHA105/ LBA4404	pGreen II	pMP90RK	Km^R, Tet^R	$SP_{CrPrx2b}$-RFP	Sec. pathway / cell wall
					$SP_{CrPrx2b}$-RFP-$CTE_{CrPrx2b}$	Vacuole
					$SP_{CrPrx2b}$-RFP-$MP_{CrPrx2b}$	Sec. Pathway / cell wall
					$SP_{CrPrx2b}$-RFP-MP-$CTE_{CrPrx2b}$	Vacuole

*Antibiotic concentration: 25 µg/mL of kanamycin (Km^R) for selection of pGreenII; 5 µg/mL of tetracycline (Tet^R) for selection of pSoup; 10 µg/mL gentamycin (Gm^R) for selection of pMP90RK. GFP - Green Fluorescent Protein; RFP - Red Fluorescent Protein.

2.2. Confirmation of already available CrPrx1- GFP fusions

Several constructs used in this work had been previously generated to study the subcelular localization of CrPrx1 [(M. M. R. Costa et al. 2008) and unpublished] and were already available in our laboratory. Since most of them had already been tested, they were used to for protocol optimization of PEG-mediated transformation of protoplasts, and are summarised in Table 4. Since these clones hadn't been used for some time, they were all analysed for confirmation of the CrPrx1-GFP fusion.

Table 4. List of GFP-CrPrx1 constructs used for optimization of PEG-mediated transformation of protoplasts. All constructs were under the control of the CaMV 35S constitutive promoter.

Construct	Abbreviation	Plasmid	Target
35S::GFP	C1	pTH-2	Cytoplasm
35S::SP_{CrPrx1}-GFP	C2	pTH-2	Sec. Pathway / cell wall
35S::SP_{CrPrx1}-GFP-CTE_{CrPrx1}	C3	pTH2-BN	Vacuole
35S::SP_{CrPrx1}-GFP-MP_{CrPrx1}	C4	pTH2-BN	ER/Golgi
35S::SP_{CrPrx1}-GFP-MP-CTE_{CrPrx1}	C5	pTH2-BN	Vacuole

Plasmid DNA of each of the constructs (Table 4) was used to transform *E. coli* as described above (section 2.1.1). Single isolated colonies were used to inoculate 5 mL of LB medium supplemented with 150 µg/mL of amplicillin and pDNA was purified using the GeneJet Plasmid Miniprep Kit (Fermentas) following the manufacturer's instructions.

pDNA identity was confirmed via restriction analysis with a single digestion with the endonuclease *SalI* (Fermentas). Double digestions with *SalI* and *PstI* (Fermentas) for C1 and C2, and *SalI* and *XhoI* (Fermentas) for C3 and C5, were also performed (Table 5).

Table 5. Composition of the restriction reactions performed with constructs C1, C2, C3 and C5 from Table 4 [a].

	Constructs							
Reagents	**C1**		**C2**		**C3**		**C5**	
Buffer O	2	2	2	2	2	2	2	2
pDNA	0.5	0.5	2	2	2	2	2	2
SalI	1	1	1	1	1	1	1	1
PstI	-	1	-	1	-	-	-	-
XhoI	-	-	-	-	-	1	-	1
H_2O	16.5	15.5	15	15	15	15	15	15
Final volume	20 (µL)	20 (µL)	20 (µL)	20 (µL)	20 (µL)	20 (µL)	20 (µL)	20 (µL)

[a] The mixtures were incubated for 1h at 37ºC.

The digestion products were visualized in 1.5% (w/v) agarose (Bio-rad) gel electrophoresis using Tris-acetate-EDTA [TAE buffer; 40 mM Tris base (Sigma), 10% (v/v) acetic acid (Merck) and 10 mM EDTA (Merck)] as running buffer. The Gene Ruler DNA Ladder Mix (0.5 µg/µL; Fermentas) was used as molecular marker and an Orange Loading Dye Solution (Sigma) was used for visual tracking of DNA migration. Ethidium bromide (EtBr; 10mg/mL; BioRad) was added to the agarose gel at a 0.5 µg/mL concentration, to allow visualization of the DNA bands under UV light. The electrophoretic run was performed at 80 V (PowerBac Basic, BioRad).

2.3. Preparation of plasmid DNA for PEG-mediated transformation of protoplasts

Preparation of pDNA for protoplast transformation, i.e. ultrapure and highly concentrated, was performed using the Plasmid Midi Kit (Qiagen), according to the manufacturer's instructions but with some modifications. A starting culture of 50 mL was used, and the bacterial cells were harvested by centrifugation at 5000 rpm for 15 min at 4ºC. The alkaline lysis procedure was carried out in 50 mL Falcon tubes as in the original protocol, however the cleaning of the lysate was done by centrifugation at 5000 rmp for 60 min at 4ºC (Universal 320R, Hettich) followed by another centrifugation for 30 min. The equilibration of the column, the DNA binding, washing and elution steps were all performed as indicated. Isopropanol precipitation was performed in 15 mL Falcon tubes, and the solution was then divided into eppendorf tubes and centrifuged as

in the original protocol. The resulting pDNA integrity was checked by agarose gel electrophoresis as described in 2.2. pDNA quantification was performed spectrophotometrically using a NanoDrop® ND1000 device.

The same procedure was also used to purify two control marker constructs additionally used in this work: 35S::SP_{CrPrx1}-GFP-$CTTP_{Phaseolin}$ (vacuolar) and 35S::SP_{CrPrx1}-GFP-KDEL (ER) (unpublished data). Both of these constructs were in pTH2-BN.

To sum up the pDNA preparations obtained through this method, gravity-flow with QIAGEN anion-exchange tips from the QIAGEN Plasmid Midi Prep kit, result in endotoxin-free, ultrapure and highly concentrated DNA, which is a key factor to improving transformation efficiency. pDNA preps isolated in such a way typically render a yield of ~1.5-2 μg/μL.

2.4. Generation of AtPrx34 –GFP fusions

The cloning strategy described by Costa et al. (2008) for CrPrx1 was followed to obtain similar constructs with AtPrx34. In summary, the amplified AtPrx34 SP was cloned in frame in pTH-2 and pTH2-BN using *Sal*I / *Nco*I to generate the construct 35S::$SP_{AtPrx34}$-GFP (C2). pTH2-BN is a derivative lacking the GFP stop codon, which is used for C-terminal fusions. The C2 construct in pTH2-BN was used to further insert amplified sequences of AtPrx34 using *Bgl*II / *Xho*I to generate the constructs: 35S::$SP_{AtPrx34}$-GFP-$CTE_{AtPrx34}$ (C3), 35S::$SP_{AtPrx34}$-GFP-$MP_{AtPrx34}$ (C4) and 35S::$SP_{AtPrx34}$-GFP-MP-$CTE_{AtPrx34}$ (C5) (Figure 13).

The empty cloning / expression vector pTH2 (C1) and pTH2-BN are describe in Figure 14A and B. In pTH2, gene expression is under the control of the cauliflower mosaic virus' constitutive promoter 35S (~400 bp). pTH2 also includes a resistance marker for ampicillin / carbenicillin, allowing the selection of positively transformed cells (not represented in the figure), a nopaline synthase (*Nos*) terminator (~250 bp) from *Agrobacterium tumefaciens*, and the reporter gene sGFP (S65T) that has cytoplasmic expression (~750 bp). pTH2-BN is a derivative from pTH2 in which a BN linker was introduced (~40 bp), and that lacks the GFP stop codon (Chiu et al. 1996; Niwa et al. 1999).

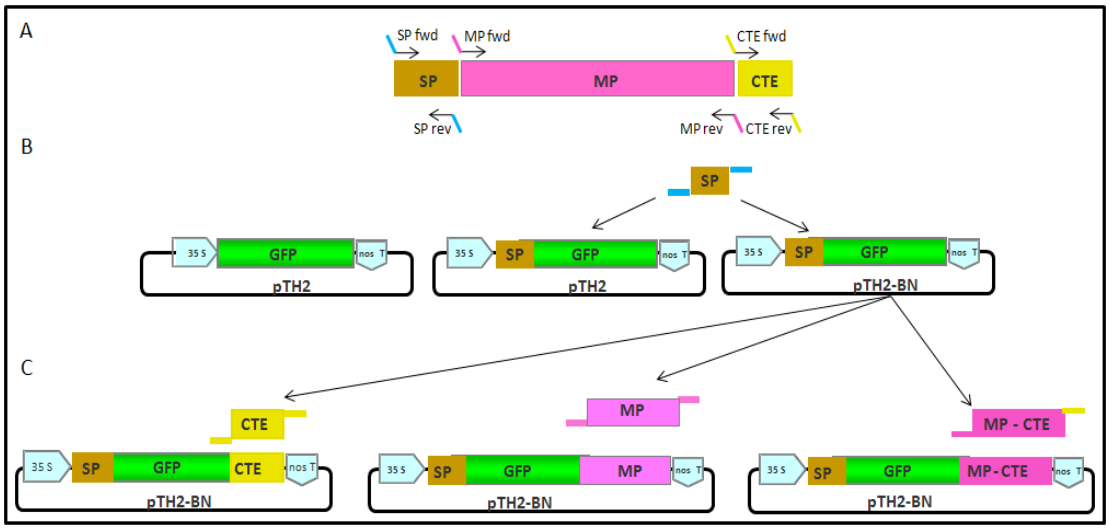

Figure 13. Schematic representation of the cloning strategy followed to obtain the AtPrx34-GFP constructs. A. Representation of the different domains of AtPrx34 and the primers used for their amplification. SP - signal peptide; MP – mature protein; CTE - C-terminal extension. B. Schematic representation of pTH-2, depicting the 35S promoter, GFP and the *nos* terminator regions (left). The SP of AtPrx34 was cloned in frame into pTH-2 (centre) and pTH2-BN (right). C. The CTE, MP and MP-CTE of AtPrx34 were all cloned at the C-terminus of GFP, on the starter construct 35S::$SP_{AtPrx34}$-GFP- in pTH2-BN (B, right).

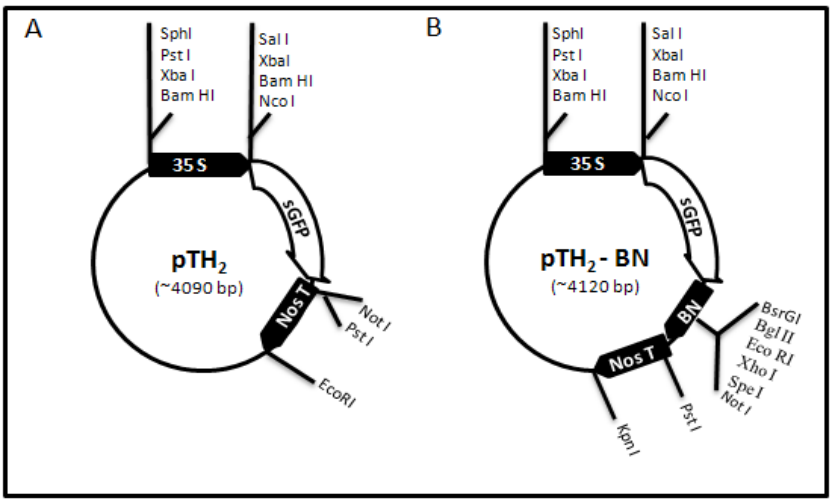

Figure 14. Schematic representation of the cloning vectors, pTH2 and pTH2-BN, depicting the most relevant restriction sites and the 35S promoter, sGFP and Nos terminator regions.

2.4.1. Transformation of *E. coli*

Initially the vector pDNAs [pTH2 and pTH2-BN; (Chiu et al. 1996; Niwa et al. 1999)] and the complete cDNA of AtPrx34 (clone RAFL03-01-G07 / resource nr. pda 13431, purchased from the RIKEN Bioresource Center, Japan) were used to transform *E. coli* DH5α by the heat sock method (section 2.1.1.). Single isolated colonies were used to

inoculate 5 mL of LB medium supplemented with 150 µg/mL of amplicillin and the liquid cultures were used to purify pDNA, with the GeneJET™ Plasmid Miniprep Kit. pDNA identity was confirmed by restriction digestion with *XhoI* (Fermentas) for AtPrx34 cDNA (Table 6) and with *Pst*I for the vectors (table 7). Digestion products were visualized in 1 % (w/v) agarose gel electrophoresis as already described (2.2.).

Table 6. Digestion reaction performed with AtPrx34 cDNA[a].

Reagents	Volume (µL)
Buffer R	2
pDNA	2
*Xho*I	1
H_2O	15
Final volume	20

[a] The mixture was incubated for 1h at 37ºC.

Table 7. Digestion reaction performed with the cloning[a] vectors*.

Reagents	Volume (µL)
Buffer O	2
pDNA	2
PstI	1
H_2O	15
Final volume	20

[a] The mixture was incubated for 1h at 37ºC.

2.4.2. Primers

The next step was to design specific primers to amplify the different domains of AtPrx34: SP (signal peptide), CTE (C-terminal extension), MP (mature protein) and MP-CTE. The localization of these domains was predicted by Welinder et al. 2002. Relatively to the SP, two sequences were amplified, a sorter using the SP primers FWD/REV and a longer one using SP primers FWD/REV2, including some aminoacids after the predicted cutting site of the SP, to be sure the endopeptidase would recognize

the cutting site. The sequences of the individual primers (Table 8) were engineered to include the appropriate restriction sites to allow directional cloning.

Table 8. List of primers used to amplify the different AtPrx34 regions to be cloned into pTH2 and pTH2-BN.

Primer	Sequence (5' to 3')[a]	Size (bp)	Tm ºC
SPAtPrx34FWD	AGCCGTCGAC**aaa**ATGCATTTCTCTTCGTCTTC	33	69.7
SPAtPrx34REV	GATGCCATGGTTGAGCAGCGGACAAAGATGCA	32	70.5
SPAtPrx34REV2	GATGCCATGGATGGTTTCTCGTACGATGTTA	31	62
MPAtPrx34FWD	CAAGATCTCAACTCACCCCTACCTTCTACGA	31	68.7
MPAtPrx34REV	CGCCTCGAGTCAGTTCACAACTCTACAGTTCAA	33	70.1
CTEAtPrx34FWD	CAAGATCTAACTCCAACTCTCTGCTCCATGAT	32	69.2
CTEAtPrx34REV	CGCCTCGAGTCACATAGAGCTAACAAAGTCAACG	34	71.5

[a] Restriction sites are underlined. Bold letters (**aaa**) correspond to sequence included in the AtPrx34 original clone.Bases in grey correspond to AtPrx34, bases in black correspond to a primer extension used to introduce the desired restriction site.

2.4.3. Polymerase chain reaction (PCR)

Firstly, all primer combinations were tested performing PCR with *Taq* DNA polymerase (Fermentas) to confirm primer specificity and the expected size of the amplification products. The composition of this reaction is shown in Table 9.

After validating the designed primers, two sets of PCRs were performed using a DNA polymerase with proofreading activity (*Pfu*; Fermentas): one to amplify small products (less than 100 bp), corresponding to the SP and CTE of AtPrx34 (PCR1), and another to amplify larger fragments (more than 1 kb), corresponding to the MP and MP-CTE of AtPrx34 (PCR2). The composition of the PCR reaction performed is shown in Table 10. The thermal cycling conditions used in the two sets of PCRs are shown in Tables 11 and 12.

Table 9. PCR reaction using *Taq* DNA polymerase.

PCR reagents	Volume (µL)
10x *Taq* with $(Nh_4^+)SO_4$ buffer	2,5
25 mM $MgCl_2$	2,5
DNA template[a] (1:20)	2
10 mM dNTPs (Fermentas)	1
10 µM *Primer*[b] fwd	2
10 µM *Primer*[b] rev	2
Taq DNA polymerase (Fermentas)	0.2
H_2O sterile	18.5
Final volume	**25**

[a] Mini prepr of AtPrx34 cDNA. b Fwd and rev primers were changed I order to amplify all the different AtPtx34 regions needed. PCR reactions were performed in 200 µL tubes in a Px2 Thermal Cycler (Thermo Electron Corporation).

Table 10. PCR reaction using *Pfu* DNA polymerase.

PCR reagents	Volume (µL)
10x Buffer *Pfu* with $MgSO_4$	5
DNA template[a] (1:20)	2
10 mM dNTPs	1
10 µM *Primer*[b] fwd	2
10 µM *Primer*[b] rev	2
Pfu DNA polymerase	0.5
H_2O sterile	37.5
Final volume	**50**

[a] Mini prepr of AtPrx34 cDNA. b Fwd and rev primers were changed I order to amplify all the different AtPtx34 regions needed. PCR reactions were performed in 200 µL tubes in a Px2 Thermal Cycler (Thermo Electron Corporation).

Table 11. PCR conditions used for amplification of the AtPrx34 SP and CTE.

	95ºC	**95 ºC**	**58 ºC**	**72 ºC**	**72 ºC**	***Hold* 6ºC**
Time	3 min	30 sec	40 sec	40 sec / 1 min [a]	5 min	∞
Number of cycles	1		35		1	

[a] When using *Pfu* DNA polymerase.

Table 12. PCR conditions used for amplification of the AtPrx34 MP and MP-CTE.

	95ºC	95 ºC	58 ºC	72 ºC	72 ºC	*Hold* 6ºC
Time	3 min	30 sec	40 sec	2 min / 3 min [a]	7min	∞
Number of cycles	1	35			1	

[a] When using *Pfu* DNA polymerase.

The amplification products from the AtPrx34 SP and CTE were separated on a 1.8 % agarose gel electrophoresis and were recovered using the GeneJET™ Gel extraction kit (Fermentas), according to the manufacturer's instructions. The amplification products from the AtPrx34 MP and MP-CTE were purified directly using the GeneJET™ PCR purification kit (Fermentas), according to the manufacturer's instructions.

All purified products were checked by 1.5% (w/v) agarose gel electrophoresis as already described (2.2.).

2.4.4. Cloning: restriction digestions and ligations

Restriction digestions were performed in both cloning vectors (pTH2 and pTH2-BN) and the purified amplification products, to prepare them for the ligation reactions.

Both expression vectors, pTH-2 and pTH2-BN, were double digested with *SalI* and *NcoI* to clone the SP1/SP2 of AtPrx34 at the N-terminus of GFP (Table 13). Digestion occurred for 3 h at 37ºC, and in the last hour of incubation 1 µL of calf intestine alkaline phosphatise (CiAP; Fermentas) was added to avoid religation of linearized pDNA by removing the 5'-phosphate from both *termini* of the vector. After this incubation time, 20 mM EDTA (pH 8.0) was added to stop the reaction, and enzymes were heat inactivated incubating at 65°C for 20 min.

Digestion of the AtPrx34 SP1 and SP2 was performed for 3 h at 37ºC (Table 14), followed by a 20 minute incubation at 65ºC to heat inactivate the restriction enzymes.

Table 13. Restriction reaction performed with the cloning vectors pTH-2 and pTH2-BN [a].

Reagents	Volume (µL)
Buffer Tango 2x	12
pDNA[a]	8
*Sal*I	4
*Nco*I	3
H_2O	33
Final volume	60

a The mixture was incubated for 1h at 37ºC. [a] Mini prep pDNA

Table 14. Restriction reaction performed with the AtPrx34 SP [a].

Digestion reagents	Volume (µL)
Buffer Tango 2x	15
DNA (PCR purified product)	20
*Sal*I	5
*Nco*I	2.5
H_2O	32.5
Final volume	75

a The mixture was incubated for 1h at 37ºC.

All the digested products were separated by agarose gel electrophoresis (2.2.), purified using the GeneJET™ Gel extraction kit (Fermentas), and checked again by agarose gel electrophoresis, to determinate the vector/insert ratio to use in the ligation reaction.

The ligation reaction was carried out for at least 4 h at RT and is described in Table 15.

Table 15. Ligation reactions performed in order to clone the AtPrx34 SP1/SP2 at the N-*terminus* of GFP in pTH2 and pTH2-BN.

Ligation reagents	pTH-2+SP (C2)	pTH-2 (-)	pTH2-BN+SP	pTH2-BN (-)
10x T4 DNA ligase buffer	1	1	1	1
pDNA	1	1	0,5	0,5
$SP1/SP2_{AtPrx34}$	3	-	3	-
T4 DNA ligase	1	1	1	1
H_2O sterile	4	7	4,5	7,5
Final Volume	10 (µL)	10 (µL)	10 (µL)	10 (µL)

(-) negative control without insert.

In order to clone the AtPrx34 CTE, MP and MP-CTE at the C-terminus of GFP in the pTH2-BN-$SP_{AtPrx34}$ background, both the construct (pTH2-BN-$SP_{AtPrx34}$) and the purified amplification products were double digested with *Bgl*II and *Xho*I, as described below (Tables 16 and 17). All the digested products were separated by agarose gel electrophoresis, purified using the GeneJET™ Gel extraction kit (Fermentas), and checked again by agarose gel electrophoresis, to determinate the vector/insert ratio to use in the ligation reaction. The ligation reaction was carried out for at least 4 h at RT and is described in Table 18.

Table 16. Composition of the restriction reaction performed to the cloning vector (pTH2-BN+SP) and the PCR purified inserts MP-CTE and MP [a].

Digestion reagents	Volume (µL)
Buffer Tango 2x (Fermentas)	12
DNA	8
*Bgl*I (Fermentas)	3
*Xho*I (Fermentas)	3
H_2O	34
Final volume	60

[a] The mixture was incubated for 1h at 37ºC.

Table 17. Composition of the restriction reaction performed to the purified CTE [a].

Digestion reagents	Volume (µL)
Buffer Tango 2x (Fermentas)	15
DNA	20
*Bgl*I (Fermentas)	3
*Xho*I (Fermentas)	3
H_2O	34
Final volume	75

[a] The mixture was incubated for 1h at 37ºC.

Table 18. Composition of the ligation reactions performed to clone the CTE, MP and MP-CTE of AtPrx34 at the C-terminus of GFP in pTH2-BN.

Ligation reagents	pTH2-BN+SP (-)	$C3_{AtPrx34}$	$C4_{AtPrx34}$	$C5_{AtPrx34}$
10x T4 DNA ligase buffer	1	1	1	1
pTH2-BN+SP	1	1	0,5	0,5
^{CTE} AtPrx34	-	4	-	-
^{MP} AtPrx34	-	-	3	-
$^{MP\text{-}CTE}$ AtPrx34	-	-	-	3
T4 DNA ligase (Fermentas)	1	1	1	1
H_2O sterile	7	3	4	4
Final Volume	10 (µL)	10 (µL)	10 (µL)	10 (µL)

(-) negative control without insert

2.4.5. Selection of positive clones

All ligation products were transformed into *E. coli* DH5α using the heat shock method (section 2.1.1.). A few colonies (at least 3) of each ligation product were selected to grow in 5 mL of LB medium supplemented with 150 µg/mL of ampicillin. After an ON incubation at 37ºC, at 200 rpm, the pDNA was purified from the bacterial culture by boiling prep. Bacterial pellets were obtained by centrifuging 3 mL of culture (2x1.5 mL in eppendorfs), at maximum speed (13000 rpm), for 3 min at RT (Centrifuge 5415 R, Eppendorf). The supernatant was discarded and the pellets were resuspended in 200 µL of sterile water. An equal volume of 2x STET [200 mM NaCl, 20 mM Tris (pH 7.5), 2 mM EDTA, 1% Triton (Sigma) with 20 µg/µL lysozyme (Sigma)] was added, the tubes were inverted and lysis occurred for no more than 5 min at RT. The tubes were boiled in a water bath for 60 sec and placed on ice to cool down. The samples were then centrifuged at 13000 rpm, for 10 min, at RT, and the pellet was removed with a sterile toothpick. One mL of cold isopropanol was added to the supernatant to precipitate the DNA, and the tubes were incubating at -20ºC for at least 20 min. This was followed by a centrifugation at 13000 rpm for 30 min at 4ºC. The supernatant were removed and the pellets were washed with 500 µL of cold 70% EtOH. The pellets were left to air-dry for 10-30 min, and were solubilised in 50 µL of sterile water.

Validation of clones was tested by restriction analysis with the enzymes shown in Table 19. RNase A (final concentration 0.1 mg/mL; Promega) was always added to the

reactions to digest contaminating RNA. Empty vectors (without respective inserts) were also restricted to act as negative controls, allowing the identification of positives clones.

Table 19. Composition of the digestion reaction performed to select the positive clones.

Digestion reagents	C2[a]	pTH2-BN with SP[b]	C3[c]	C4[c]	C5[c]
Buffer O	2	2	2	-	-
Buffer Tango 2x	-	-	-	4	4
DNA (Boiling prep)	2	2	2	2	2
***Sal*I**	1	1	1	-	-
***Eco*RI**	1	-	-	-	-
***Bgl*II**	-	1	-	1	1
***Xho*I (Fermentas)**	-	-	1.5	1	1
RNase A (0.1 mg/mL)	1	1	1	1	1
H_2O	13	13	12.5	11	11
Final volume	20 µL	20 µL	20 µL	20 µL	20 µL

[a]C1 was used as negative control for C2. [b] pTH2BN was used as negative control for pTH2-BN with SP. [c] pTH2-BN with SP was used as negative control for C3-C5. The mixtures were incubated for 1h at 37ºC.

For each construct, two positive clones were chosen in order to be sequenced (STAB Vida) and to check the absence of errors in the nucleotide sequence. pDNA to be sequenced was purified with the GeneJET™ Plasmid Miniprep Kit. Sequence homology analysis was performed using a multiple sequence alignment program, *MultiAlin*[1] (Corpet 1988). Again, for each construct, error-free clones were used for midiprep purifications of pDNA with the Plasmid Midi Kit (Qiagen) to obtain highly pure and concentrated DNA to transform protoplasts (section 2.3.).

[1] "Multiple sequence alignment with hierarchical clustering": http://multalin.toulouse.inra.fr/multalin/multalin.html

2.5. Isolation of *Arabidopsis* mesophyll protoplasts

Arabidopsis thaliana mesophyll protoplasts were prepared according to Yoo *et al.*, (2007) and the method is summarized in Figure 15.

Ten to twenty *Arabidopsis* leaves (fully expanded, corresponding to 1-2 plants) were cut into strips (0.5-1 mm wide) with a new sharp razor blade, over a Petri dish cover. The leaf strips were transferred into a Petri dish containing 10 mL of the freshly prepared enzyme solution [1.5% (w/v) cellulase Onozuka R10 (Duchefa), 0.4% macerozyme R10 (Serva), 0.4 M mannitol (Sigma), 20 mM KCl (Merck), 10 mM $CaCl_2.2H_2O$ (Merck), 20 mM MES (pH 5.7) - enzymes must dissolve slowly for at least 30 min, with gentle stir and in the dark]. Vacuum was applied on the open Petri dish for 15 min using an excicator and a vacuum pump, the Petri dish was sealed with Parafilm and was incubated for 2-3 h, at 28ºC, in the dark. After this time, the colour of the enzyme solution is expected to change, becoming greenish, due to protoplast release. More protoplasts were gently released from the leaf pieces with the help of a sawn-off plastic Pasteur pipette, and the suspension was filtered through a 100 μm nylon mesh into a new Petri dish. An additional volume of 2 to 3 mL of W5 solution [154 mM NaCl, 125 mM $CaCl_2.2H_2O$, 5 mM KCl, 2 mM MES (pH 5.7)] was added to the initial Petri dish in order to recover the maximum number of protoplasts.The filtrate was transferred into 15 mL Falcon tubes (no more than 8 mL/tube) and was centrifuged for 5 min at 600 rpm at RT in a clinical centrifuge (Compact Star CS4, VWR) to pellet the protoplasts. The supernatant was removed (the discarded supernatant contains broken cells and the enzymes that we want to get rid of) and cold W5 solution was added regenerating the original volume of enzymatic solution. The protoplasts were resuspended very gently, by inverting the tube very gently, were centrifuged again at 600 rpm for 5 min at RT, and gently resuspended in 5 mL of cold W5 medium. The protoplasts were kept on ice for 30 min, were again centrifuged at 600 rpm for 5 min at RT, and resuspended in MMg solution [0.4 M mannitol (Sigma), 15 mM $MgCl_2$ (Merck) and 4 mM MES (pH 5.7)] to a final concentration of $2x10^5$ cells/mL. At this stage the protoplasts were ready for PEG-mediated transformation.

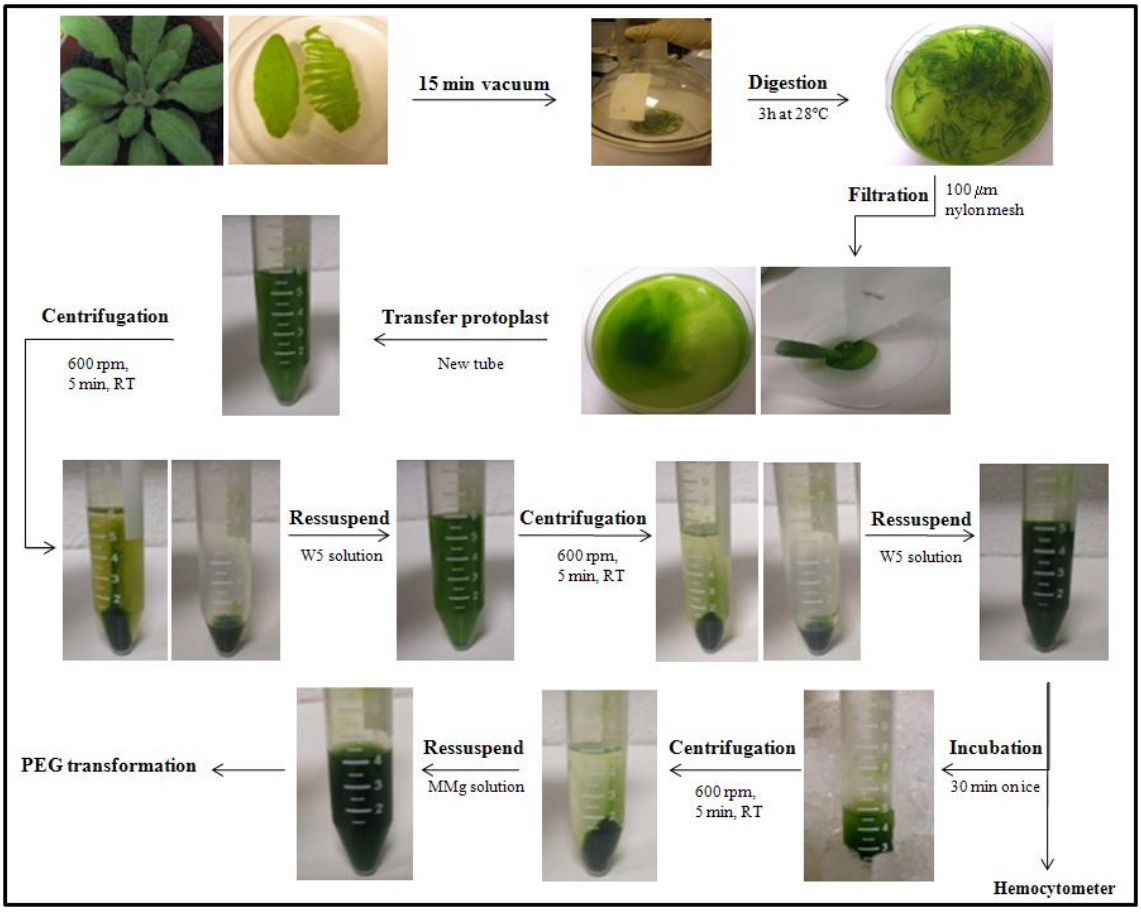

Figure 15. Isolation of *Arabidopsis* mesophyll protoplasts.

Protoplast concentration was determined using a hemocytometer, under the optical microscope (Figure 16). The hemocytometer chamber used was composed of 25 small squares with 0.1 mm^2 of area and 0.1 mm of height, therefore a volume capacity of 0.1 µL, and the total of the 25 squares corresponded to a volume of 2.5 µL. To determine the total number of protoplasts obtained, cells were counted in at least 5 squares, then the average number of cells per square was calculated and finally this number was used to extrapolate for the total area (25 squares=2.5 µL). To avoid overestimation of the total number of cells, two border lines were chosen to count cells, e.g. the upper and left hand side ones; the cells positioned over these lines were counted and considered to be inside the square, whereas cells on the bottom and right hand side lines were not taken into consideration. For routine experiments, 10–20 *Arabidopsis* leaves, i.e. 1-2 plants, digested in 10 mL of enzyme solution typically yielded 0.5-1x10^6

protoplasts, which is enough for up to 50 transformations ($2x10^4$ protoplasts/sample). It is essential to use plants that still have not differentiated the primary floral bud.

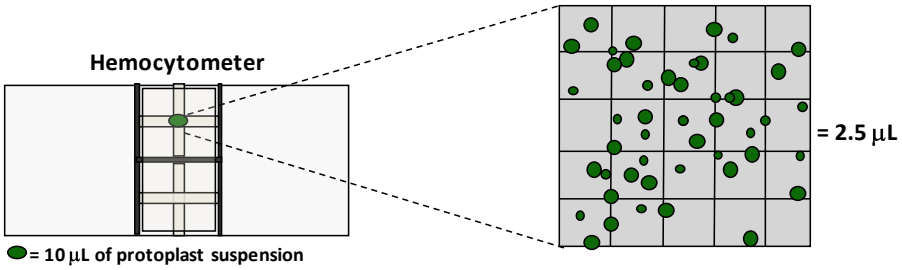

Figure 16. Representation of the hemocytometer used to count the cells.

The integrity of the isolated protoplasts was checked by observation under an optical microscope (Olympus Optical Microscope) and images were acquired by a coupled Olympus DP 25 Digital Camera and respective software (Cell B, Olympus). Image analysis was done with Adobe Photoshop CS3 software, and a set of images representative of all population was chosen.

2.6. Isolation of *C. roseus* mesophyll protoplasts

Catharanthus roseus mesophyll protoplasts were prepared according to Duarte et al. (2008), with some modifications (Figure 17). Ten to twenty young leaves of *C. roseus* (typically 2nd and 3rd pairs), to which the mid rib was removed, were cut into strips (1-2 mm wide) with a new sharp razor blade, over a Petri dish cover. The leaf strips were transferred into a Petri dish containing 20 mL of the freshly prepared enzyme solution [2% (w/v) cellulase Onozuka R10 (Duchefa), 0.3% macerozyme R10 (Serva) and 0.1% (v/v) pectinase (Sigma) - enzymes must dissolve slowly for at least 30 min, with gentle stir and in the dark] in TEX medium [0.32% (w/v) Gamborg's B5 medium (Duchefa), 5.1 mM $CaCl_2.2H_2O$, 0.4 M Sucrose (Merck) and 2.6 mM MES, with the pH adjusted to 5.6-5.8 with KOH] and were incubated ON, in the dark, at RT. On the following day, the Petri dishes were placed on an orbital shaker at 60-75 rpm, for 1h, in the dark. After this step, the colour of the enzyme solution becomes greenish due to the release of protoplasts. More protoplasts were gently released from the leaf pieces with the help of a sawn-off plastic Pasteur pipette, and the suspension was filtered through a 100 μm

nylon mesh into a new Petri dish. An additional volume of 3 mL of TEX medium was added to the initial Petri dish in order to recover the maximum number of protoplasts.

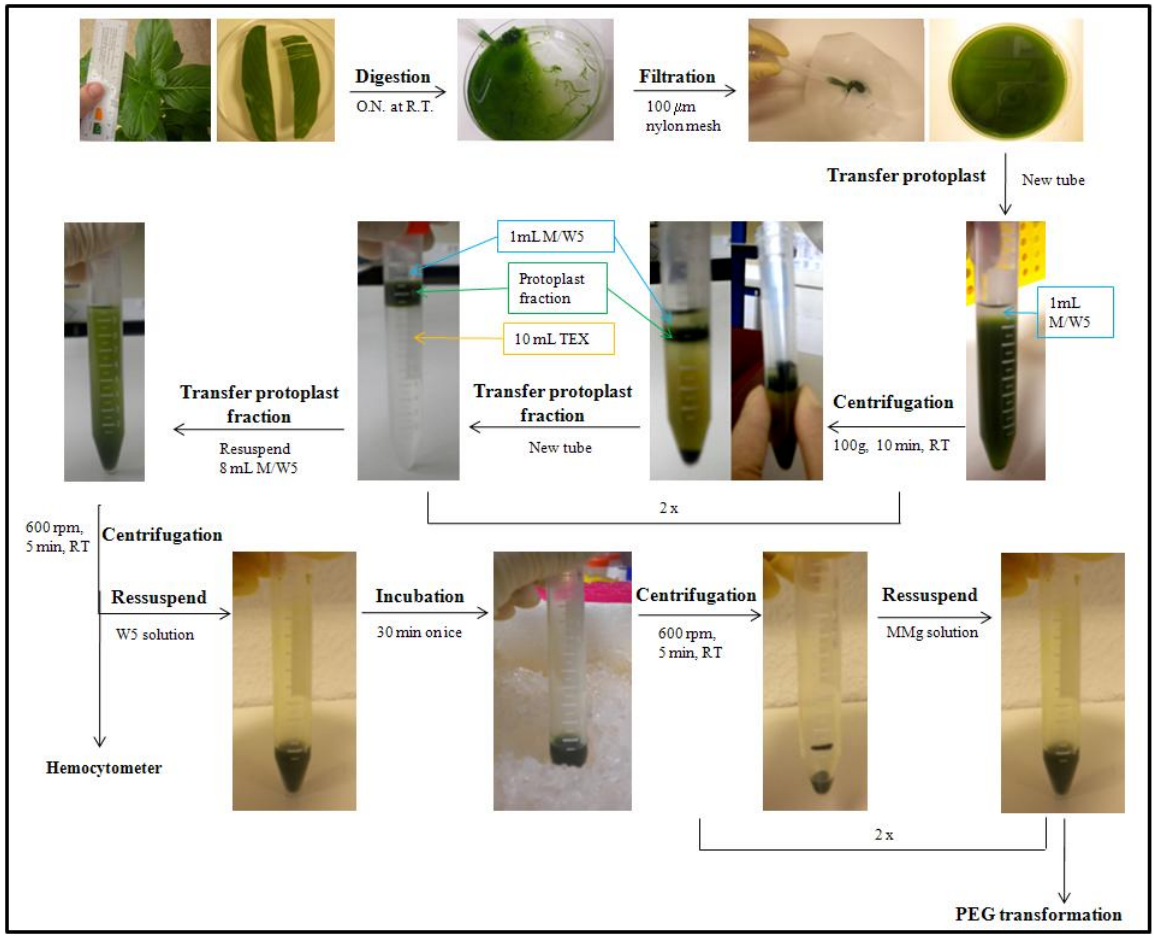

Figure 17. Isolation of *C. roseus* mesophyll protoplasts.

The filtrate was transferred into 15 mL Falcon tubes (no more than 8 mL/tube) and was overlaid with 1 mL of Mannitol/W5. Mannitol/W5 solution is composed of 0.32 M mannitol (Sigma), 1 mM D-glucose (Sigma), 30 mM NaCl, 25 mM CaCl2, 1 mM KCl and 0.3 mM MES; the pH must be adjusted to 5.6-5.8 with KOH. The tubes were then centrifuged at 100 g for 10 min at RT, in a swing-out rotor with minimal acceleration/deceleration (Centrifuge 3K15, Sigma). The living protoplast fraction was recovered from underneath the Mannitol/W5 layer and was transferred into new 15 mL Falcon tubes containing 10 mL of TEX medium. The protoplasts were overlaid with 1 mL of Mannitol/W5 and a new centrifugation followed, as above. The living protoplast fraction was collected and transferred into new 15 mL Falcon tube, this time containing 8 mL of Mannitol/W5 solution. The solution was gently mixed and the protoplasts were

centrifuged as above. The supernatant was removed without disturbing the pellet, deliberately leaving ~1 mL to carefully resuspend the protoplasts, by promoting gentle movements in the bottom of the tube. Protoplast concentration was determined using a hemocytometer under the optical microscope (section 2.5.). The protoplasts were resuspended in W5 to a final concentration of $2x10^5$ cells/mL. The protoplasts were kept on ice for 30 min, and were centrifuged for 5 min, at 600 rpm, at RT, in a clinical centrifuge. The supernatant was removed carefully without disturbing the pellet, the protoplasts were resuspended in the same volume of MMg solution at R.T. [0.4 M mannitol (Sigma), 15 mM $MgCl_2$ (Merck) and 4 mM MES (pH 5.7)]. This last step was repeated once more and the protoplasts were resuspended in MMg solution for a final concentration of $2x10^5$ cells/mL. At this stage the protoplasts are ready for PEG transformation. For routine experiments, 10–20 *C. roseus* leaves digested in 20 mL of enzyme solution typically yielded enough protoplasts for up to 50 transformations ($2x10^4$ protoplasts/sample).

The integrity of the isolated protoplasts was checked by observation under an optical microscope (Olympus Optical Microscope) and images were acquired by a coupled Olympus DP 25 Digital Camera and respective software (Cell B, Olympus). Bright field and fluorescence (UV filter) observations were also performed on a Zeiss Axio Imager Z1 inverted epifluorescence microscope. Images were captured with an Axiocam MR in automatic exposure mode, and processed with Axiovision 4.4 software. Image analysis was done with Adobe Photoshop CS3 software, and a set of images representative of all population was chosen.

2.7. PEG-mediated transformation of *Arabidopsis* and *C. roseus* protoplasts

Transformation of *Arabidopsis* and *C. roseus* mesophyll protoplasts was performed as described in Yoo *et al.*, 2007 with little modifications. Firstly, 10-20 μg of highly pure and concentrated plasmid DNA (1.5-2 μg/μL) were added to round-bottom 2 mL eppendorfs. Twenty μg of pDNA were used in all cases except when using C1 (empty vector) for which 10 μg of pDNA were enough to efficiently transform. One hundred μL ($2x10^4$ cells) of the protoplast suspension were added to the DNA containing tubes,were gently mixed, and 110 μL of polyethylene glycol (PEG) solution [40% (w/v)

PEG 4000 (Sigma), 0.2 M mannitol and 0.1 M $CaCl_2$) were slowly added (drop by drop), gently flicking the tube after each drop. To control the effect of PEG on the survival rate of protoplasts, two controls were made, one with protoplasts only, and another with protoplasts and PEG without DNA .

The transformation mixture and the two controls were incubated for 15 min at RT, and after this, 440 µL of W5 solution were added. The tubes were centrifuged at 600 rpm for 2 min (acc/dec 1; Universal 320R Centrifuge, Hettich), the supernatant was removed, and the pellet was resuspended in 100 µL of W5 solution. The samples were then transferred to new 15 mL falcon tubes containing 900 µL of W5 and were incubated in the dark at 25ºC for ~ 2 days (40 h) with the tubes in an angle. Before observation under the confocal microscope, cells were subjected to a 3 h pulse at 35ºC since this proved to increase GFP expression or fluorescence.

2.8. Confocal Laser Scanning Microscopy (CLSM) analysis of the transformed protoplasts

The expression and localization of GFP in transformed protoplasts was monitored by observation under the confocal microscope (SP2 AOBS SE, Leica Microsystems) with an excitation wavelength of 488 nm and an emission wavelength of 522±16 nm. Chloroplast autofluorescence under blue light excitation was also registered at an emission wavelength ranging from 650 to 700 nm. Image analysis was done with Adobe Photoshop CS3 software's, and a set of images representative of the whole population was chosen for each construct.

The survival and transformation efficiency rates of the protoplasts subjected to PEG-mediated transformation was registered for both species, for the C1 construct (pTH2). An average of all experimental data (~8 individual experiments) was used for the determination of both rates in *Arabidopsis* protoplasts. For *C. roseus* protoplasts this statistical analysis was conducted attending to a single experiment performed in April and June, due to the seasonality of this plant.

2.9. *Agrobacterium*-mediated transformation by leaf infiltration

Two methodologies were employed in order to perform *Agrobacterium*-mediated transformation of *Arabidopsis* and *C. roseus* leaves. The first consisted of a simple method that is ordinarily used to Agro-infiltrate tobacco leaves using an $MgCl_2$ infiltration buffer. The second was a slightly different approach described in Di Fiore *et al.* (2004) to which we have done some modifications.

In the first method, 8 mL of LB medium supplemented with the appropriate antibiotics was inoculated with the *A. tumefaciens* clones of interest and the cultures were grown ON at 28ºC with vigorous agitation (200 rpm) until reaching an $O.D._{600nm}$ of 1.5 – 2 (stationary phase). Three mL of culture were centrifuged at 13000 rpm, for 3 min, at RT, the supernatant was discarded, and the bacterial pellet was resuspended in $MgCl_2$ infiltration buffer (10 mM $MgCl_2$ and 10 mM MES, pH 5.6) with 100 µM acetosyringone. An $O.D._{600nm}$ of 0.6-0.8 was used to perform the infiltration. Infiltration was done using a syringe (without needle) and pressing it against the abaxial leaf epidermis (lower epidermis) of the leaves (Figure 18 A). The plunger was then pushed down gently, while supporting the adaxial side of the leaf with a finger. The *A. tumefaciens* cell suspension diffuses through the leaf as it fills the extracellular air spaces. Noninfiltrated leaves were used as negative control. In the case of *Arabidopsis*, most of the leaves in the rosette were infiltrated (Figure 18, A to C). For *C. roseus*, only the first and the second pair of leaves from adult plants were used to infiltrate (Figure 18, D and E). For both cases infiltration was always performed *in planta*. The infiltrated plants were incubated for 48h, at 21ºC, under a 16 h photoperiod, prior to observation under the confocal microscope.

In the second protocol, which was based on the method published by Di Fiore et al. (2004), the *A. tumefaciens* clones were grown in selective 100 mL YEB medium, ON, at 28ºC, with agitation (200 rpm), until the $O.D._{600nm}$ reached ~0.8. The suspension was centrifuged and the bacteria were resuspended in MMA [0.43% (w/v) Murashige and Skoog basic salt mixture (Duchefa), 10 mM MES (pH 5.6), 2% (w/v) sucrose and 200 µM acetosyringone)] to an $O.D._{600nm}$ of ~2 to 2.4. The *Agrobacterium* suspension was kept at 22°C, stirring at <75 rpm, for 1h, to induce virulence, and was then used for infiltration. Two methods of infiltration were used: with a syringe (described above), and applying vacuum. *Arabidopsis* and *C. roseus* leaves (adult leaves

and seedlings) were syringe infiltrated as described above (Figure 18, A to H). In this case, leaves from *in vitro* regenerated *C. roseus* plants were also infiltrated (Figure 18, I to K). The infiltration was performed *in planta* and on detached leaves, using the seringe approach. When vacuum infiltration was performed, young *C. roseus* leaves (first and second pairs) from adult plants and seedlings, as well as leaf discs (1 cm ∅; Figure 19), were submerged and incubated for 25 min under a constant negative pressure (100 mbar) generated by a vacuum pump. Following infiltration, the leaves were briefly washed in water and dried on paper to remove excess liquid. The leaves were then placed on wet Whatman paper in plastic sterile Petri dishes, sealed, and incubated for 48 h at 21ºC under in the dark. In all cases non-infiltrated leaves were used as negative controls (Figure 19).

Figure 18. Agro-infiltration of *Arabidopsis* and *C. roseus* leaves using a syringe. A to C. Infiltration of *Arabidopsis* leaves. D and E. Infiltration of *C. roseus* leaves. F. Infiltrated *C. roseus* leaves detached from the plant. G and H. Infiltration of *C. roseus* seedlings. I to K. Infiltration of *C. roseus in vitro* regenerated plants. Arrows indicate infiltrated regions.

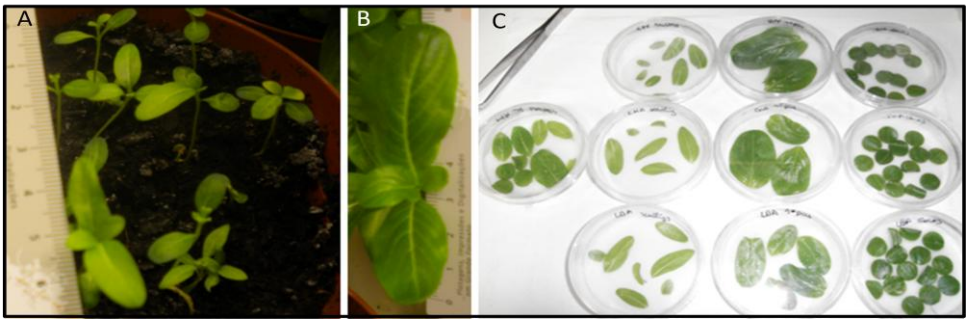

Figure 19. Agroinfiltration of *C. roseus* leaves using vacuum. A. Seedlings. B. 1st and 2nd leaf pairs of an adult plant. C. Detached leaves and leaf discs obtained from the 2nd pair of leaves of *C. roseus* adult plants, in the Petri dishes used for vacuum infiltration.

2.10. Confocal Laser Scanning Microscopy (CLSM) analysis of the infiltrated leaf regions

The expression and localization of GFP in Agro-infiltrated leaves was monitored by observation of fresh hand-cut sections of the leaves under the confocal microscope (SP2 AOBS SE, Leica Microsystems) as described for transformed protoplasts (2.8.).

Results

3. Results

3.1. Confirmation of the CrPrx1-GFP fusions

CrPrx1 is the main Prx expressed in the leaves of *C. roseus*, and its vacuolar sorting has been previously characterized using several CrPrx1-GFP fusions (M. M. R. Costa et al. 2008), Table 4 in section 2.2.).

In this work, these CrPrx1-GFP fusions were used as positive controls to validate the optimization of transient expression protocols. Since the cloned constructions hadn't been used for some time, they were checked for plasmid DNA (pDNA) integrity and for the presence and identity of the different constructs, by restriction analysis followed by agarose gel electrophoresis (Figure 20).

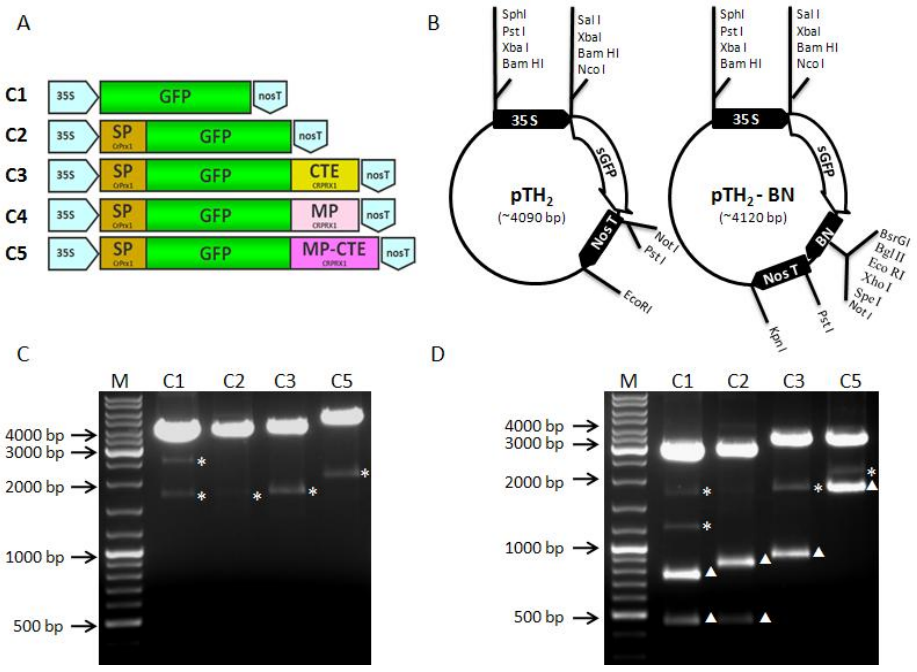

Figure 20. Schematic representations and restriction analysis of the CrPrx1-GFP fusions. A. Schematic representation of the CrPrx1-GFP constructs. B. Schematic representation of the cloning vectors, pTH2 and pTH2-BN, depicting the most relevant restriction sites and the 35S promoter, sGFP and Nos terminator regions. C. Agarose gel electrophoresis showing the plasmids bearing the different cosntructs linearized with *Sal*I. The lower molecular weight bands (asterisks) correspond to undigested plasmid and can also be seen in D. D. Agarose gel electrophoresis showing the restriction analysis of the same plasmids as in C. C1 and C2 were double digested with *Sal*I and *Pst*I excising the 35S promoter (~400bp) and sGFP (~750bp) for C1, and the 35S promoter (~400bp) and SP-GFP (~850bp) for C2 (arrowheads). C3 and C5 were double digested with *Sal*I and *Xho*I releasing SP-GFP-CTE (~950bp) for C3 and SP-GFP-MP-CTE (~1500bp) for C5 (arrowheads). M – Molecular weight marker, GeneRuler^{TM} DNA Ladder Mix (Fermentas). 1.5 % agarose gels.

*Sal*I was used to linearize all plasmids (Figure 20C), and no major differences were observed between C1, C2 and C3 (~4 kb) since these differ from one another only in ca. 100 bp. C2 contains the SP_{CrPrx1} (~100 bp) absent in C1, while C3, relatively to C2, additionally possesses the CTE_{CrPrx1} (and BN linker). C5 is perfectly distinguishable from all the others because it includes the complete sequence of CrPrx1, therefore having 1 kb more than the remaining constructs (~5 kb). Double digestions confirmed further the identity of each construct (Figure 20D). Restriction with *Sal*I and *Pst*I released the 35S promoter (~400 bp) and sGFP (~750 bp) for C1, and the 35S promoter (~400 bp) and SP-GFP (~850 bp) for C2, as expected. Restriction with *Sal*I and *Xho*I released SP-GFP-CTE (~950bp) for C3, and SP-GFP-MP-CTE (~1500 bp) for C5, also as expected. Extra bands in Figure 20C and 20D (asterisks) correspond to uncut plasmid DNA. The C4 construct was not subjected to restriction analysis, although its integrity was confirmed by agarose gel electrophoresis (Figure 21A).

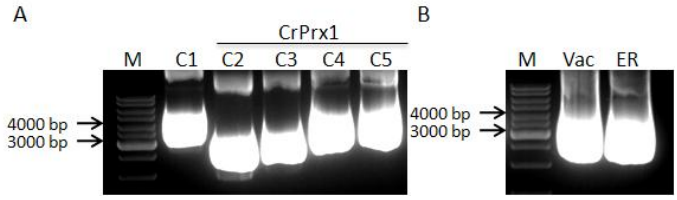

Figure 21. Agarose gel electrophoresis of all pDNAs used for protoplast transformation. A. pTH2 empty vector (C1) and CrPrx1-GFP fusions (C2-C5). B. Vacuolar (Vac) marker construct (35S::SP_{CrPrx1}-GFP-$CTTP_{Phaseolin}$) and ER (ER) marker construct (35S::SP_{CrPrx1}-GFP-KDEL**)**. M – Molecular weight marker, GeneRuler^{TM} DNA Ladder Mix (Fermentas). In both cases, 2 µL of each sample were loaded onto 1.5 % agarose gels.

Figure 21 shows all the constructs used for protoplast transformation after midiprep purification using the QIAGEN Plasmid Midi Prep kit. Uncut DNA is not reliable to estimate the molecular weight of the isolated pDNA, however all plasmids ran accordingly to their relative size, with exception to C1 construct that should have had an inferior position in relation to all the others. This unexpected *location* of C1 may be related with a specific conformation on the pDNA molecule, since when linearized it showed the expected relative position (Figure 20C). Figure 21B shows two additional control constructs used in this work, also after midiprep isolation. One is a vacuolar marker and corresponds to SP_{CrPrx1}-GFP-$CTPP_{phaseolin}$ (unpublished data), the other targets GFP to the ER and corresponds to SP_{CrPrx1}-GFP-HDEL (unpublished data). Both markers were in pTH2-BN.

3.2. Generation of the AtPrx34-GFP fusions

AtPrx34 (At3g49120; GenBank accession no. NM_114771) is the main Prx activity present in *A. thaliana* leaves (Carqueijeiro 2008) and, in order to investigate its subcellular localization, several AtPrx34-GFP fusions were generated here. The full cDNA sequence of AtPrx34 showing the different putative regions, SP, MP and CTE, as well as the location of the primers used for construct generation are represented in Figure 22.

In order to determine the AtPrx34 SP sequence to be used in the GFP fusion constructs, we used the program SignalP 3.0 server[2] (Emanuelsson et al. 2007). The program identified the AtPrx34 SP at the N-terminal region of the protein, and predicted the cleavage site for the signal peptidase to be located between position 29 and 30 (LSA-AQ; Figure 22B). Prediction of the AtPrx34 CTE to be used in the fusion constructs was done by analyzing the multiple alignments of the deduced amino acid sequences corresponding to the 73 Prx genes identified in the *Arabidopsis* genome [Figure 22C; (Welinder et al. 2002)]. The CTE region was chosen to start three amino acids after the last conserved cysteine (C) residue (Figure 22A, yellow box), one amino acid upstream the site predicted by Welinder et al. 2002 (Figure 22C) .

The next step was to design specific primers to amplify the selected AtPrx34 domains to be fused with GFP. Primers were designed in order to include restriction sites to be used for the directional cloning of all AtPrx34 domains, and their annealing sites are represented in Figure 22A (coloured boxes). Two SP sequences were chosen: a shorter one (SP1) that ended immediately after the predicted cleavage site (on the aa glutamine - Q; Figure 22A, light blue box), and a longer one (SP2) that ended further downstream (Figure 22A, navy blue box). The SP2 was used later in the work and after poor results with SP1. The idea was to ensure recognition of the SP2 sequence by the endopeptidase by including extra downstream amino acids.

[2]SignalP 3.0: **http://www.cbs.dtu.dk/services/SignalP/**

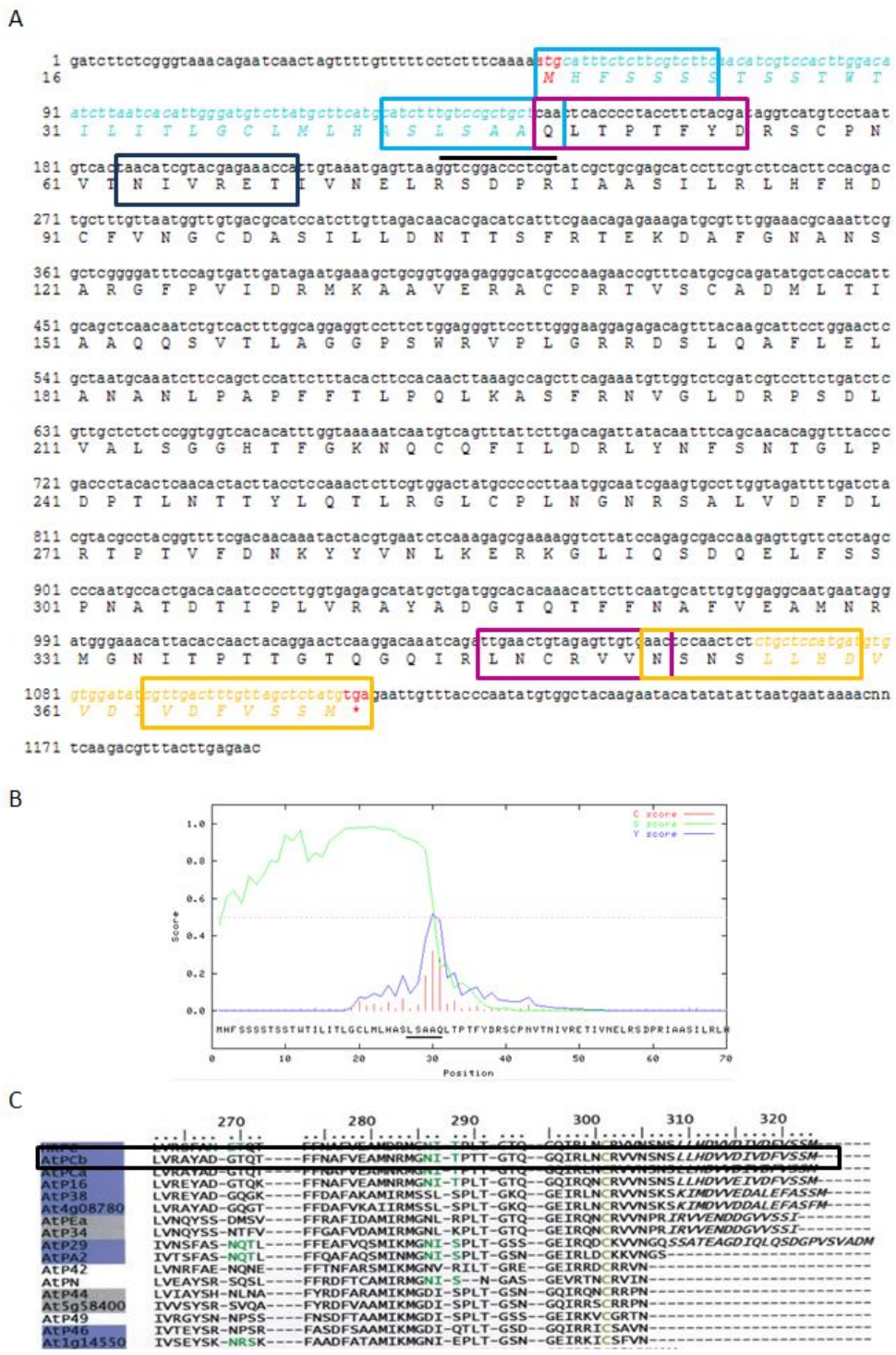

Figure 22. Coding sequence and deduced translated protein sequence of AtPrx34, the main Prx in *A. thaliana* leaves. A. Coding sequence and deduced amino acid sequence for AtPrx34. The predicted SP sequence in is blue and the predicted CTE sequence is in yellow. Coloured boxes mark the annealing sites of all primers used: light blue for SP (navy blue for SP2), pink for MP and yellow for CTE. The underlined sequence marks the predicted cleavage site of the SP. B. Prediction of the AtPrx34 SP region and cleavage site using the SignalP 3.0 program. C. Multiple alignment of the C-terminal regions of the deduced amino acid sequences of several *Arabidopsis* class III peroxidases. The box marks the AtPrx34 sequence, previously named AtPCb. The CTE regions are in italic and are thought to be absent in the mature proteins. Adapted from Welinder et al. 2002.

Before proceeding with amplifications and ligations, the several plasmids were analysed by restriction digestion. The ATPrx34 cDNA was obtained commercially and it had been cloned into a pRAFL03 vector (Figure 23A) with approximately 3.0 kb, with the insert corresponding to the AtPrx34 having approximately 1.3 kb. This clone was linearized with *Xho*I and generated a single band with the expected size of ca. 4.3 kb. The expression vectors pTH2 and pTH2-BN (Figure 24A) were digested with *Pst*I, and, as expected, these restrictions released a fragment of ~1200 bp corresponding to 35S::GFP, and a fragment of ~1250 bp corresponding to 35S::GFP-BN linker, respectively (Figure 24B).

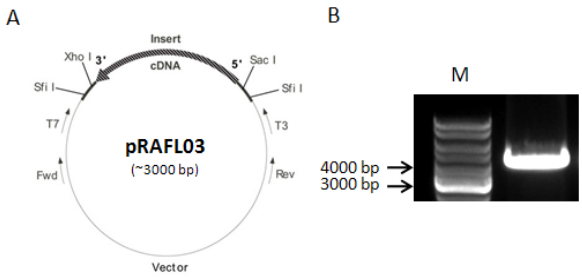

Figure 23. Restriction analysis of the original clone containing the complete cDNA of AtPrx34. A. Schematic representation of vector pRAFL03. B. pRAFL03-AtPrx34 individual clones digested with *Sal*I. A single band with ~4.3 kb was observed. M – Molecular weight marker, GeneRuler^{TM} DNA Ladder Mix (Fermentas). 1.5 % agarose gel.

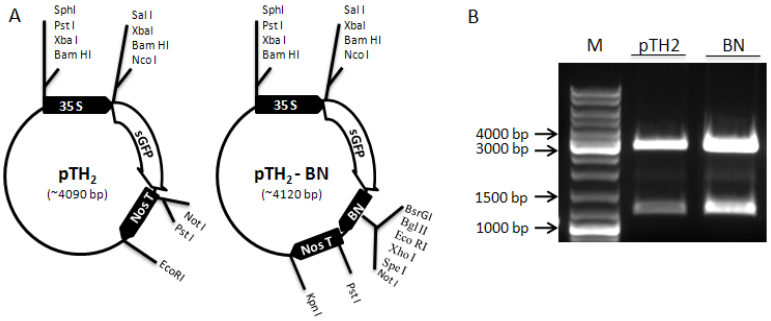

Figure 24. Restriction analysis of the expression vectors pTH2 and pTH2-BN. A. Schematic representation of pTH2 and pTH2-BN, depicting the most relevant restriction sites and the 35S promoter, sGFP and Nos terminator regions. B. Individual clones of pTH2 and pTH2-BN digested with *Pst*I, releasing a fragment of 1.2 kb (35S::GFP) for pTH2, and 1.25 kb (35S::GFP-BN linker) for pTH2-BN. M – Molecular weight marker, GeneRuler^{TM} DNA Ladder Mix (Fermentas). 1.5 % agarose gel.

The complete AtPrx34 cDNA (in pRAFL03) was used as template to amplify the SP, CTE, MP and MP-CTE regions, by PCR. First of all, the specificity of the designed primers was tested by PCR using a *Taq* DNA polymerase to amplify the fragments. The resulting PCR products were ran on an agarose gel and can be observed

in Figure 25. All primer combinations gave products with the expected molecular weight: ~100 bp for the SP and ~60 bp for the CTE in Figure 25A), ~1100 bp for the full CDS, ~900 bp for the MP and ~980 bp for the MP-CTE in Figure 25B.

To generate the AtPrx34 fragments to be used in the constructs, a *Pfu* DNA polymerase was used. The main difference between *Pfu* and alternative enzymes, like *Taq* DNA polymerase, is that *Pfu* has superior thermostability and , 3' to 5' exonuclease proofreading activity correcting for nucleotide-misincorporation errors, resulting in PCR fragments with fewer errors Agarose gel electrophoresis of the PCR fragments generated with *Pfu* and used for insertion are shown in figure 26.

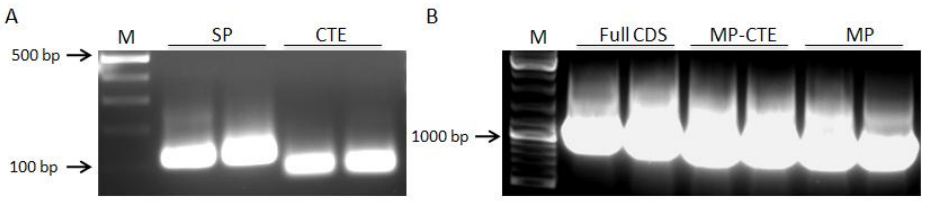

Figure 25. PCR amplification of the selected AtPrx34 regions using *Taq* DNA polymerase (Fermentas). All observed bands had the expected molecular weight. A. SP ~100 bp and CTE ~60 bp. 1.5% agarose gel. B. Full CDS ~1100 bp, MP-CTE ~950 bp and MP ~900 bp. 1.0 % agarose gel. M – Molecular weight marker, GeneRuler^{TM} DNA Ladder Mix (Fermentas).

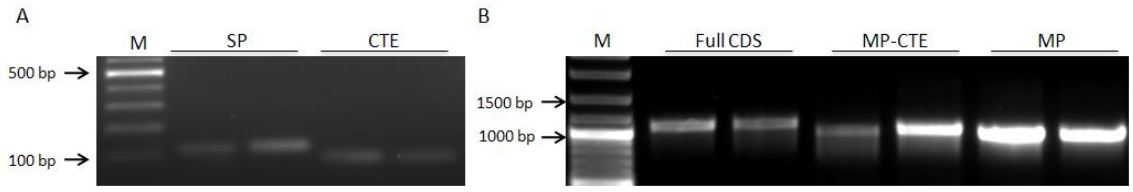

Figure 26. PCR amplification of the selected AtPrx34 regions using *Pfu* DNA polymerase (Fermentas). All observed bands had the expected molecular weight. A. SP ~90 bp and CTE (~60 bp). 1.5% agarose gel. B. Full CDS (~1100 bp), MP-CTE (~950 bp) And MP (~900 bp). 1.0 % agarose gel. M – Molecular weight marker, GeneRuler^{TM} DNA Ladder Mix (Fermentas).

For the cloning of the SP1 of AtPrx34, the corresponding fragment and the expression vectors pTH2 and pTH2-BN were digested with *Sal*I and *Nco*I, were purified, and ran on an agarose gel (Figure 27). Ligation of $SP1_{AtPrx34}$ and pTH2 generated the construct 35S::$SP1_{AtPrx34}$-GFP. Ligation between $SP1_{AtPrx34}$ and pTH2-BN generated the backbone construct that allowed further insertions at the C-terminus of GFP.

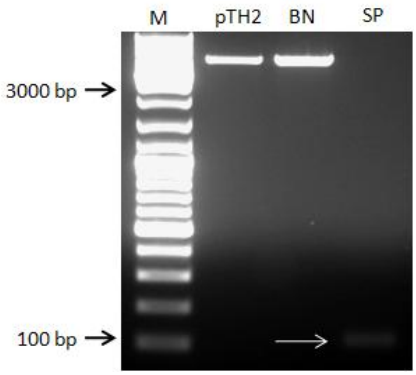

Figure 27. Preparative agarose gel electrophoresis for the ligation reactions between $SP1_{AtPrx34}$ and the expression vectors pTH2 and pTH2-BN. All DNAs were previously digested with *Sal*I and *Nco*I and purified. 2 µL of each vector (pTH2 and BN) and 4 µL of $SP1_{AtPrx34}$ (arrow) were loaded on the gel. M – Molecular weight marker, GeneRuler^{TM} DNA Ladder Mix (Fermentas). 1.5% agarose gel.

The ligation products were used to transform *E. coli* DH5α cells and pDNAs were extracted from 3 selected colonies and were digested either with *Sal*I and *Eco*RI for pTH2-$SP1_{AtPrx34}$ (Figure 28A), or with *SalI* and *BglII* for pTH2-BN-$SP1_{AtPrx34}$ (Figure 28B). Confirmation of positive clones could have been performed with *Sal*I and *Nco*I to excise the insert, however due to its reduced size (~100 bp) its observation would not have been easy. Therefore, we decided to cut empty pTH2 and pTH2-$SP1_{AtPrx34}$ (C2 or $SP1_{AtPrx34}$-GFP) with *Sal*I and *Eco*RI, which excise respectively a fragment of ~1.0 and ~1.1 kb, corresponding to +-$SP1_{AtPrx34}$ (~100 bp)+GFP (~750 bp)+nos terminator (~250 bp), run these together, and identify the positive clones by a ~100 bp difference between the two excised fragments. Among all positive clones (not all are shown), clones 23 and 24 were selected to be sequenced (Figure 28A).

The same strategy was followed to identify positive pTH2-BN- $SP1_{AtPrx34}$ clones, but using *Sal*I and *Bgl*II . This digestion excises a fragment of ~850 bp corresponding to $SP1_{AtPrx34}$ (~100 bp)+GFP (~750 bp), again with more 100 bp than the empty vector. Among positive clones, clones 1 and 2 were selected to be sequenced (Figure 28B).

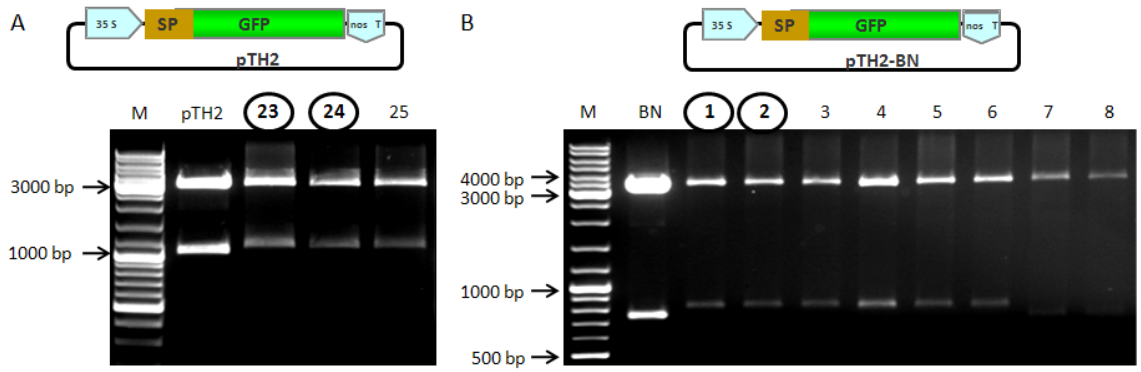

Figure 28. Restriction analysis of the clones obtained after ligation between SP1$_{AtPrx34}$ and the expression vectors pTH2 and pTH2-BN. A. Schematic representation of the SP1$_{AtPrx34}$-GFP construct (top) and restriction analysis of the pTH2-SP1$_{AtPrx34}$ clones with *Sal*I and *Eco*RI (bottom).The lane marked with pTH2 corresponds to the digestion of the empty vector. All the represented clones are positive, which is translated by the presence of a band with 1.1 kb. B. Schematic representation of the SP1$_{AtPrx34}$-GFP BN construct (top) and restriction analysis of the pTH2-BN-SP1$_{AtPrx34}$ clones with *Sal*I and *Bgl*II (bottom) .The lane marked with BN corresponds to a digestion of the empty vector. Positive clones were identified by the presence of a band with ~850 bp. M – Molecular weight marker, GeneRuler^{TM} DNA Ladder Mix (Fermentas). 1.5% agarose gels.

Sequencing of the selected clones revealed a perfect match between query and original sequence (Figure 29).

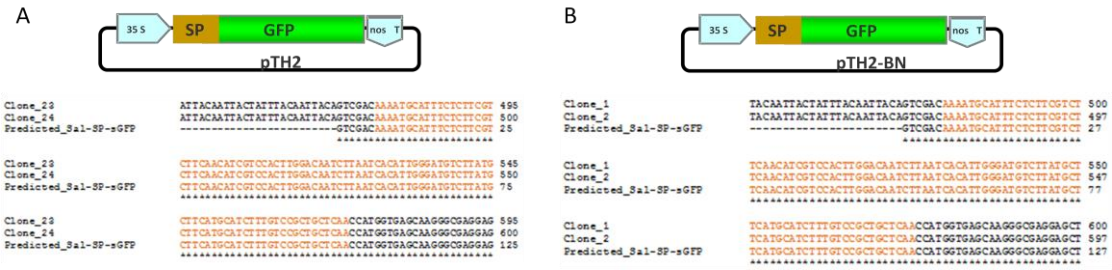

Figure 29. Alignment between the SP1$_{AtPrx34}$ sequence and sequences obtained for the generated clones. A. Schematic representation of the SP1$_{AtPrx34}$-GFP construct (top) and alignments (bottom). Alignments were performed with the sequences obtained for clones 23 and 24 from Figure 28A. B. Schematic representation of the SP1$_{AtPrx34}$-GFP BN construct (top) and alignments (bottom). Alignments were performed with the sequences obtained for clones 1 and 2 from Figure 28B. Asterisks (*) represent perfect matches. SP sequence is marked in brown. Sequencing reactions were performed with primer M13Fwd, that anneals with both expression vectors upstream the 35S promoter region.

At this point we had successfully obtained our SP1$_{AtPrx34}$-GFP construct (C2) and the backbone to clone the AtPrx34 CTE, MP and MP-CTE regions, downstream to the GFP sequence. For the cloning of the CTE, MP and MP-CTE, all the obtained fragments and pTH2-BN-SP1$_{AtPrx34}$ were digested with *Bgl*II and *Xho*I, were purified and ran on an agarose gel (Figure 30).

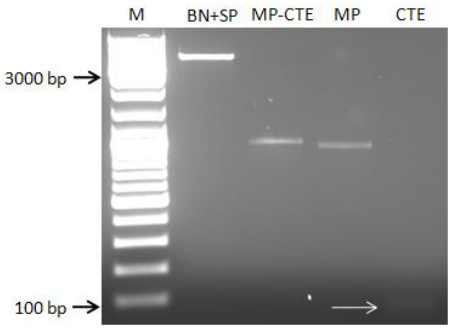

Figure 30. Preparative agarose gel electrophoresis for the ligation reactions between CTE, MP and MP-CTE of AtPrx34 and the backbone pTH2-BN-SP1$_{AtPrx34}$. All DNAs were previously digested with *Bgl*II and *Xho*I and purified. 2 µL of the vector (BN+SP), MP and MP-CTE, and 4 µL of CTE (arrow) were loaded on the gel. M – Molecular weight marker, GeneRuler^{TM} DNA Ladder Mix (Fermentas). 1.5% agarose gel.

Ligations of pTH2-BN-SP1$_{AtPrx34}$ and the CTE, MP and MP-CTE regions of AtPrx34 were performed as above, and ligation reaction products were used to transform *E. coli* DH5α cells. Confirmation of positive clones for SP1$_{AtPrx34}$-GFP-CTE construct, for the same reasons as stated for the previous ligation reactions, was performed by digestion with *Sal*I and *Xho*I leading to excision of a fragment of ~900 bp [SP1$_{AtPrx34}$ (~100 bp)+GFP (~750 bp)+CTE (~60 bp)], with more 60 bp than the fragment excised from the backbone construct pTH2-BN-SP1$_{AtPrx34}$.. Results are shown in Figure 31A. Among all positive clones (not all are shown), clones 8 and 16 were selected to be sequenced and revealed a perfect match between query and the original sequence (Figure 32A).

Confirmation of positive clones for the SP1$_{AtPrx34}$-GFP-MP construct was performed digesting with *Bgl*II and *Xho*I, which led to the excision of the inserted fragment (MP$_{AtPrx34}$) with ~900 bp. Results are shown in Figures 31B and clones 4 and 10 were selected to be sequenced. Sequencing of the selected clones revealed a perfect match between query and the original sequence (Figure 32B).

Confirmation of positive clones for the SP1$_{AtPrx34}$-GFP-MP-CTE construct was performed digesting also with *Bgl*II and *Xho*I, which led to the excision of the inserted fragment (MP-CTE$_{AtPrx34}$) with ~950 bp. Results are shown in Figures 31C and clones 10 and 17 were selected to be sequenced (Figure 32C). For both cases the same digestion was performed with the backbone construct and, as expected, no visible band was excised. The agarose gel shown in Figure 31C had to be stained after the run and this resulted in a less effective DNA labelling by the EtBr. In some lanes it was not possible to accurately confirm the presence of the insert MP-CTE (lanes 2 and 3), but in most cases the band corresponding to MP-CTE was undoubtedly present. For the last

two constructs, sequencing of the selected clones also revealed perfect matches between queries and original sequences (Figure 32C).

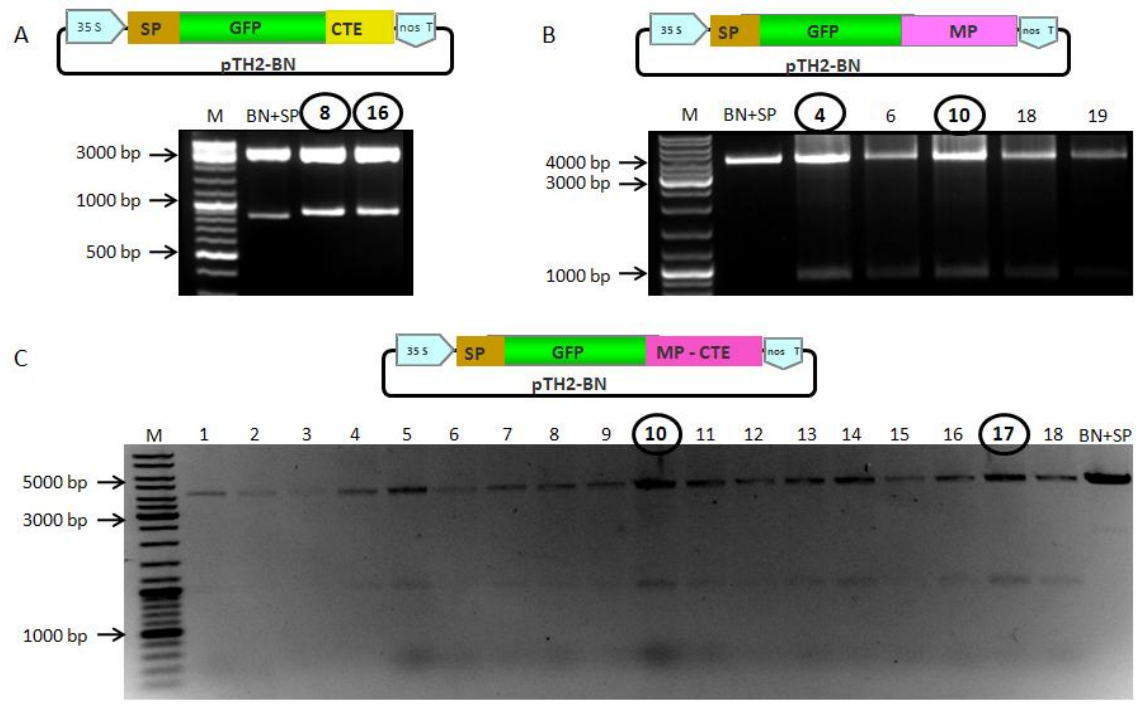

Figure 31. Restriction analysis of the clones obtained after ligation between pTH2-BN-SP1$_{AtPrx34}$ and the CTE, MP and MP-CTE regions of AtPrx34. A. Schematic representation of the SP1$_{AtPrx34}$-GFP-CTE construct (top) and restriction analysis of the pTH2-SP1$_{AtPrx34}$-GFP-CTE clones with *Sal*I and *Xho*I (bottom). All the represented clones are positive, which is translated by the presence of a band with ~900 bp. 1.5% agarose gel. B. Schematic representation of the SP1$_{AtPrx34}$-GFP-MP$_{AtPrx34}$ construct (top) and restriction analysis of the pTH2-SP1$_{AtPrx34}$-GFP-MP$_{AtPrx34}$ clones with *Bgl*II and *Xho*I (bottom). All the represented clones are positive, which is translated by the presence of a band with ~900 bp corresponding the MP$_{AtPrx34}$ fragment. C. Schematic representation of the SP1$_{AtPrx34}$-GFP-MP-CTE$_{AtPrx34}$ construct (top) and restriction analysis of the pTH2-SP1$_{AtPrx34}$-GFP-MP-CTE$_{AtPrx34}$ clones with *Bgl*II and *Xho*I (bottom). All the represented clones are positive, which is translated by the presence of a band with ~950 bp corresponding the MP-CTE$_{AtPrx34}$ fragment. 1.5% agarose gels. Lanes marked with BN+SP correspond to digestions of the backbone construct. M – Molecular weight marker, GeneRuler^{TM} DNA Ladder Mix (Fermentas).

Figure 32. Alignment between the predicted CTE$_{AtPrx34}$ / MP$_{AtPrx34}$ / MP-CTE$_{AtPrx34}$ sequence and the generated clones. A. Schematic representation of the SP1$_{AtPrx34}$-GFP-CTE$_{AtPrx34}$ construct (top) and alignments (bottom). Alignments were performed with the sequences obtained for clones 8 and 16 from Figure 31A. Sequencing reactions were performed with custom primer sGFP-Fwd that anneals with sGFP. B. Schematic representation of the SP1$_{AtPrx34}$-GFP-MP$_{AtPrx34}$ construct (top) and alignments (bottom). Alignments were performed with the sequences obtained for clones 4 and 10 from Figure 31B. Sequencing reactions were performed with custom primer sGFP-Fwd and complemented custom primer AtPrx34-Fwd that anneals within AtPrx34 mature protein. C. Schematic representation of the SP1$_{AtPrx34}$-GFP-MP-CTE$_{AtPrx34}$ construct (top) and alignments (bottom). Alignments were performed with the sequences obtained for clones 10 and 17 from Figure 31C. Sequencing reactions were performed with custom primer sGFP-Fwd and complemented custom primer AtPrx34-Fwd. Asterisks (*) represent perfect matches. All inserts sequences are marked in the same color as portrayed in the schematic representation of he constructs. Nucelotides in grey represent the vectors sequence. Between the inserts sequence and te vectors sequence are the restrion enzymes sequence.

Molecular cloning of AtPrx34-GFP fusions, SP2

Although there were no apparent problems with neither of the constructs generated for AtPrx34, the fact was that regardless of the construct, GFP fluorescence was always observed in the cytoplasm (section 3.5.2., Figure 49). This led us to speculate that maybe the SP was not being perceived as such by the cell machinery and we decided to generate a second round of constructs with a longer SP ($SP2_{AtPrx34}$) as mentioned before.

A second round of constructs was prepared differencing only in the SP sequence and using exactly the same strategy. The SP2 was initially amplified with *Taq* DNA polymerase, to check primers specificity (figure 33A), and later with *Pfu* DNA polymerase to generate the ligation fragment (figure 33B). This new SP is larger than the first one, with ~160 bp, as it can be seen in both gels.

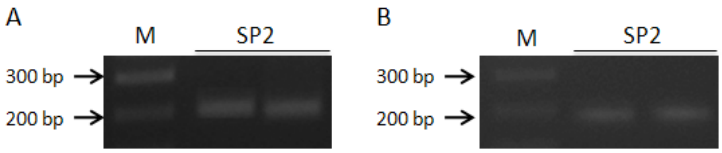

Figure 33. PCR amplification of the SP2 region from AtPrx34. A. Amplification performed with *Taq* DNA polymerase. B. Amplification performed with *Pfu* DNA polymerase. All the P2 bands had the expected molecular weight of 160 bp. M - Molecular marker, *Gene Ruler*. 1.5% agarose electrophoresis gel.

SP2 and the cloning vectors were digested with *Sal*I and *Nco*I, purified and ran on an agarose gel to proceed for ligation reactions, as before (Figure 34). The ligation reaction products were used to transform *E. coli* DH5α and pDNAs of selected colonies was analysed as before by digestion with *Sal*I and *Eco*RI to yield a ~1200 bp that this time has more 160 bp than the empty vector (Figure 35A). The enzymatic verification of pTH2-BN+SP2, was performed with *Sal*I and *Bgl*II (figure 35B), and again a difference in the agarose gell between pTH2-BN and pTH2-BN+SP2 is clear, corresponding to the SP2 (~160 bp). For both constructs all clones were positive, and two clones were chosen to go to sequencing, 3 and 5 for C2 and 4 and 7 for pTH2-BN+SP2.

Sequencing of the selected clones revealed a perfect match between query and original sequence, figure 36.

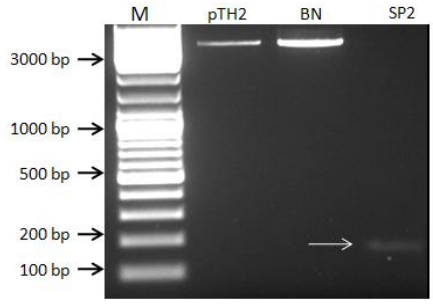

Figure 34. Preparative agarose gel electrophoresis for the ligation reactions between $SP2_{AtPrx34}$ and the expression vectors pTH2 and pTH2-BN. All DNAs were previously digested with *Sal*I and *Nco*I, and purified accordingly. 2 µL of each vector (pTH2 and BN) and 4 µL of $SP2_{AtPrx34}$ (arrow) were loaded on the gel. M – Molecular weight marker, GeneRuler™ DNA Ladder Mix (Fermentas). 1.5% agarose gel.

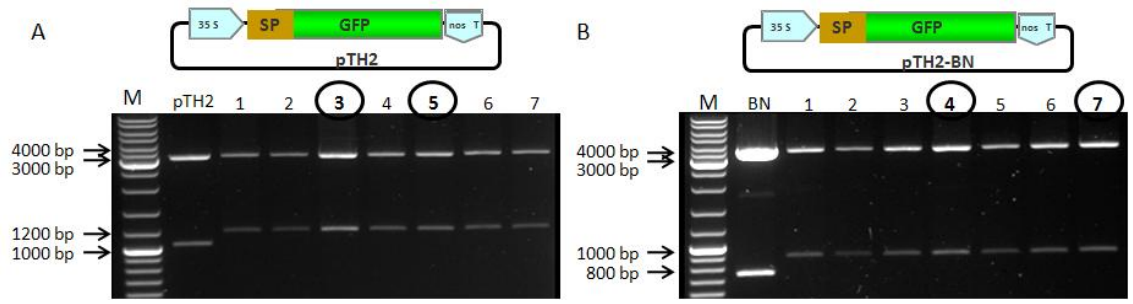

Figure 35. Restriction analysis of the clones obtained after ligation between $SP2_{AtPrx34}$ and the expression vectors pTH2 and pTH2-BN. A. Schematic representation of the $SP1_{AtPrx34}$-GFP construct (top) and restriction analysis of the pTH2-$SP2_{AtPrx34}$ clones with *Sal*I and *Eco*RI (bottom).The lane marked with pTH2 corresponds to the digestion of the empty vector. All the represented clones are positive, which is translated by the presence of a band with 1.2 kb. B. Schematic representation of the $SP1_{AtPrx34}$-GFP BN construct (top) and restriction analysis of the pTH2-BN-$SP2_{AtPrx34}$ clones with *Sal*I and *Bgl*II (bottom) .The lane marked with BN corresponds to a digestion of the empty vector. Positive clones were identified by the presence of a band with ~950 bp. M – Molecular weight marker, GeneRuler™ DNA Ladder Mix (Fermentas). 1.5% agarose gels.

For the cloning of the CTE, MP and MP-CTE of AtPrx34, all the obtained fragments and pTH2-BN-$SP2_{AtPrx34}$ were digested with *Bgl*II and *Xho*I, were purified and ran on an agarose gel (Figure 37A and B). The ligation reactions were performed as before, with one exception, a ratio of 4:1 insert to vector was used to clone the CTE into the vector. Transformed, selected clones of *E. coli* were analysed as before and results are shown in Figre 38. Enzymatic verification of $SP2_{AtPrx34}$-GFP-CTE construct was performed with *Sal*I and *Xho*I (Figure 38A) leading to the release of a band of ~ 1000 bp in positive clones, with more 100 bp than the backbone construct . The identification of the positive clones for $SP2_{AtPrx34}$-GFP-MP construct and $SP2_{AtPrx34}$-GFP-MP-CTE construct was conducted with the enzymes used in their cloning, *Bgl*II and *Xho*I,

revealing a band with ~900 bp and ~980 bp for positive clones, while the vector, pTH2-BN+SP2, missed that band (Figure 38B). For all three constructs all clones were positive, and clones 1 and 2 were chosen to be used in transformation for all the constructs.

Figure 36. Alignment between the predicted $SP2_{AtPrx34}$ sequence and the generated clones. Schematic representation of the $SP1_{AtPrx34}$-GFP construct for pTH2 and pTH2-BN(top) and alignments (bottom). Alignments were performed with the sequences obtained for clones 3 and 5 from Figure 35A, and for clones 4 and 7 from Figure 35B. Asterisks (*) represent perfect matches. SP sequence is marked in brown. Sequencing reactions were performed with primer M13Fwd that anneals with both expression vectors upstream the 35S promoter region.

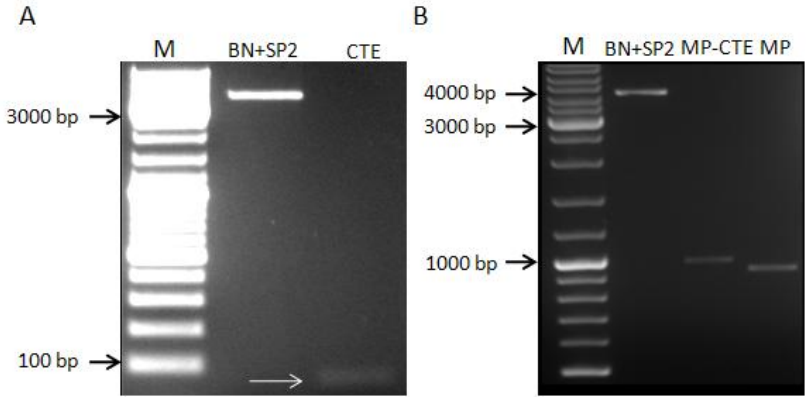

Figure 37. Preparative agarose gel electrophoresis for the ligation reactions between CTE, MP and MP-CTE of AtPrx34 and the backbone pTH2-BN-$SP2_{AtPrx34}$. A. Ligation between AtPrx34 CTE and pTH2-BN-SP2. B. Ligation between AtPrx34 MP / MP-CTE and pTH2-BN-SP2. All DNAs were previously digested with *Bgl*II and *Xho*I and purified. 2 µL of the vector (BN+SP), MP and MP-CTE, and 4 µL of CTE (arrow) were loaded on the respective geis. M – Molecular weight marker, GeneRuler™ DNA Ladder Mix (Fermentas). 1.5% agarose gel.

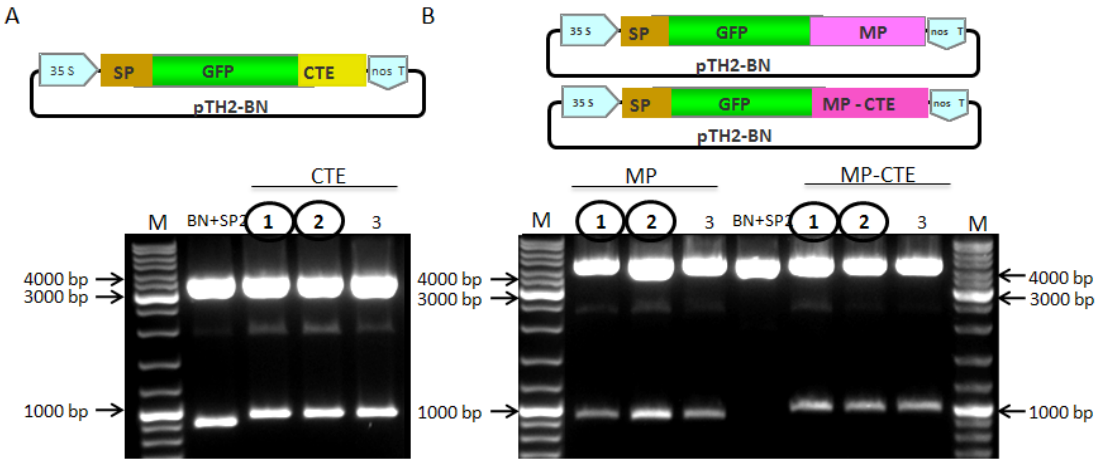

Figure 38. Restriction analysis of the clones obtained after ligation between pTH2-BN-SP2$_{AtPrx34}$ and the CTE, MP and MP-CTE regions of AtPrx34. A. Schematic representation of the SP1$_{AtPrx34}$-GFP-CTE construct (top) and restriction analysis of the pTH2-SP2$_{AtPrx34}$-GFP-CTE clones with *Sal*I and *Xho*I (bottom). All the represented clones are positive, which is translated by the presence of a band with ~1000 bp. 1.5% agarose gel. B. Schematic representation of the SP2$_{AtPrx34}$-GFP-MP$_{AtPrx34}$ and SP2$_{AtPrx34}$-GFP-MP-CTE$_{AtPrx34}$ constructs (top) and restriction analysis of the same construct clones with *Bgl*II and *Xho*I (bottom). All the represented clones are positive, which is translated by the presence of a band with ~900 bp corresponding the MP$_{AtPrx34}$ fragment (left) and 1000 bp corresponding the MP-CTE$_{AtPrx34}$ fragment (right). 1.5% agarose gels. Lanes marked with BN+SP correspond to digestions of the backbone construct. M – Molecular weight marker, GeneRuler^{TM} DNA Ladder Mix (Fermentas).

The constructs for C3, C4 and C5 with SP2 weren't sequenced because they were produced with already sequenced inserts from the previous constructs. pDNAs of all the generated AtPrx34-GFP constructs were purified using the QIAGEN Plasmid Midi Prep kit, through gravity-flow with QIAGEN anion-exchange tips, resulting in ultrapure and highly concentrated pDNA shown in Figure 39. Although it is not possible to accurately determine the size of uncut pDNA, all plasmids ran accordingly to their relative size.

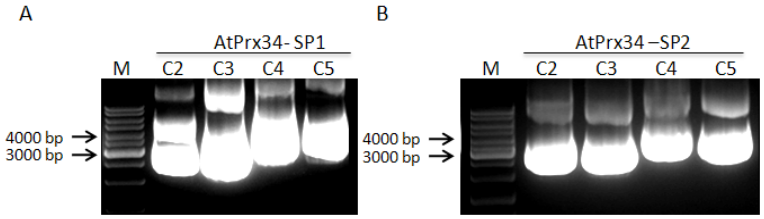

Figure 39. Agarose gel electrophoresis of all AtPrx34-GFP pDNAs used for protoplast transformation. A. C2-C5 AtPrx34-GFP fusions, generated with SP1. B. C2-C5 AtPrx34-GFP fusions, generated with SP2. M – Molecular weight marker, GeneRuler^{TM} DNA Ladder Mix (Fermentas). In all cases, 2 µL of each sample were loaded onto 1.5 % agarose gels.

3.3. Isolation of *Arabidopsis* mesophyll protoplasts

The method used for isolation of *Arabidopsis* mesophyll protoplasts resulted in highly pure fractions of mesophyll protoplasts (Figure 40) with average yields of $0.5x10^5 \pm 0.2$ protoplasts mL^{-1} g^{-1}(FW). Protoplasts appeared spherical, clearly three-dimensional, with chloroplasts pushed against the plasma membrane by the large central vacuole (Figure 40).

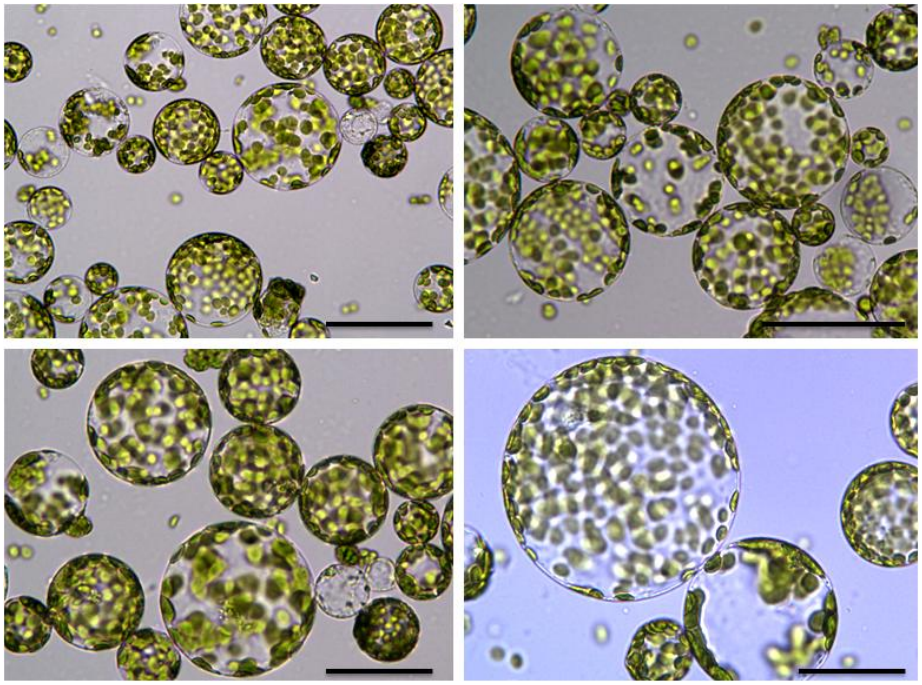

Figure 40. Bright field images of *A. thaliana* mesophyll protoplasts at different magnifications. Bars = 50 µm. Magnification = 40x.

Protoplasts were suspended in MMg solution, which is thought to be essential to make the protoplasts competent for the uptake of DNA during PEG-mediated transformation, due the presence of $MgCl_2$.

3.4. Isolation of *C. roseus* mesophyll protoplasts

The methos used for isolation of *C. roseus* mesophyll protoplasts resulted in highly pure fractions of mesophyll protoplasts (Figure 41) with average yields of $0.8x10^5 \pm 0.2$ protoplasts.mL^{-1}.g^{-1}(FW).

Direct observation of *C. roseus* protoplasts by bright field and fluorescence microscopy showed spherical healthy cells (Figure 41). Among the protoplast population, a fraction of cells exhibited blue fluorescence under UV light. These cells are larger, possess fewer chloroplasts and are thought to be fluorescent due to the accumulation of the alkaloid serpentine inside their vacuoles. These specialized alkaloid accumulating cells are called idioblasts. Idioblasts occur in several plant families, are most probably morphologically related to laticifers, and may be associated with the biosynthesis and accumulation of secondary products, like the Vinca alkaloids (St-Pierre et al. 1999)

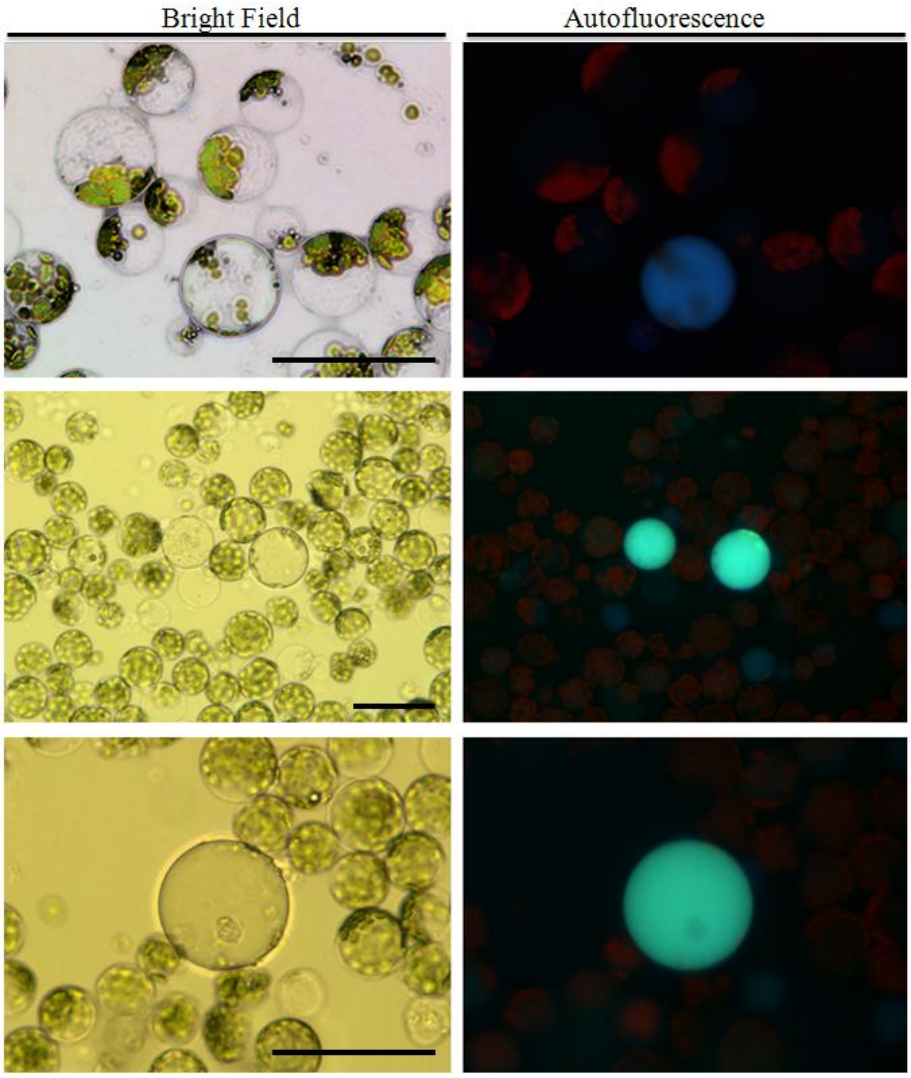

Figure 41. Bright field (left column) and autofluorescence under UV light (right column) images *of C. roseus* mesophyll protoplasts.. Blue fluorescence under UV light is due to the accumulation of the alkaloid serpentine in the vacuoles of mesophyll specialized cells named idoblasts. Under UV light, chloroplasts also slightly fluoresce in red. Bars = 50 µm. Magnification = 40x.

After isolation, *C. roseus* protoplasts were resuspended and incubated in MMg solution in order to turn them competent for PEG-mediated transformation.

3.5. PEG-mediated transformation of *Arabidopsis* protoplasts

3.5.1. Transformation with control/marker constructs

In order to prove and optimize the PEG-mediated technique of transient expression in *Arabidopsis* protoplasts, these cells were transformed with GFP (construct C1), with marker constructs coding for GFP targeted to the ER and the vacuole, and with already tested CrPrx1-GFP fusions.

PEG-mediated transformation of protoplasts is a very simple and species independent procedure, where the DNA, protoplasts and PEG solution are mixed and incubated. DNA uptake by plant cells requires high concentrations of PEG, which acts only in combination with divalent cations. At the high concentration of PEG used for the transformation experiments, the hydration of DNA is strongly reduced. Such changes in the hydration economy are known to cause structural changes in the form of DNA which cause protection against digestion (Mi Jeon et al. 2007). The transformation of cells is thought to occur during the incubation period with PEG, and after that the protoplasts are kept to rest for 48 h in W5 solution.

In this work, the first construct to be used was 35S::GFP (C1). Protoplasts transformed with C1 showed GFP fluorescence in the cytoplasm, and absence of signal in the ER, vesicles or vacuole (Figure 42). The nucleoplasm was also labelled. Merging of the images acquired in the green (GFP) and red (chlorophyll autofluorescence) channels clearly allowed the distinction of the nucleus, the cytoplasm, and also the outline of the organelles.

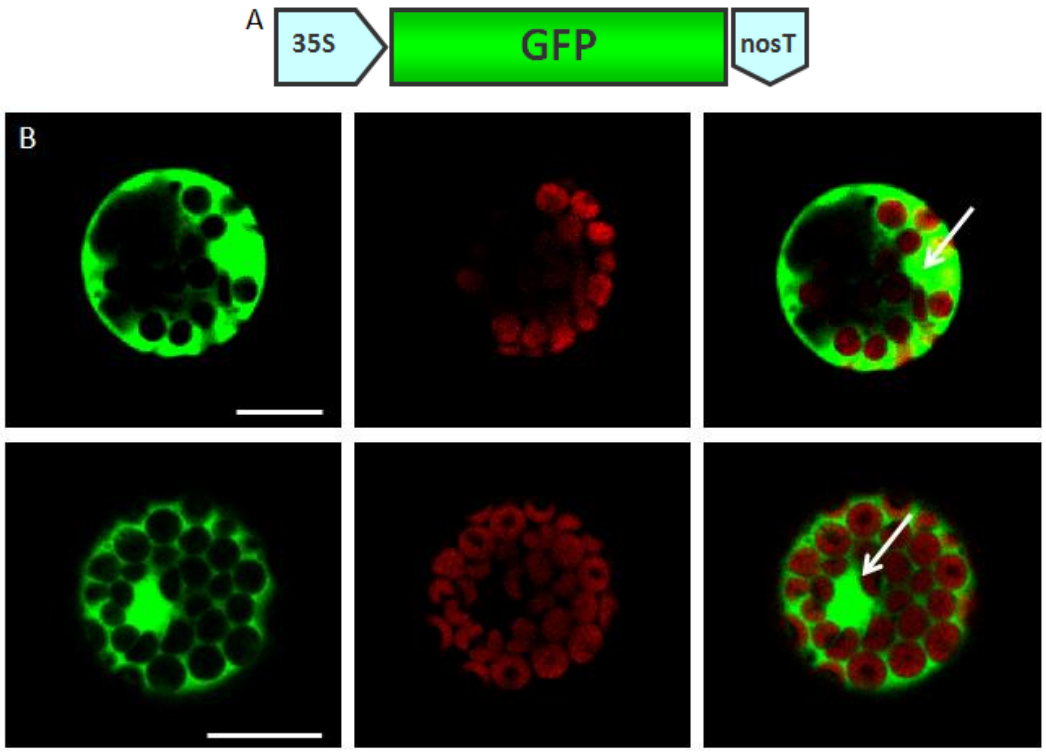

Figure 42. Transient transformation of *Arabidopsis* protoplasts with a control GFP fusion observed under the confocal microscope. A. Schematic representation of the 35S::GPF construct (C1). B. Typical GFP fluorescence pattern observed for transformation with the C1 cosntruct. GFP accumulates in the cytoplasm**.** Arrows are pointing to the nucleus of cells. Left - GFP channel; Middle – Red channel showing chloroplast autofluorescence; Right – merged images. Bars = 10 µm. Magnification = 40x.

Transformation of *Arabidopsis* protoplasts was also performed using a marker 35S::SP_{CrPrx1}-GPF-KDEL construct. The SP of CrPrx1 included in the construct directs the fusion protein to the secretory pathway, while the tetrapetide KDEL will determine its retention in the ER, the first organelle of the secretory pathway. The results obtained are shown in Figure 43 and show GFP accumulation in a typical reticulate / network pattern recognized as the ER, proving retention of this fusion protein in this compartment. Another distinctive feature observed is the labelling of the perinuclear ER, in contrast to what the nucleoplasm labelling observed when expressing cytGFP.

The tetrapeptide KDEL is commonly found at the C terminus of soluble proteins of the endoplasmic reticulum (ER), and it contributes to their localization by interacting with a receptor, ERD2, that recycles between the Golgi complex and the ER (Lorenzo Frigerio et al. 2001), thus the K/HDEL signal is sufficient to confer variable extents of accumulation in the plant ER.

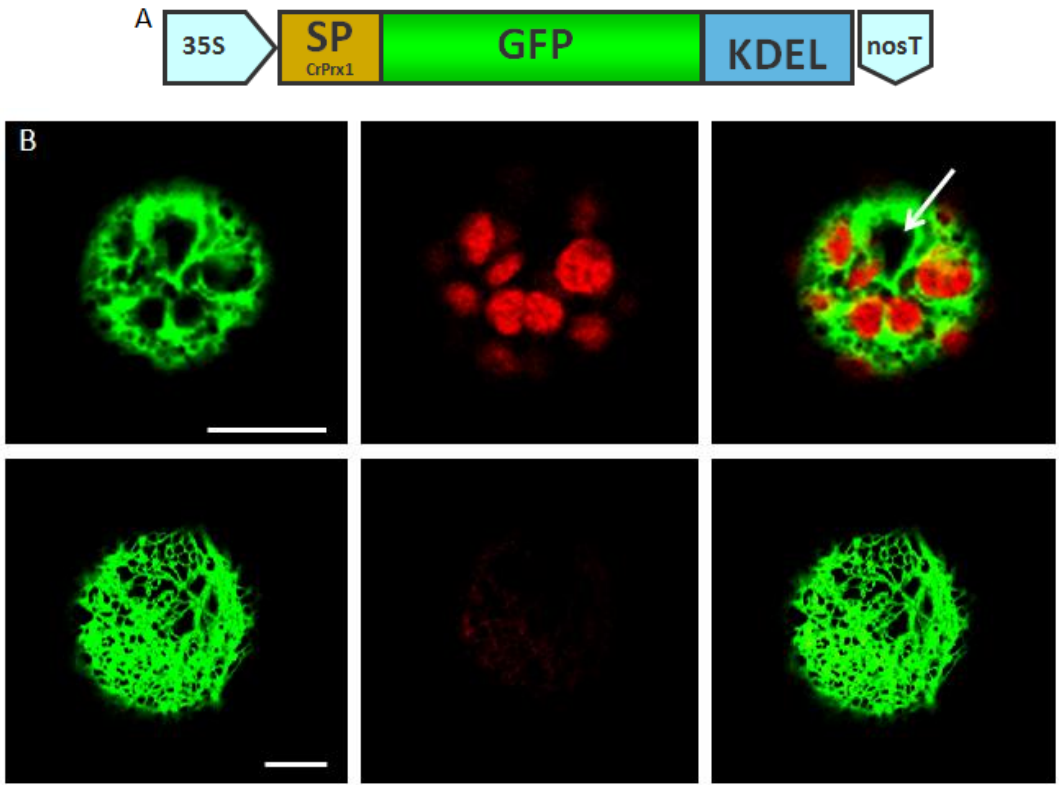

Figure 43. Transient transformation of *Arabidopsis* protoplasts with an ER located GFP fusion observed under the confocal microscope. A. Schematic representation of the 35S::SP_{CrPrx1}-GPF-KDEL construct. B. GFP is targeted to, and accumulated in the ER. The arrow is pointing to the perinuclear ER. Left - GFP channel; Middle – Red channel showing chloroplast autofluorescence; Right – merged images. Bars = 10 µm. Magnification = 40x.

Results obtained with *Arabidopsis* protoplasts expressing the fusion protein encoded by the 35S::sGFP SP_{CrPrx1}-GFP construct (C2) are shown in Figure 44. In this figure one can clearly see that the presence of the SP of CrPrx1 seems to target the fusion protein to some compartment of the secretory pathway. Unlike what happened with C1, in this situation no cytoplasmic labelling is observed. In this case, the typical ER network is as visible as for the previous construct, indicating that at the time these images were acquired, most of the GFP had already left the ER network and travelled to the Golgi apparatus or beyond. The existence of perinuclear and thin strands fluorescence indicates that GFP is still present at least in part of the ER (Figure 44, arrow). Most fluorescence is present in small spheroid compartments, possibly corresponding to Golgi or secretory intermediate compartments. Of course, one can only speculate about the true nature of these structures, since accurate identification could only be achieved using specific markers for different subcellular compartments. It

is also noteworthy that cell wall (apoplast) localized GFP, the final localization expected in this case, cannot be visible in this system since the cell wall is absent.

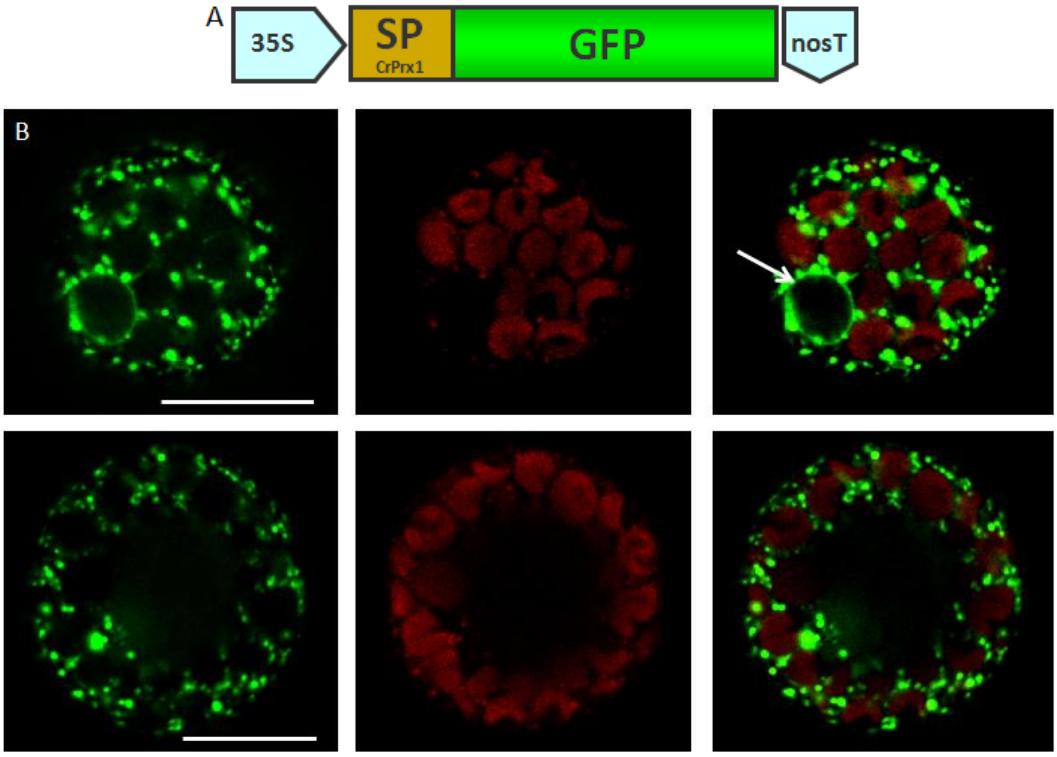

Figure 44. Transient transformation of *Arabidopsis* protoplasts with the SP_{CrPrx1}-GFP fusion (C2), observed under the confocal microscope. A. Schematic representation of the 35S::SP_{CrPrx1}-GPF construct (C2). B. GFP is targeted to an unidentified compartment of the secretory pathway. Arrow points to the perinuclear ER. Left - GFP channel; Middle – Red channel showing chloroplast autofluorescence; Right – merged images. Bars = 10 µm. Magnification = 40x.

The C-terminal extension (CTE) of CrPrx1 has been shown to be the vacuolar sorting determinant of this protein. Accordingly, expression of SP_{CrPrx1}-GPF-CTE_{CrPrx1} (C3) targeted GFP to the central vacuole of *Arabidopsis* mesophyll protoplasts and confirmed that our system can be used to study vacuolar sorted GFP fusions (Figure 45). In this case, smaller bright vesicles could also be observed. These may correspond to small vacuoles or to post-Golgi intermediate compartments like the PVCs (section 1.4.; Figure 9). Very similar results were obtained with protoplasts expressing the SP_{CrPrx1}-GPF-MP-CTE_{CrPrx1} fusion (C5). Again, GFP was targeted and accumulated in the central vacuole and smaller bright structures were also present (Figure 46).Comparison between the results of the expression of C3 and C5, with the ones obtained while expressing the vacuolar control SP_{CrPrx1}-GPF-$CTPP_{Phaseolin}$ (Figure 47), confirmed vacuolar accumulation of GFP in both constructs in which the CTE of CrPrx1 was present. In Figure 47 one can also see a healthy untransformed cell (signal

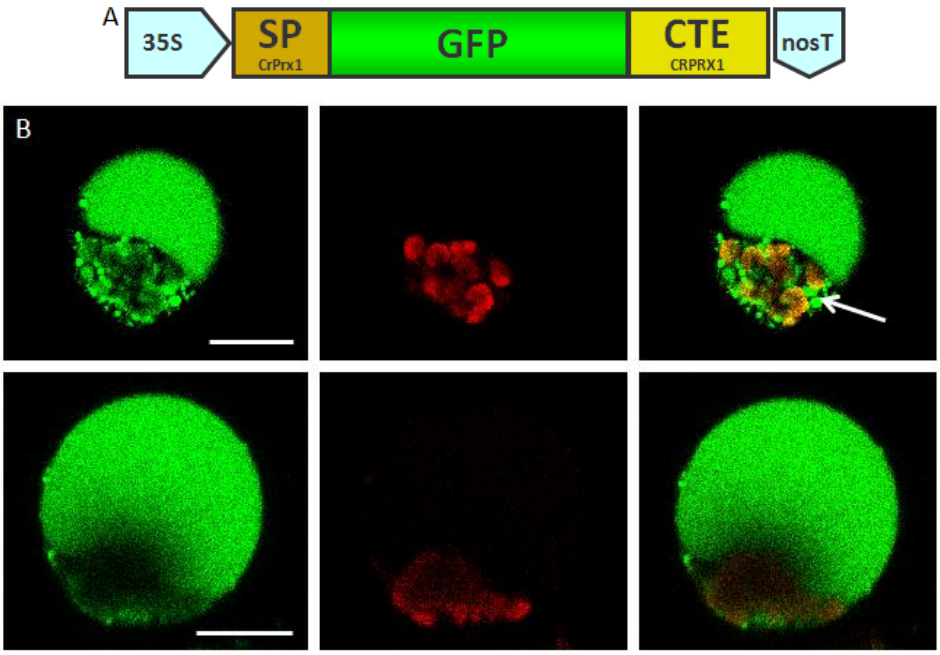

Figure 45. Transient transformation of *Arabidopsis* protoplasts with SP_{CrPrx1}-GFP-CTE_{CrPrx1} fusion (C3), observed under the confocal microscope. A. Schematic representation of the 35S::SP_{CrPrx1}-GPF-CTE_{CrPrx1} construct (C3). B. The presence of the CTE of CrPrx1 targets GFP to the central vacuole**.** Arrows indicates unidentified smaller structures also eccumulating GFP. Left - GFP channel; Middle – Red channel showing chloroplast autofluorescence; Right – merged images. Bars = 10 µm. Magnification = 40x.

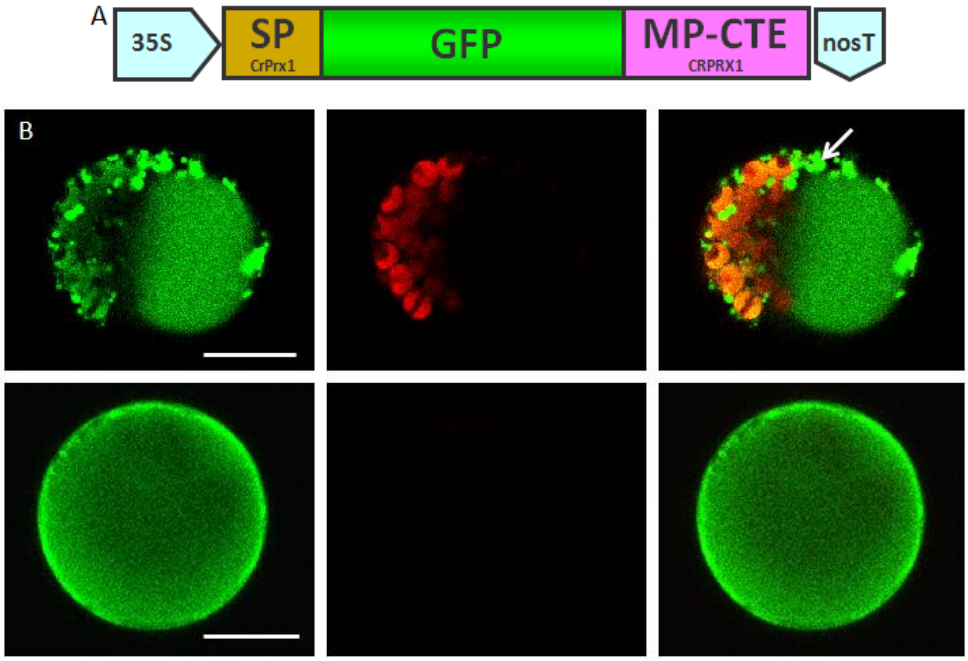

Figure 46. Transient transformation of *Arabidopsis* protoplasts with SP_{CrPrx1}-GFP-MP-CTE_{CrPrx1} fusion (C5), observed under the confocal microscope. A. Schematic representation of the 35S::SP_{CrPrx1}-GPF-MP-CTE_{CrPrx1} construct (C5). B. GFP accumulates in the large central vacuole. Arrows indicates small vacuoles or intermediate compartments (possibly PVCs). Left - GFP channel; Middle – Red channel showing chloroplast autofluorescence; Right – merged images. Bars = 10 µm. Magnification = 40x.

is restricted to the red channel) next to a GFP expressing cell with a bright green vacuole. The results with constructs targeting GFP for vacuolar localization also clearly show that the vacuole occupies most of the cell space.

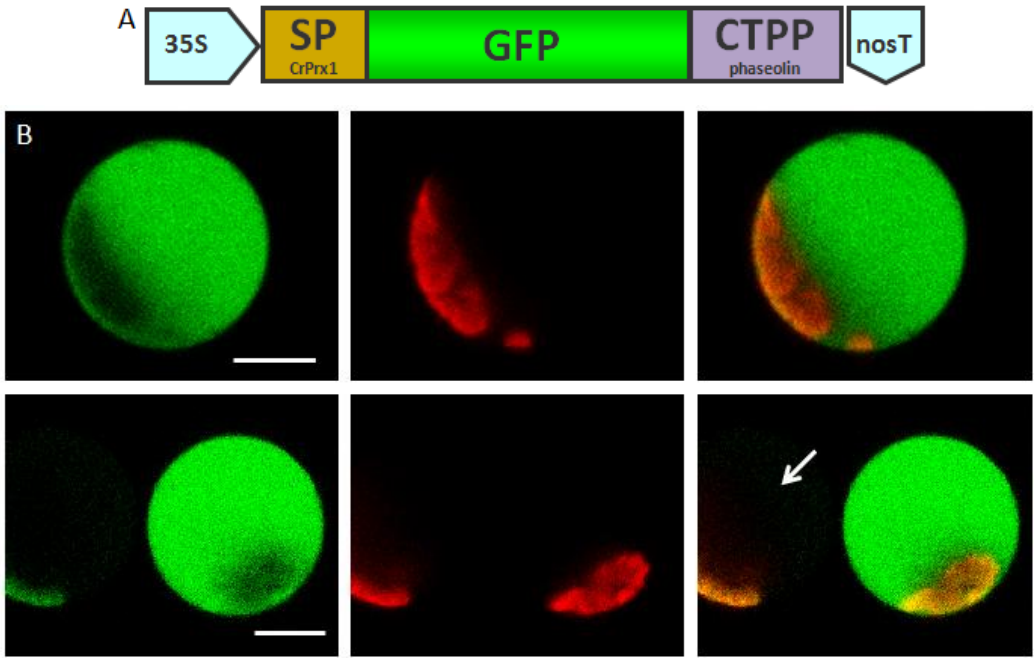

Figure 47. Transient transformation of *Arabidopsis* protoplasts with a vacuole located GFP fusion, observed under confocal laser-scanning microscopy. A. Schematic representation of the 35S::SP_{CrPrx1}-GPF- $CTPP_{Phaseolin}$ construct. B. GFP target to the vacuole. Arrow shows a nontransformed cell next to a transformed cell. Left - GFP channel; Middle – Red channel showing chloroplast autofluorescence; Right – merged images. Bars = 10 µm. Magnification = 40x.

Finally, expression of the SP_{CrPrx1}-GPF-MP_{CrPrx1} construct (C4) in *Arabidopsis* mesophyll protoplasts resulted in accumulation of GFP fluorescence in the secretory pathway (ER/Golgi/post-Golgi) and not in the vacuole, in a pattern similar to what was observed for C2 (Figure 48). Therefore, exclusion of the CTE of CrPrx1 from the fusion protein, supports the role of the CTE as necessary for vacuolar sorting of CrPrx1. This result, obtained in a heterologous expression system, confirms the vacuolar localization of CrPrx1 and suggests a conserved mechanism for the recognition of the CTE sorting signal present in this protein.

The results obtained with the markers and CrPrx1-GFP constructs validated the methodology of isolation and transformation of *Arabidopsis* mesophyll protoplasts, and showed this technique could be used for investigating the sorting through the secretory pathway and vacuoles of other uncharacterized proteins.

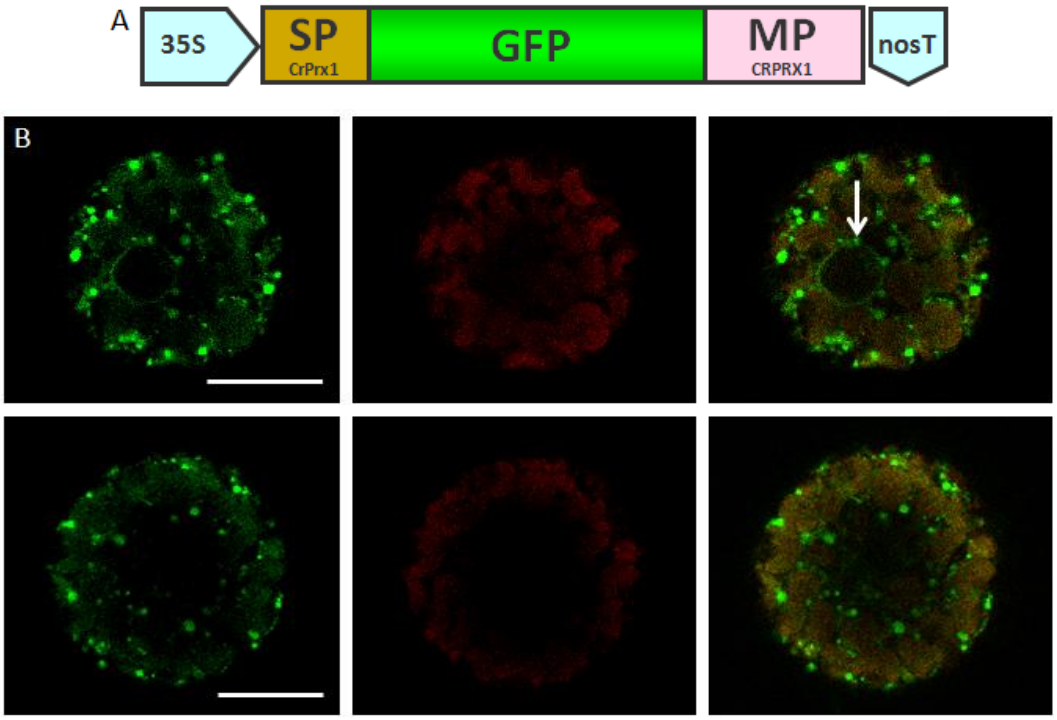

Figure 48. Transient transformation of *Arabidopsis* protoplasts with SP_{CrPrx1}-GFP-MP_{CrPrx1} fusion (C4), observed under confocal laser-scanning microscopy. A. Schematic representation of the C4: 35S::SP_{CrPrx1}-GPF-MP_{CrPrx1} construct. B. GFP is targeted to an unidentified compartment of the secretory pathway. Arrow points to the perinuclear ER. Left - GFP channel; Middle – Red channel showing chloroplast autofluorescence; Right – merged images. Bars = 10 µm. Magnification = 40x.

3.5.2. Transformation with AtPrx34-GFP fusions

After validation, PEG-mediated transformation of *Arabidopsis* protoplasts was, therefore, used to study the subcellular sorting of AtPrx34 in the homologous system, using the fusions generated earlier in the course of this work.

Although there were no mutations or errors in the sequences of all AtPrx34-GFP constructs (with SP1), the results obtained when transforming *Arabidopsis* mesophyll protoplasts with these constructs were, unexpectedly, always the same: all the AtPrx34-GFP fusions resulted in labelling of the cytoplasm, as if no SP was present (Figure 49), meaning that the AtPrx34-GFP fusion proteins were not being successfully targeted to the secretory pathway.

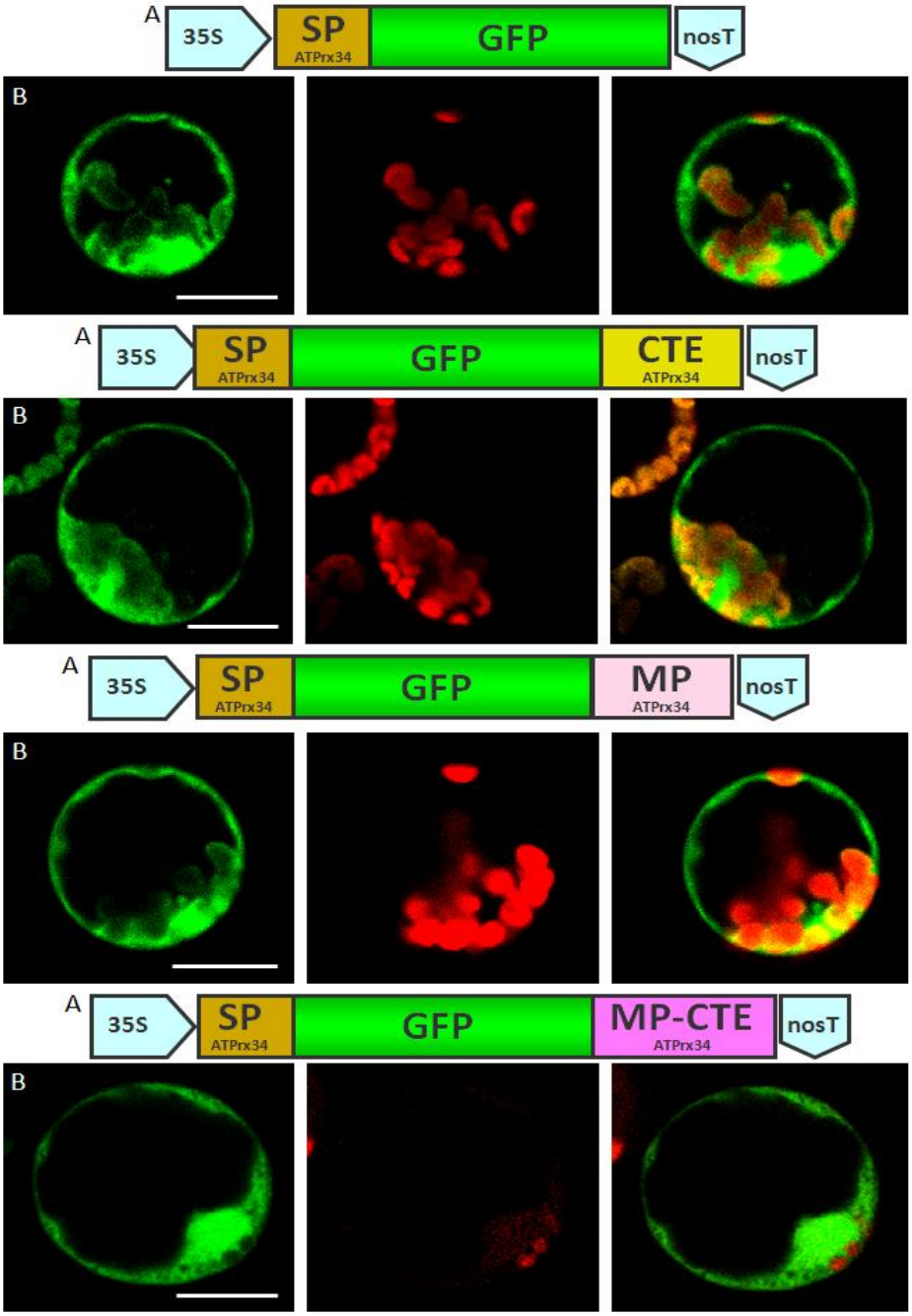

Figure 49. Transient transformation of *Arabidopsis* protoplasts with several AtPrx34-GFP fusions observed under the confocal microscope. A. Schematic representation of all used constructs is shown: 35S::SP1$_{AtPrx34}$-GFP (C2), 35S::SP1$_{AtPrx34}$-GFP-CTE$_{AtPrx34}$ (C3), 35S::SP1$_{AtPrx34}$-GFP-MP$_{AtPrx34}$ (C4) and 35S::SP1$_{AtPrx34}$-GFP-MP-CTE$_{AtPrx34}$ (C5). B. In all cases GFP accumulates in the cytoplasm. Left - GFP channel; Middle – Red channel showing chloroplast autofluorescence; Right – merged images. Bars = 10 µm. Magnification = 40x.

This poor results led us to generate new constructs with a longer SP for AtPrx34 (SP2), since out idea was that the SP1 cutting site was not being recognised as such by the cell. Unfortunately, the newly generated constructs also proved ineffective and did not express any of the expected GFP patterns for subcellular localization of the fusions

(Figure 50). In fact, the majority of the cells were either not transformed or not expressing the fluorescent protein (Figure 50D). In some cells, a weak fluorescent signal was observed in a pattern suggestive of components of the secretory pathway (Figure 50B and C). However, any role of the CTE of AtPrx34 in the vacuolar localization of this protein remains purely speculative, since we did not generate any results supporting or denying this hypothesis.

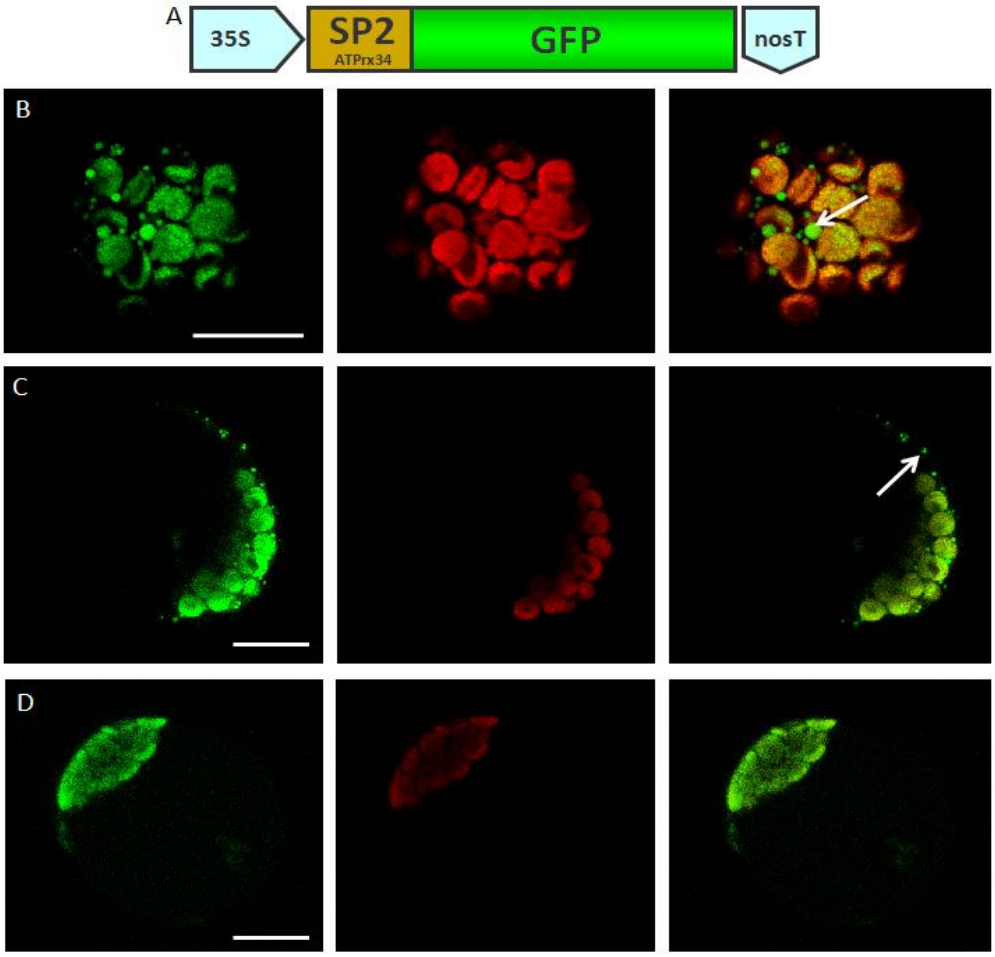

Figure 50. Transient transformation of *Arabidopsis* protoplasts with $SP2_{AtPrx34}$-GFP fusion, observed under confocal laser-scanning microscopy. A. Schematic representation of the 35S::$SP2_{AtPrx34}$-GFP (C2) construct. B and C. No specific GFP pattern is explicit for protoplasts transformed with the C2 construct described. Arrow indicate a weak fluorescent signal observed in a pattern suggestive of components of the secretory pathway. D. Signal emission to all other AtPrx34-GFP fusions with SP2. Left - GFP channel; Middle – Red channel showing chloroplast autofluorescence; Right – merged images. Bars = 10 µm. Magnification = 40x.

3.5.3. Transformation efficiency and protoplast survival rates

The survival rate of protoplasts throughout the transformation procedure was determined (Figure 51). Protoplasts that were not exposed to PEG had a survival rate of about 54%, while PEG exposed cells but not transformed had a lower survival rate, of 25 %, similar to the survival rate of *Arabidopsis* mesophyll protoplasts transformed with C1. This construct was chosen for calculation of survival rate and efficiency because cytoplasmic GFP showed a brighter fluorescence and rendered an invariable GFP localization pattern. These results mean that exposure to PEG and not to DNA has negative effects on protoplasts. Moreover, the handling of protoplasts through the protocol is agressive for the cells and therefore all steps have be carried out very gently (Figure 51A).

Of the 25% of protoplasts that survived the transformation process, 21% successfully expressed cytoplasmic GFP (Figure 51B). These results also show that the life span of isolated protoplasts is short, but long enough to successfully transiently express fusion proteins in order to study subcellular localisation, protein-protein interactions, etc.

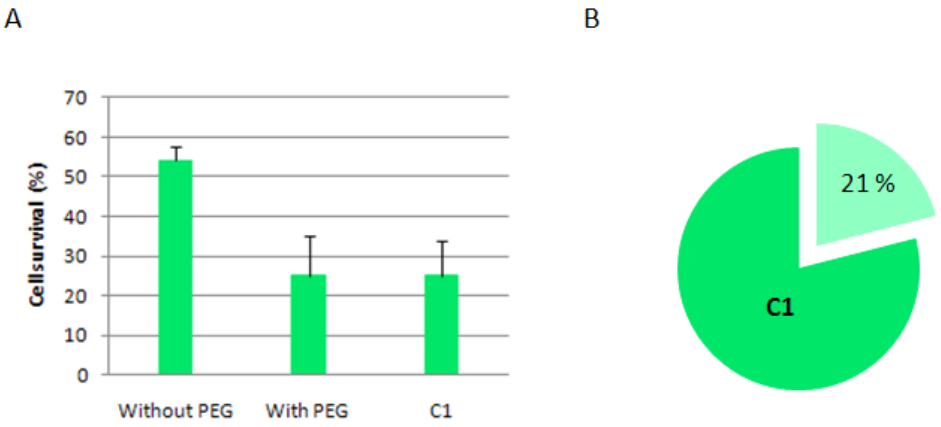

Figure 51. Quantitative data for PEG-mediated transformation of *Arabidopsis* protoplasts. A. Cell survival rate for untransformed protoplasts not exposed and exposed to PEG (without and with PEG, respectively), and for protoplasts submitted to the complete protocol of transformation with C1 construct. B. Transformation rate of protoplasts with C1 construct. Statistical data calculated from an average of 8 individual experiments.

Despite the unsuccessful results with the AtPrx34-GFP fusions, the isolation of *Arabidopsis* mesophyll protoplasts and the subsequent PEG-mediated transformation of

these cells were proven straightforward and reliable techniques that are now successfully established in our laboratory.

3.6. PEG-Mediated Transformation of *C. roseus* Protoplasts

3.6.1. Tranformation with control/marker constructs

The PEG-mediated transformation protocol was also developed for *C. roseus* protocols, since for the characterization of candidate gene implicated in the biosynthesis, regulation or transport of TIA biosynthesis, the homologous system is preferential.

The protocol used for *Arabidopsis* was applied directly to *C. roseus* protoplasts and after applying a 35ºC treatment prior to observation, the technique worked very well, also with this species. Resembling what was done in *Arabidopsis* protoplasts, the C1 construct and the ER marker construct were first used to validate the technique. Transformation with these constructs worked well and resulted in cytoplasm and ER accumulation of green fluoresecence, with the exactly patterns observed for *Arabidopsis* proitoplasts, as expected (Figure 52 and 53, respectively).

The fusions that included the CrPrx1 SP located at the N-*terminus* of GFP were targeted to the ER, resulting in ER accumulation of green fluorescence, or to intermediate secretory compartments, as observed for *Arabidopsis* protoplasts (C2, Figure 54 for C2 and Figure 56 for C4). The fusions that had the CrPrx1 CTE located at the C-*terminus* of GFP, C3 and C5, led to GFP accumulation in the vacuole (Figure 55 for C3 and 57 for C5). The same subcelular localization was observed for the vacuolar marker fusion, confirming those results (Figure 58). In fact, in figures 55, 57 and 58, it can be seen that in all constructions, even with the CTE, ER labelling can be seen in some cells, oposite to what happened with *Arabidopsis* protoplasts, indicating that in C. roseus protoplasts, either transient expression or protein traffic through the secretory pathways are slower. In this case it also seems that the presence of the MP together with the CTE results in more efficient accumulation in the vacuole of the fusion protein (Figures 57).

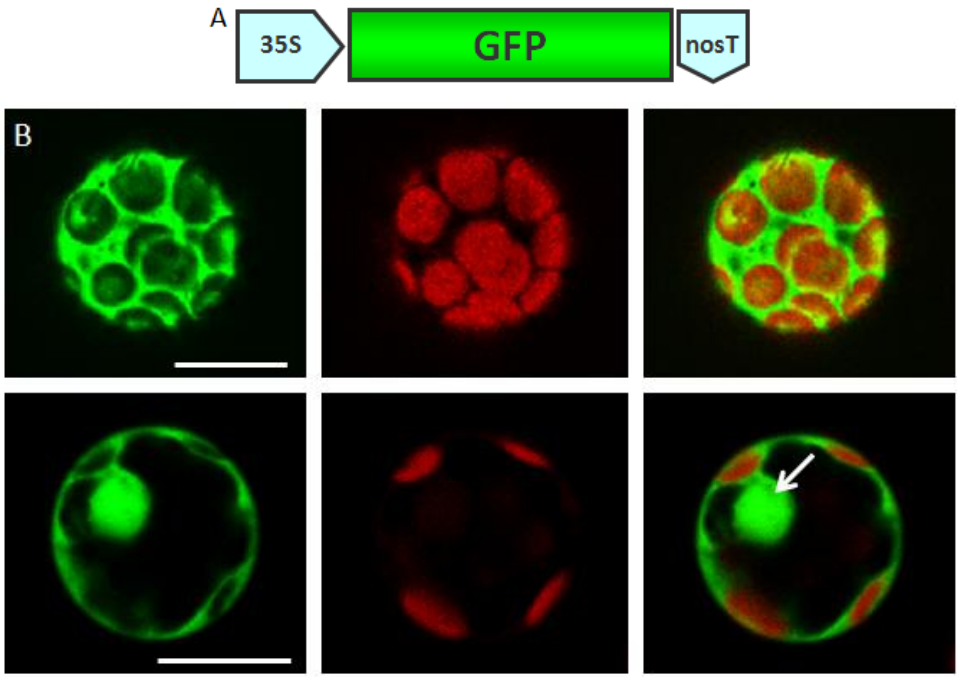

Figure 52. Transient transformation of *C. roseus* protoplasts with a control GFP construct observed under the confocal microscope. A. Schematic representation of the 35S::GPF construct (C1). B. Typical GFP fluorescence pattern observed for transformation with the C1 cosntruct. GFP accumulates in the cytoplasm**.** Arrow is pointing to the nucleus of cells. Left - GFP channel; Middle – Red channel showing chloroplast autofluorescence; Right – merged images. Bars = 10 µm. Magnification = 40x.

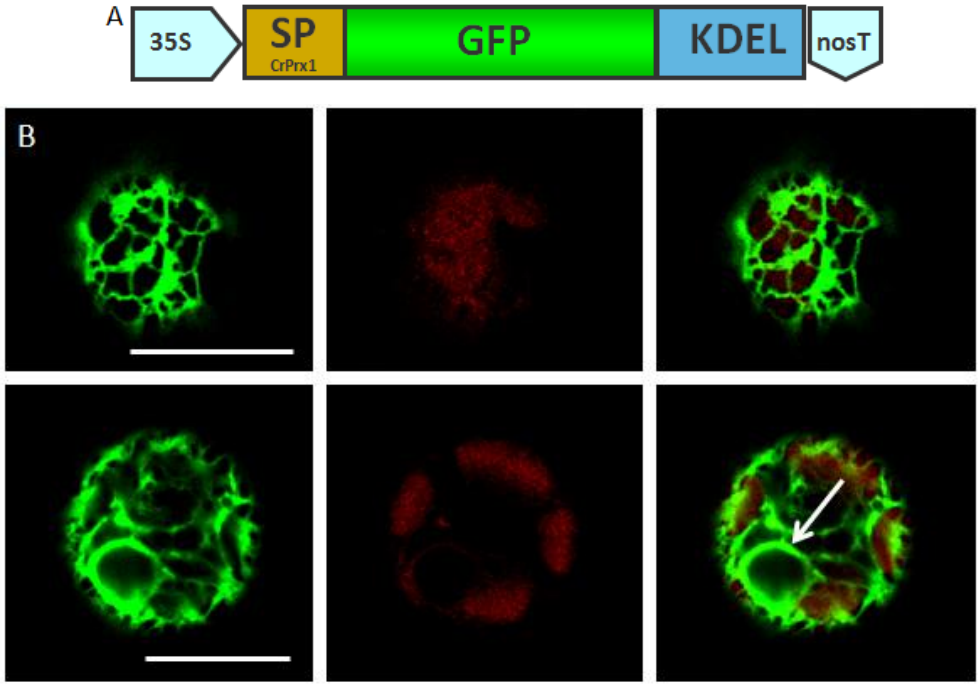

Figure 53. Transient transformation of *C. roseus* protoplasts with an ER located GFP fusion observed under the confocal microscope. A. Schematic representation of the 35S::SP_{CrPrx1}-GPF-KDEL construct. GFP is target to, and accumulated in the ER. The arrow is pointing the perinuclear ER. Left - GFP channel; Middle – Red channel showing chloroplast autofluorescence; Right – merged images. Bars = 10 µm. Magnification = 40x.

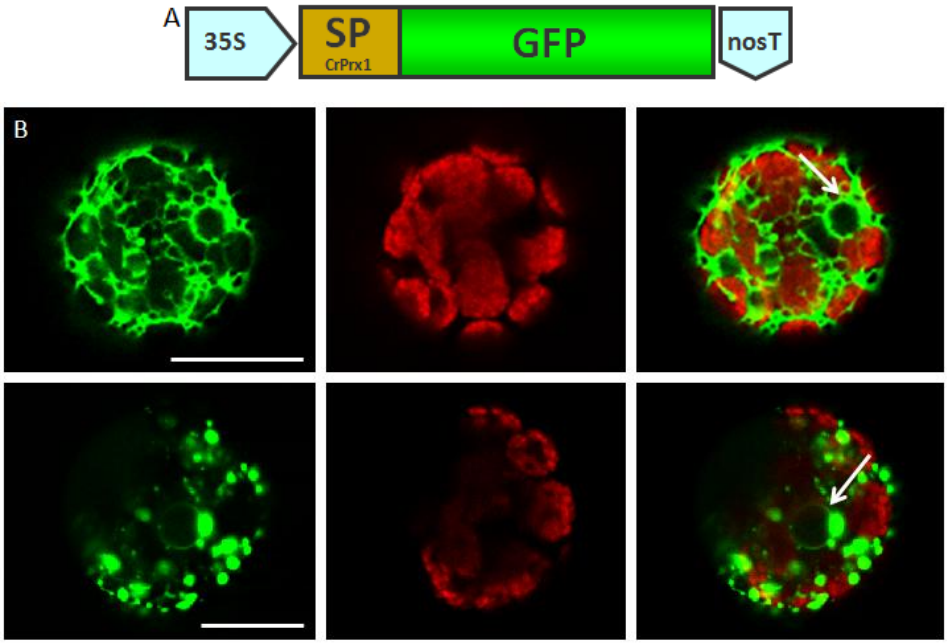

Figure 54. Transient transformation of *C. roseus* protoplasts with the SP_{CrPrx1}-GFP fusion (C2), observed under the confocal microscope. A. Schematic representation of the 35S::SP_{CrPrx1}-GPF construct (C2). B. GFP is targeted to an unidentified compartment of the secretory pathway. Arrow points to the perinuclear ER. Left - GFP channel; Middle – Red channel showing chloroplast autofluorescence; Right – merged images. Bars = 10 µm. Magnification = 40x.

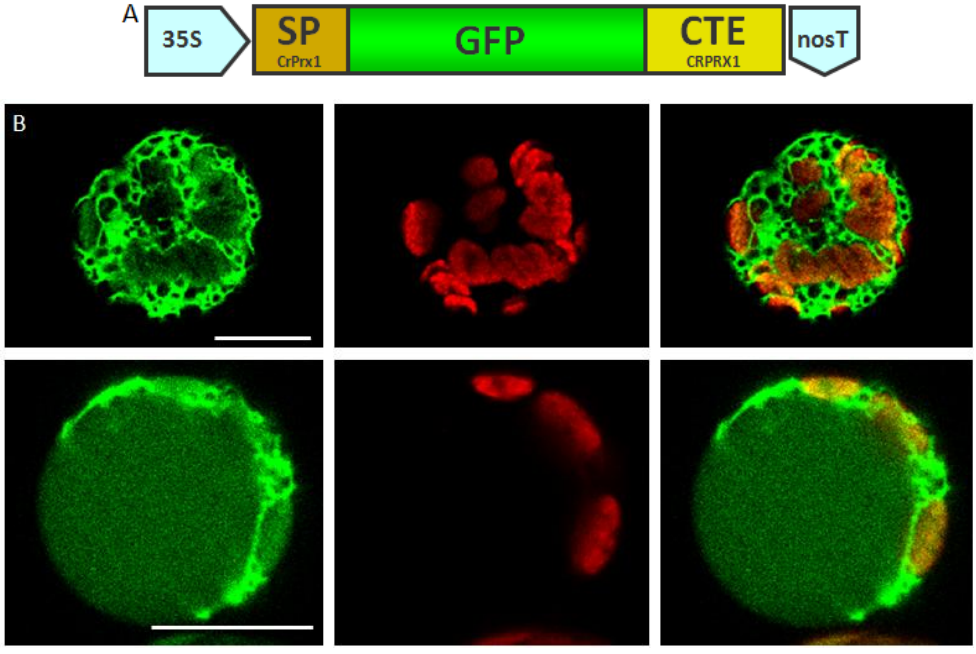

Figure 55. Transient transformation of *C. roseus* protoplasts with SP_{CrPrx1}-GFP-CTE_{CrPrx1} fusion (C3), observed under the confocal microscope. A. Schematic representation of the 35S::SP_{CrPrx1}-GPF-CTE_{CrPrx1} construct (C3). B. The presence of the CTE of CrPrx1 targets GFP to the central vacuole, but still is observedl ER acummulation. Left - GFP channel; Middle – Red channel showing chloroplast autofluorescence; Right – merged images. Bars = 10 µm. Magnification = 40x.

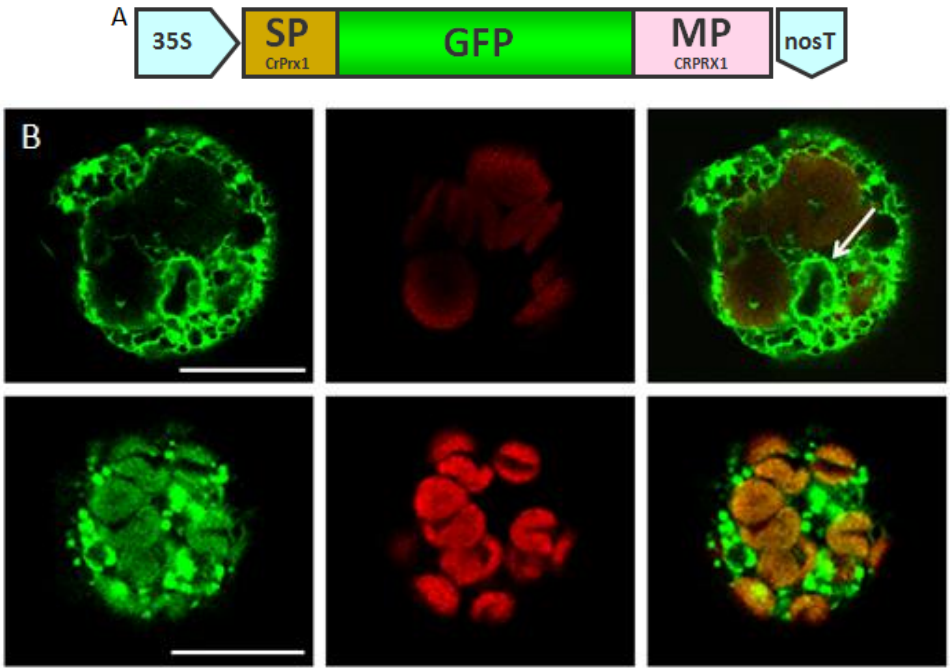

Figure 56. Transient transformation of *C. roseus* protoplasts with C4 CrPrx1-GFP fusion, observed under confocal laser-scanning microscopy. A. Schematic representation of the 35S::SP_{CrPrx1}-GPF-MP_{CrPrx1} construct (C4). B. GFP is targeted to an unidentified compartment of the secretory pathway. Arrow points to the perinuclear ER. Left - GFP channel; Middle – Red channel showing chloroplast autofluorescence; Right – merged images. Bars = 10 µm. Magnification = 40x.

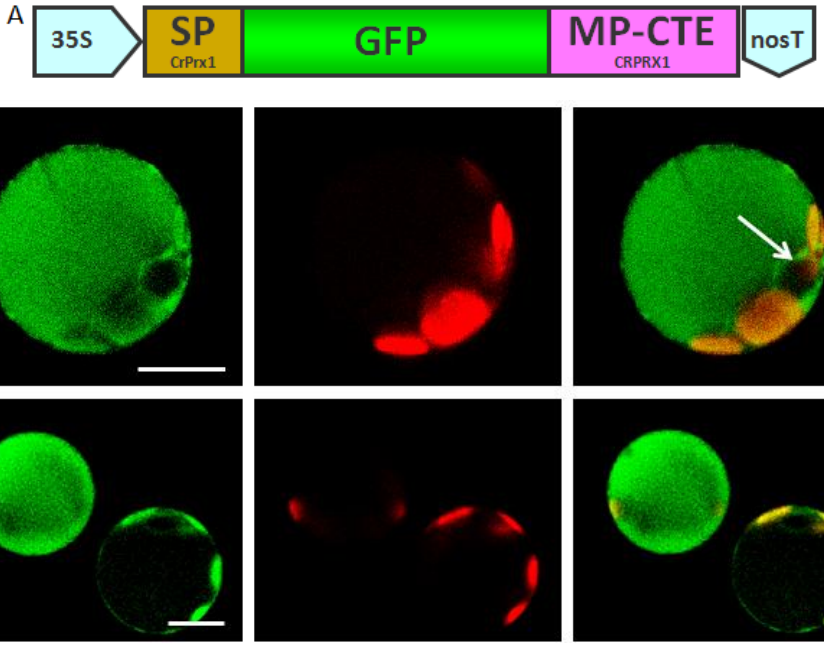

Figure 57. Transient transformation of *C. roseus* protoplasts with SP_{CrPrx1}-GFP-MP-CTE_{CrPrx1} fusion (C5), observed under the confocal microscope. A. Schematic representation of the 35S::SP_{CrPrx1}-GPF-MP-CTE_{CrPrx1} construct (C5). In this case, GFP also accumulates in the large central vacuole. Arrow points to the perinuclear ER. Left - GFP channel; Middle – Red channel showing chloroplast autofluorescence; Right – merged images. Bars = 10 µm. Magnification = 40x.

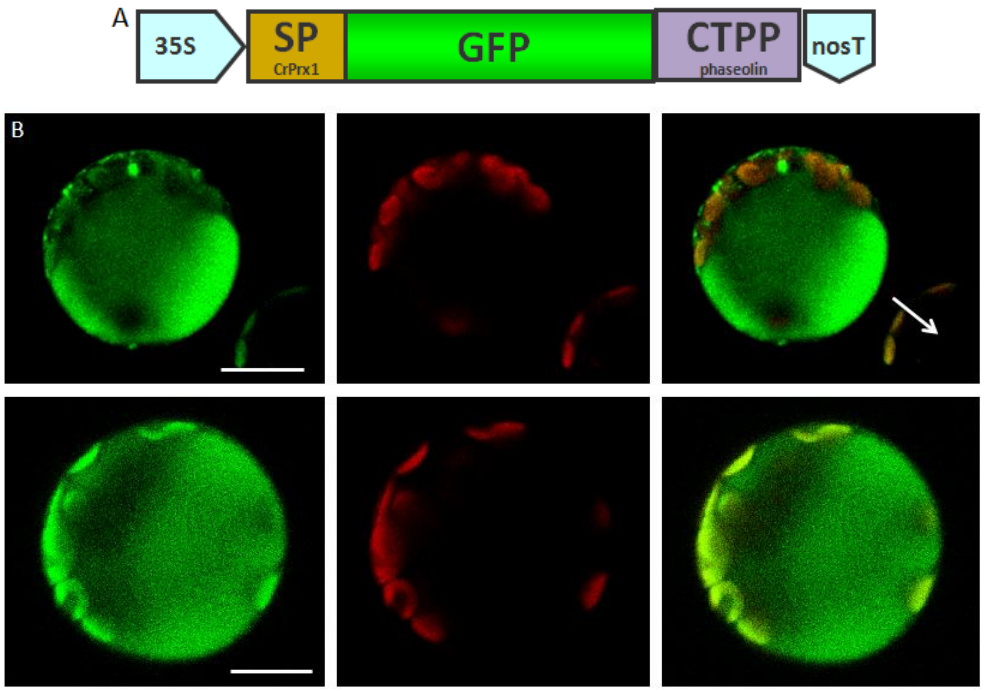

Figure 58. Transient transformation of *C. roseus* protoplasts with vacuole control-GFP fusion, observed under confocal laser-scanning microscopy. A. Schematic representation of the 35S::SP_{CrPrx1}-GPF- $CTPP_{Phaseolin}$ construct. B. GFP target to the vacuole. Arrow is poiting to a nontransformed cell next to an undoubtedly transformed cell. Left - GFP channel; Middle – Red channel showing chloroplast autofluorescence; Right – merged images. Bars = 10 µm. Magnification = 40x.

3.6.2. Transformation efficiency and protoplast survival rates

The survival rate for *C. roseus* protoplasts was also determined, in two single experiments, one in April and the other in June (Figure 59). The survival rate of transformed protoplasts with C1, in April, was 78%. From those 78 % of protoplasts that survived the transformation process, 40% of were successfully expressing cytoplasmic GFP. In this experience, exposure to PEG was not considered.

For the experience conducted in June (Figure 59), a 40% cell survival was observed for the protoplasts that weren't exposed to PEG, this parameter decreased to 20% for the protoplasts exposed to PEG, and for 36% for protoplasts transformed with the C1 construct. Apparently, in this case, the incubation with DNA of the protoplasts-PEG mixture seems to introduce some protective effect, since the survival rate for protoplasts transformed with C1 is actually similar to the protoplasts not exposed to PEG. 22% of the 36% of protoplasts that survived the transformation process were expressing successfully GFP cytoplasmic. These results show that the life span of

transformed protoplasts is short, but nevertheless, long enough to successfully transiently express fusion proteins in order to study subcellular localisation, protein-protein interactions, etc.

Therefore, in *C. roseus*, protoplast survival rates and transformation efficiencies seem to vary considerably between experiments, which may be due to plants being in a different physiological state due to slightly different developmental stages of environmental conditions between the two experiments.

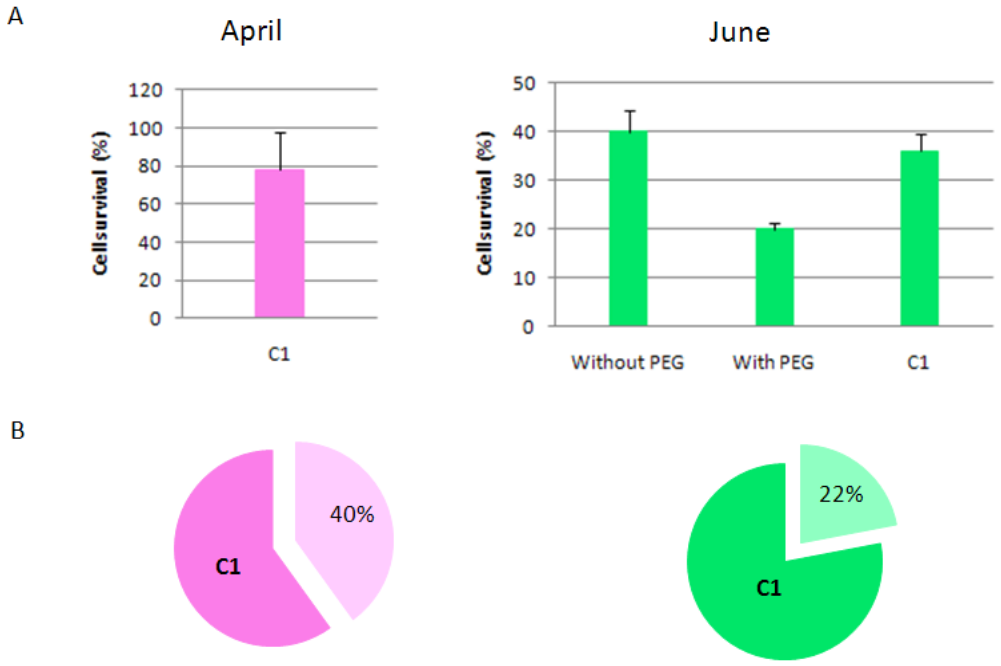

Figure 59. Quantitative data for PEG-mediated transformation *C. roseus* protoplasts. A. Cell survival rate for untransformed protoplasts not exposed and exposed to PEG (without and with PEG, respectively), and for protoplasts submitted to the complete protocol of transformation with C1 construct. B. Transformation rate of protoplasts with C1 construct. Statistical data calculated from an average of single experiments performed in April and June.

3.7. *Agrobacterium*-mediated transformation of *Arabidopsis* leaves

The *Agrobacterium*-mediated transient gene expression in intact plant leaves is another rapid and useful method of analysis of gene expression *in vivo*. In this work, two different approaches were used to attempt *Agrobacterium* infiltration of *Arabidopsis* leaves: $MgCl_2$ infiltration method and Di Fiore-based method (see section 2.9.). However, neither was successful, and only the results obtained from the first approach are showed as an example.

The method used is based in a simple method ordinarily used to Agro-infiltrate tobacco leaves using an $MgCl_2$ infiltration buffer. *Arabidopsis* leaves were infiltrated with a $SP2_{AtPrx34}$-GFP fusion cloned in a modified version of the binary plasmid pGreen II containing GFP as a reporter gene. In this case, theoretically, GFP should label subcellular compartments in the secretory pathway, namely ER, Golgi or cell wall. Labelling of the vacuole was not expected due to the absence of the putative vacuolar sorting signal – $CTE_{AtPrx34}$. The results obtained can be observed in Figure 60 and, unfortunately, in all cases, a convincing GFP signal was never observed. Most of the green fluorescence observed actually co-localizes with chloroplasts, meaning that fluorescence detection is being made at a level that the signal detected is actually mostly coming from autofluorescence.

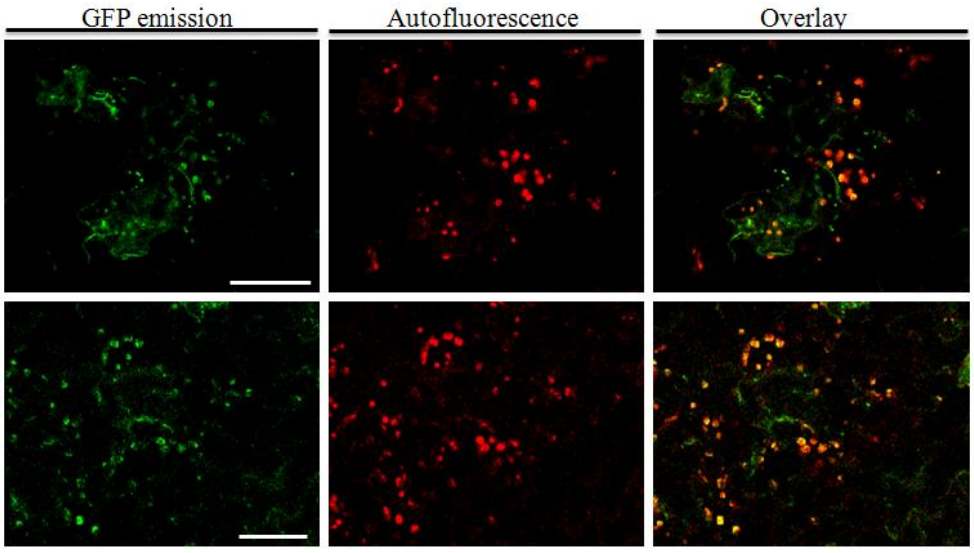

Figure 60. Transient Transformation of *Arabidopsis* leaves infiltrated with *A. tumefaciens* harbouring a $SP2_{AtPrx34}$-GFP construct (GV3101), observed under the confocal laser-scanning microscopy. *Agrobacterium* infiltration was performed in $MgCl_2$ buffer. Left - GFP channel; Middle – Red channel showing chloroplast autofluorescence; Right – merged images. Bars = 10 µm. Magnification = 40x.

RFP-fusions designed to assess the vacuolar-targeting capacity of the CTE of another *C. roseus* Prx, CrPrx3, (table 3, see section 2.1.1.) were also used, since the constructs were available in the lab in a binary vector which could therefore be used for *Agrobacterium* transformation. Again, no positive results were obtained, and therefore, no data is presented here.

3.8. *Agrobacterium*-mediated transformation of *C. roseus* leaves

Agroinfiltration of *C. roseus* leaves was performed with material from several sources, namely: leaves from seedlings, leaves from healthy young plants, leaves from adult flowering plants, and leaves from *in vitro* regenerated plants (from mature zygotic embryos).

The same two different approaches, $MgCl_2$ infiltration method and Di Fiore-based method, were also used to attempt Agro-infiltration in *C. roseus* leaves (see section 2.9.), however in this case only the Di Fiore-based method was successful, and just in one attempt, when young regenerated *in vitro* plants were used. This method has a more complex procedure to induce virulence, and uses a bacteria suspension 10 times more concentrated that may explain the relative success. Leaf epidermis of *in vitro* regenerated plants was infiltrated by the syringe method with an *Agrobacterium* clone harbouring $SP2_{AtPrx34}$-GFP fusion.

Although only one cell appeared to be transformed, the use of *in vitro* plants can represent a starting point to further optimizations of this protocol, but at this stage a milestone was achieved: transient expression in *C. roseus* leaves was also accomplished. This fact reveals the potential of this transient expression methodology, after complete optimization. An evident fluorescent signal was observed for at least one cell, showing an ER distinctive pattern (Figure 61B, arrow).

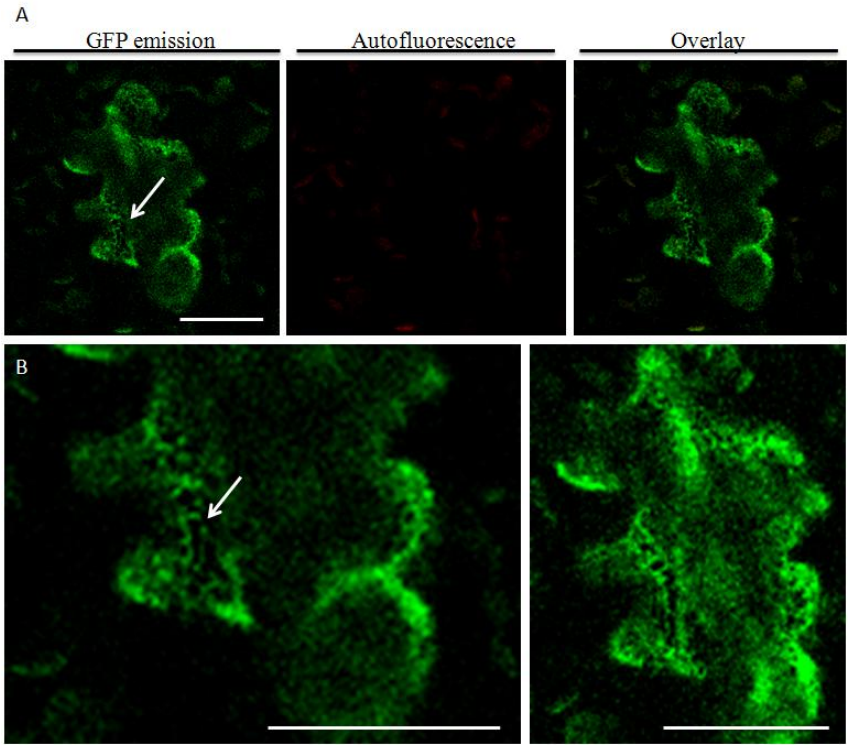

Figure 61. Transient transformation of *C. roseus* leaves infiltrated with *A. tumefaciens* harbouring a $SP2_{AtPrx34}$-GFP construct (GV3101), observed under the confocal laser-scanning microscopy. *Agrobacterium* infiltration was performed in MMA buffer. A. At least one cell appeared transformed and showing GFP fluorescence mainly in the ER. B. Magnification of the same cell as in A. Bars = 20 µm . Magnification = 40x.

The RFP-fusions designed to assess the vacuolar-targeting capacity of the CrPrx3 CTE (table 3, section 2.1.1.) were also used but no positive results were obtained.

Discussion

4. Discussion

Here, we have put to work efficient and reproducible protocols for the PEG-mediated transformation of *Arabidopsis* and *C. roseus* leaf protoplasts, and we have shown its suitability for the investigation of the subcellular and vacuolar sorting of proteins by using GFP fusions. Namely, subcellular sorting of several Prx-GFP fusions was confirmed or investigated. Transient expression by agroinfiltration of leaves of the two plants was also tried with only limited success, but some future improvements may be foreseen.

In this work, we managed to successfully isolate protoplasts from *A. thaliana* and *C. roseus* leaves (Figure 40 and 41, Chapter 3). Several factors influence protoplast release and recovery at different steps of the isolation method, namely plant growth conditions and digestion of cell walls (enzyme solution, time of digestion) (Abel & Theologis 1994; Mi Jeon et al. 2007; Yoo et al. 2007). In fact, plants are very sensitive to all kinds of environmental changes, e.g., drought, flooding, extreme temperature and constant mechanical perturbation, so a constant environment should be maintained when growing plants to use for protoplast isolation, which was done in this work. Selection of healthy leaves at a proper developmental stage is also a very important factor for the success in experiments involving protoplasts. Protoplasts prepared from leaves grown under stress conditions may look similar to those obtained from healthy leaves, however they can exhibit low transformation efficiency rates (Yoo et al. 2007). In this work, protoplast isolation was almost always obtained with high recovery of protoplast cells, meaning that the developmental stage and growing conditions were well adapted to this objective. For *Arabidopsis*, non-flowering healthy plants were always used (stage 4 of development as defined by Boyes et al. 2001 and for *C. roseus*, well expanded dark green leaves, usually from the 2^{nd}-3^{rd} pairs of healthy flowering plants were also used with success.

When isolating protoplasts, the time of incubation in the enzyme solution depends on enzyme concentration and the type of material used. For *A. thaliana* col. 0 leaves, 3 h of digestion in the enzyme solution (28ºC, in the dark), were enough to release most protoplasts from the leaf strips. However, the efficiency of protoplast isolation differs significantly for different ecotypes and genotypes (Yoo et al. 2007). In the case of *C.*

roseus, due to the composition and the higher thickness of the cell wall, an O.N. incubation in enzyme solution was required and a more complex enzymatic cocktail was used. Immediate dipping and submerging of the leaf strips after cutting is also critical to obtain a higher protoplast yield (Yoo et al. 2007). When leaf strips are dried out, the enzyme solution cannot penetrate and the protoplast yield decreases significantly. Another important requisite about the enzymatic solution is that it must be prepared fresh (Yoo et al. 2007).

Protoplasts must be used as soon as possible after their isolation. However, they are stable and can be kept on ice for a few hours prior to use. Fresh and healthy protoplasts should remain intact throughout the isolation and transformation procedures (Yoo et al. 2007). One major limitation of the protoplast system includes the variation of protoplast transformation frequency that occurs both within and between experiments. Therefore, this system may be of limited value for quantitative analysis. In fact, we observed a large difference in the survival rate (78 / 40%) and transformation efficiency (40 / 22%) between the two experiments perfomed for *C. roseus*. Relatively to *Arabidopsis* experiments no variations were observed.

PEG stimulates the uptake of DNA into plant protoplasts allowing transient expression of foreign genes (Mathur & Koncz 1998; Mi Jeon et al. 2007). The advantage of PEG is that no expensive technical equipment is needed and that no major adaptation for different protoplast origins is required (Yoo et al. 2007). Similarly to the protoplast isolation procedure, some critical factors influence the efficiency and stability of PEG-mediated transformation. Nevertheless, the concentration of the PEG solution, the incubation time of the protoplast/DNA/PEG mixture, and the plasmid to protoplasts ratio may have to be optimized. In this work, the procedure described in Yoo *et al.* (2007) was followed with minor changes. A higher concentration of PEG and lower molecular weights of PEG might favor higher gene expression (Mi Jeon et al. 2007). For example, some protocols use 40% (w/v) PEG-4000 solution while others opt by 25% (w/v) PEG-6000. In this work, we used a 40% (w/v) PEG-4000 solution, but the ultimate requisite about the PEG solution is that it must be prepared and used within 5 days otherwise the transformation will simply not occur.

The pDNA:protoplast ratio must be optimized, depending on the reporter's sensitivity. A highly sensitive reporter needs only half the amount of pDNA. In this work, we started with 10 µg of pDNA to transform $2x10^4$ protoplasts. This amount was

afterwards doubled (20 µg) for all constructs, except for cytoplasmic GFP (C1) that worked perfectly even with half the amount of pDNA. Cytoplasmic GFP always exhibited a strong fluorescence, appearing much brighter and intense than the remaining fusions. On the other hand, an interesting decrease in fluorescent signal was observed as more target sequences were added to the vector, both in *Arabidopsis* and *C. roseus* protoplasts. Records of confocal observations of *C. roseus* protoplasts expressing C3, C4 and C5 (Figure 55-57, respectively; Chapter 3) had to be acquired at maximum laser power and with increased gain, in a few cases resulting in some bleed-through of the red signal (chloroplast autofluorescence). Nevertheless, even in these cases the localization and intensity of the GFP signal was unequivocal. This decrease of fluorescence associated with the increase of the GFP-fusion protein may result from an increased influence in the conformation of GFP responsible for fluorescence, but may also have to do with the influence of the environmental conditions of the different target compartments.

It is noteworthy that whenever GFP was localized in the large central vacuole – CrPrx1 C3 / C5 and the vacuolar marker, the fluorescence was dimmer when compared to the one observed for GFP in other compartments of the secretory pathway. One can hypothesize that the amount of GFP necessary to produce a strong signal in such a large compartment like the vacuole has to be much higher than the one necessary to produce a strong signal in the cytoplasm, ER or secretory pathway vesicles. Another explanation for the decreased fluorescence in the vacuole relates to the luminal pH of this organelle. It is well established that throughout the secretory pathway there is a pH gradient, with higher values for the ER and lower values in the acidic vacuole. In fact, Tamura et al. (2003) showed that light induced the import of H^+ to the vacuole by action of H^+-ATPases, leading to a decrease in pH in this organelle which affected GFP stability and fluorecence. The same authors found that vacuolar-targeted GFP only fluoresced in the vacuole if the plants were placed in the dark for 2 days. The fluorescence on the ER network and of small granular structures within the cytosol was not affected by exposure to light conditions (Tamura et al. 2003). These authors also found that leaf epidermal cells showed a lower fluorescent intensity than root cells, suggesting that the vacuoles of the leaf cells have a higher GFP degradation activity than those of the roots.

Therefore, in this work, and in order to avoid loss of the vacuolar GFP signal, transformed protoplasts were always kept in the dark for 2 days prior to observation.

Althoughonly vacuolar GFP fluorescence seems to be affected by light, all samples were kept in the dark regardless of the construct, to maintain the same incubation conditions. The constant higher fluorescence observed for the vacuolar constructs whenever expressed in *Arabidopsis* (in comparison to *C. roseus*), may also point out to different characteristics of the vacuoles in these two species, namely regarding pH values.

Focusing on the set of CrPrx1-GFP constructs used in this work, both SP-GFP, targeted to the ER – Golgi - cell wall, and GFP targeted to the vacuole, (i.e., whenever the CTE of CrPrx1 was present), sometimes led to the observation of spheroid structures showing bright green fluorescence, besides the ER or the vacuoles, respectively. For the CTE constructs, the vacuolar localization of GFP was unmistakable and it was further validated using the vacuolar control containing the CTPP of phaseolin. However, the identification of the smaller fluorescent structures was not confirmed using specific markers. These may be Golgi or intermediate compartments of the secretory pathway. Inside a plant cell, besides the central vacuole, multivesicular bodies, prevacuolar compartments and/or storage protein-containing vacuoles may co-exist in a single cell (Neuhaus & Rogers 1998). Fluckiger et al. 2003 reported different aspects of the vacuolar system in *Arabidopsis*, related to cell differentiation and environment, and identified the presence of different types of vacuoles – lytic (LV) and protein storage (PSV), and pre-vacuolar compartments (PVCs), a composition that changes during cell development. Later, Hunter et al. 2007 reported that mature *Arabidopsis* cells only contain LVs and that PSVs are restricted to the first three days of seed germination.

In this work the vacuolar localization of CrPrx1 was further confirmed, using two PEG-mediated protoplast transformation/expression systems – one homologous (*C. roseus*) and another heterologous (*A. thaliana*). The fact that the CrPrx1-GFP fusions were only localized in the vacuole whenever the CTE of this protein was present, unmistakably shows that the vacuolar sorting determinant(s) of CrPrx1 is located in the CTE domain of this protein. Additionally, placing the CrPrx1 CTE at the C-terminus of GFP sorted the FP to the vacuole, meaning that this domain is necessary and sufficient to target a protein to the central vacuole. The observation of the same fluorescence pattern when using the same constructs in the two expression systems, *Arabidopsis* and

C. roseus, suggests a conserved mechanism for the recognition and sorting of soluble proteins to the vacuole in different plant species.

Our next goal was to investigate the subcellular localization of AtPrx34 (Carqueijeiro 2008), and whether the CTE present represent a vacuolar sorting signal. In *A. thaliana*, only 10 out of the 73 identified Prx in the plant's genome possess a CTE and are therefore putatively vacuolar (Welinder et al. 2002). To try to answer this question we decided to study the subcelular sorting of AtPrx34, the main leaf Prx in *Arabidopsis*, purified in our lab (Carqueijeiro 2008). AtPrx34 was actually previously identified as vacuolar in a report describing the *Arabidopsis* vacuole proteome (Carter et al. 2004). To investigate the subcellular sorting determination of AtPrx34, its amino-acid sequence was analyzed for the presence of putative sorting signals, and as a result, two were identified (Figure 22, Chapter 3). A signal peptide (SP) that should target the protein to the secretory pathway (ER), and a CTE present in all vacuolar Prxs identified so far, proved to be the vacuolar sorting signal in the case of CrPrx1 (Costa et al. 2008 and results presented here). The presence of vacuolar sorting signals in soluble proteins (usually carried within a propeptide) determines receptor recognition within the lumen of the secretory pathway and consequentially selective transport to the vacuole (Welinder et al. 2002; Carter et al. 2004). To determine whether the SP of AtPrx34 targets an otherwise cytoplasmic GFP marker to the secretory pathway, and if the CTE is sufficient for the vacuolar targeting of AtPrx34, both the putative SP and various sequences of AtPrx34 [CTE, complete protein (MP-CTE), mature protein (MP)] were fused to the C-terminus of sGFP and used for transient expression in *Arabidopsis* protoplasts mediated by PEG.

For the first AtPrx34-GFP set of fusion constructs, GFP always appeared to be localized in the cytoplasm (Figure 49, Chapter 3). This led us to think that probably the region selected to be used as SP for AtPrx34 ($SP1_{AtPrx34}$) was not successfully targeting GFP to the secretory pathway. A reason for such a result could be that the region selected as SP, which ended just one amino acid after the predicted cleavage site, was not being recognized by the ER endopeptidase, and consequently the fusion protein finished to be synthetized by the ribosomes at the cytosol, with translocation to the ER being compromised. With this hypothesis in mind, we decided to generate a second AtPrx34-GFP set of fusions, with a longer SP region ($SP2_{AtPrx34}$) that ended 15 amino acids after the predicted cleavage site. Unfortunately, still no fluorescent signal was ever

observed in the secretory pathway (ER/Golgi/intermediate compartments) (Figure 50, Chapter 3). In a reduced number of cells, bright spots were seldom observed, but in these cases the fluorescent signal was always very weak and bleed-through of the red channel occurred. However, the same SP sequence ($SP2_{AtPrx34}$), cloned in a binary vector (pGreenII) modified to contain eGFP, and used to agroinfiltrate *C. roseus* leaves, revealed GFP fluorescence in an ER like pattern (Figure 61, Chapter 3). Indeed, previous results obtained in our lab with agroinfiltration of tobacco leaf epidermis showed the same results (unpublished data). All together, these results seem to validate the $SP2_{AtPrx34}$ sequence as a SP, and points to possibly some undetected problem with the pTH2 plamid constructions. In any case, evidence that AtPrx34 is vacuolar is still lacking and further experiences must be conducted to confirm this hypothesis. The identification of the CTE as the vacuolar sorting signal of AtPrx34 would be very important since it would lead to the identification for the first time of a ct-VSD in a protein of *Arabidopsis thaliana*.

Summarizing, a PEG-mediated transformation protocol of *Arabidopsis* and *C. roseus* protoplasts was successfully set up and revealed to be a trustworthy transient expression assay, in which highly reproducible results were achieved, and a satisfactory transformation rate was also obtained (more the 20% in all cases). However, some modifications could probably still be done to increase both cell survival and transformation rates. Namely, the medium where the protoplasts are incubated until the observation could be changed to a medium containing also an osmolarity agent, as mannitol, to reduce protoplast bursting. The buffer M/W5 could be a plausible substitute for this purpose.

Agrobacterium-mediated transient assays have become the favorite choice in many functional analyses and, in particular, leaf agroinfiltration represents nowadays an easy and non-invasive technique for investigating sub-cellular localization and intracellular trafficking of gene products. However, such a wide spread technique has only very seldom been reported for any of the two plant systems used in this work.

In order to validate and improve our agroinfiltration protocol for successful subcellular localization analyses, *Arabidopsis* and *C. roseus* leaves were agroinfiltrated with *Agrobacterium* harbouring plasmids with GFP and RFP constructs. The constructs used were $SP2_{AtPrx34}$-GFP and a set of CrPrx3-RFP constructs. CrPrx3 as already

mentioned, is a Prx present in *C. roseus* roots, previously identified and purified in our lab. This Prx also possesses a CTE, therefore it is potentially vacuolar.

Regardless the variety of available constructs and Agrobaterium strains, all attempts of transient expression through Agro-infiltration of *Arabidopsis* leaves proved unsuccessful, and the same happened with all but one attempt with *C. roseus* leaves.

Nevertheless, it is worthy to point out that RFP fusions expressed in green cells (aerial parts of the plant) are usually hard to observe if using a regular fluorescence microscope under which the RFP signal and chloroplast auto-fluorescent are practically undistinguishable. The use of an ultra spin confocal microscope overcomes this difficulty, and RFP (mRFP in the case of this work) is a better choice when the expected subcellular localization of a fusion is the vacuole, since RFP is brighter and more stable than GFP in this organelle (Duarte et al. 2010).

Given that *Arabidopsis* is not recalcitrant to *Agrobacterium* transformation (M. J. Kim et al. 2009), it is expected that maybe the use of diverse strains of *Agrobacterium*, different bacterial titres and even distinct infiltration buffers could eventually result in a positive result. There are also the need to test further developmental stages and possibly incubation conditions of the plants, since tobacco plants are actually susceptible to agroinfiltration if they are grown under very specific light and temperature conditions (Duarte et al. 2008).

Agroinfiltration of *C. roseus* leaves was performed with material from several sources, namely: leaves from seedlings, leaves from healthy young plants, leaves from adult flowering plants, and leaves from *in vitro* regenerated plants (from mature zygotic embryos). Vacuum infiltration with the bacterial suspension was also carried out, besides syringe infiltration. Actually, difficulties were already expected when transforming *C. roseus* leaves with *Agrobacterium* since this species has been reported to be recalcitrant to *Agrobacterium* transformation (Zárate & Verpoorte 2007). In fact, most of the successful reports of *Agrobacterium* transformation of *C. roseus* were done with roots and *A. rhizogenes* (Ayora-Talavera et al. 2002; Hughes, Hong, Gibson, Shanks & San 2004a; Hughes, Hong, Gibson, Shanks & San 2004b), and transient or stable expression in *C. roseus* is usually performed by particle bombardment of cells (Duarte et al. 2010). In spite of all this, we were able to successfully transiently express the $SP2_{AtPrx34}$-GFP construct in leaves from *in vitro* regenerated *C. roseus* plants, using a method previously described by Di Fiore et al. 2004. As expected, the SP2 of AtPrx34

directed GFP to the secretory pathway and this was translated by the observed localization of GFP in an ER distinctive pattern (Figure 61, Chapter 3). Zottini et al. 2008 showed that the problem raised by different susceptibility of distinct cultivars towards *Agrobacterium* infection, and recalcitrance of several species to *Agrobacterium* transformation, can be overcome by infiltrating leaves resulting from *in vitro* regenerated plants. In this work, we have shown that this seems to be also true for *C. roseus*. All **plants** have defense systems to **protect** them against external agents (Huckelhoven 2007) and growing plants *in vitro*, where all environment factors are controlled, and plants are not exposed to stress conditions, seems to constitute a way to obtain a positive response to an *Agrobacterium* infection. Over all, the results we obtained were highly promising and represent another successful goal of this work.

To finish, some topics must be considered when *Agrobacterium* transformation is the preferred method. The genetic background and plant growth conditions are key factors in performing successful leaf agroinfiltration experiments, as it was proved above. The compatibility of *Agrobacterium* strains with the plant species represents another important variable to be considered in this kind of assay. Three bacterial strains were used to induce transient gene expression, GV3101, EHA105 and LBA4404, and only the first one was successful. Infiltration via syringe induced mechanical damage due to the pressure applied to leaves during manipulation. This led in some cases to restricted areas of necrosis that can result in an overproduction of phenolic compounds by the plant that instead of inducing *Agrobacterium* infection could in fact kill the bacteria (Franklin et al. 2008). The concentration of acetosyringone and the composition of the infiltration medium can also affect the outcome of transient gene expression mediated by *Agrobacterium*.

Conclusions and Final Remarks

5. Conclusions and final remarks

The intent of this work was to develop an efficient and straightforward approach that will allow, among others, to systematically unravel the subcellular localization of enzymes involved in the *C. roseus* TIA biosynthetic pathway, *in vivo* and through a simple transient expression system. Furthermore, the universality of the CTE as a vacuolar sorting determinant for Prxs was studied, using as examples a well characterized enzyme (CrPrx1), and the most abundant Prx in *Arabidopsis* leaves (AtPrx34).

The successful establishment of PEG-mediated transformation of *Arabidopsis* and *C. roseus* mesophyll protoplasts was reported herein, and validated as an excellent transient expression system. Application of this methodology in these two important plant models will allow the rapid testing of the subcellular localization of proteins of interest, sorting capability of protein regions encoded by selected candidate genes of interest, and also of protein-protein interactions, namely between Prxs and putative interacting proteins for which there are several candidates, etc.

Transient expression by agroinfiltration revealed a much more difficult technique to implement than protoplast transformation, and only in one instance it worked, when using *in vitro C. roseus* plants. Plant developmental stage and environmental constions are probably crucial to the success of this technique, a sthey were not yet found for *Arabidopsis* and *C. roseus*.

The vacuolar sorting capacity of the CrPrx1 CTE was further demonstrated in our work, but it was not possible to obtain conclusive results for AtPrx34, since in this case, all the GFP fusions generated for protoplast transformation were sorted to the cytoplasm and not to the secretory system, as expected. This is probably due to some malfunctioning of the vector plasmid used for protoplast infiltration, since agroinfiltration of *C. roseus* in vitro plants showed, as expected, sorting to the ER of an SP-AtPrx34 construct harboured in a binary vector plasmid (used for *Agrobacterium*-mediated transformation but not PEG-mediaed transformation).

The transient expression assays described in the present study constitute reliable and inexpensive methods that can be performed in most labs, and that are suitable test-systems to characterize genes of unknown function or candidate genes to a specific

function, such as candidate genes implicated in the TIA biosynthetic pathway in C. roseus. The use of the transient expression methods optimized in this work will definitely contribute to the study of candidate genes identified *in silico* or by omic approaches, in both plant systems tested. It is clear that both methodologies, PEG-mediated transformation of protoplasts and *Agrobacterium* infiltration of leaves, also have disadvantages, but together, these transient expression techniques are extremely useful tools for characterization of subcellular localization and protein-protein interactions of uncharacterized proteins, and are also useful for evaluating expression of recombinant plant proteins in vivo, and to the analysis of protein function before committing to time-consuming generation of transgenic plants.

References

6. References

Abel, S. & Theologis, A., 1994. Transient transformation of Arabidopsi leaf protoplasts: a versatile experimental system to study gene expression. *The Plant Journal*, 5(3), pp.421-427.

Almagro, L. et al., 2009. Class III peroxidases in plant defence reactions. *Journal of Experimental Botany*, 60(2), pp.377-390.

Ayora-Talavera, T. et al., 2002. Overexpression in *Catharanthus roseus* hairy roots of a truncated hamster 3-hydroxy-3-methylglutaryl-CoA reductase gene. *Appl ed Biochemistry and Biotechnology*, 97(135-145).

Barcelo, P. & Lazzeri, P.A., 1998. Direct gene transfer: chemical, electrical and physical methods. In *Transgenic Plant Research*. pp. 35-55.

Bent, A.F., 2000. Transformation *Arabidopsis* in Planta Transformation . Uses , Mechanisms , and Prospects for Transformation of Other Species. *Plant Physiology. Update on Plant*, 124, pp.1540-1547.

Boyes, D.C. et al., 2001. Growth Stage – Based Phenotypic Analysis of *Arabidopsis*: A Model for High Throughput Functional Genomics in Plants. *The Plant cell*, 13, pp.1499-1510.

Cardoso, L., 2009. Transformation and regeneration of the medicinal plant *Catharanthus roseus*. *Master Thesis, UTAD*.

Carqueijeiro, I., 2008. Behaviour of class III peroxidases from leaves of *Arabidopsis* thaliana during biotic stress. Master thesis, Faculty of Sciences of the University of Porto.

Carter, C. et al., 2004. The Vegetative Vacuole Proteome of *Arabidopsis* thaliana Reveals Predicted and Unexpected Proteins. *The Plant Cell*, 16, pp.3285-3303.

Chiu, W.-ling et al., 1996. Engineered GFP as a vital reporter in plants. *Current Biology*, 6(3), pp.325-330.

Chowrira, G.M., Akella, V. & Lurquin, P.F., 1995. Electroporation-mediated gene transfer into intact nodal meristemsin planta. *Molecular biotechnology*, 3(1), pp.17-23.

Corpet, F., 1988. Multiple sequence alignment with hierarchical - clustering. *Nucleic acids research*, 16(22), pp.10881-10890. Cosio, C. & Dunand, C., 2008. Specific

functions of individual class III peroxidase genes. *Journal of Experimental Botany*, 16, pp.1-18.

Costa, M.M.R. et al., 2008. Molecular Cloning and Characterization of a Vacuolar Class III Peroxidase Involved in the Metabolism of Anticancer Alkaloids in *Catharanthus roseus* 1 [C]. *Plant Physiology*, 146, pp.403-417.

Crossway, A. et al., 1986. SpringerLink - Molecular and General Genetics MGG, Volume 202, Number 2. *MGG Molecular & General Genetics*, 202(2), pp.179-185.

Dessaux, Y., Petit, A. & Tempé, J., 1992. Opines in *Agrobacterium* biology. In *Verma DPS (ed) Molecular signals in plant-microbe communications*. p. 109–136.

Dewick, P.M., 2002. *Medicinal Natural Products: A Biosynthetic Approach*,

Di Fiore, S. et al., 2004. Transient Gene Expression of Recombinant Terpenoid Indole Alkaloid Enzymes in *Catharanthus roseus* Leaves. *Plant Molecular Biology Reporter*, 22, pp.15-22.

Duarte, P., Memelink, J. & Sottomayor, M., 2010. Fusion with Fluorescent Proteins for subcellular localization of enzymes involved in plant alkaloid biosynthesis. In *Plant Secondary Metabolism Engineering. Methods and applications*. pp. 215-290.

Duarte, P., Pissarra, J. & Moore, I., 2008. Processing and trafficking of a single isoform of the aspartic proteinase cardosin A on the vacuolar pathway. *Planta*, 227(6), pp.1255-1268.

Dupree, P. & Sherrier, D.J., 1998. The plant Golgi apparatus. *Biochimica et Biophysica Acta*, 1404, pp.259-270.

El-sayed, M. & Verpoorte, R., 2007. Catharanthus terpenoid indole alkaloids: biosynthesis and regulation. *Phytochemistry Reviews*, 6, pp.277-305.

Emanuelsson, O. et al., 2007. Locating proteins in the cell using TargetP, SignalP and related tools. *Nature protocols*, 2(4), pp.953-71.

Facchini, P.J., 2001. Alkaloid Biosynthesis in Plants: Biochemistry , Cell Biology , Molecular Regulation , and Metabolic Engineering Applications. *Annual Review in Plant Physiology*, 52, pp.29-66.

Faye, L. et al., 2005. Protein modifications in the plant secretory pathway: current status and practical implications in molecular pharming. *Vaccine*, 23(15), pp.1770-8.

Finer, J.J., Finer, K.R. & Santarém, E.R., 1996. Plant Cell Transformation, physical methods for. In *MEYERS, R.A. Encyclopedia of Molecular Biology and Molecular Medicine.*

Fluckiger, R. et al., 2003. Vacuolar system distribution in *Arabidopsis* tissues, visualized using GFP fusion proteins. *Journal of Experimental Botany*, 54(387), pp.1577-1584.

Foresti, O. et al., 2008. Protein Domains Involved in Assembly in the Endoplasmic Reticulum Promote Vacuolar Delivery when Fused to Secretory GFP, Indicating a Protein Quality Control Pathway for Degradation in the Plant Vacuole. *Molecular Plant*, 1(6), pp.1067-1076.

Framond, A.J. de, Barton, K.A. & Chilton, M.-D., 1983. Ti: A New Vector Strategy for Plant Genetic Engineering. *Nature Biotechnology*, 1(3), pp.262-269.

Franklin, G. et al., 2008. Hypericum perforatum plant cells reduce *Agrobacterium* viability during co-cultivation. *Planta*, 227(6), p.1401–1408.

Frigerio, Lorenzo et al., 2001. Influence of KDEL on the Fate of Trimeric or Assembly-Defective Phaseolin: Selective Use of an Alternative Route to Vacuoles. *The Plant cell*, 13, pp.1109-1126.

Fromm, M., 1985. Expression of genes transferred into monocot and dicot plant cells by electroporation. *Proceedings of the National Academy of Sciences*, 82(17), pp.5824-5828. Available at: http://www.pnas.org/cgi/content/abstract/82/17/5824.

Gelvin, S.B., 2009. *Agrobacterium* in the Genomics Age. Update on Genomics of *Agrobacterium*-Mediated Plant Transformation. *Plant Physiology*, 150, pp.1665-1676.

Gelvin, S.B., 2003. *Agrobacterium*-Mediated Plant Transformation: the Biology behind the " Gene-Jockeying " Tool. *Microbiology and Molecular Biology Reviews*, 67(1), pp.16-37.

Guirimand, G. et al., 2009. Optimization of the transient transformation of *Catharanthus roseus* cells by particle bombardment and its application to the subcellular localization of hydroxymethylbutenyl 4-diphosphate synthase and geraniol 10-hydroxylase. *Plant Cell Reports*, 28(8), pp.1215-1234.

Gutensohn, M. et al., 2006. Toc, Tic, Tat et al.: structure and function of protein transport machineries in chloroplasts. *Journal of plant physiology*, 163(3), pp.333-47.

Hawes, C. & Satiat-Jeunemaitre, B., 2005. The plant Golgi apparatus--going with the flow. *Biochimica et biophysica acta*, 1744(3), pp.466-80.

Helenius, A. & Aebi, M., 2001. Intracellular Functions of N-Linked Glycans. *Science*, 291(5512), pp.2364-2369.

Hellens, R. et al., 2000. pGreen: A versatile and flexible binary Ti vector for *Agrobacterium*-mediated plant transformation. *Plant Molecular Biology*, 42, p.819–832.

Hiraga, S. et al., 2001. A Large Family of Class III Plant Peroxidases. *Plant Cell Physiology*, 42(5), pp.462-468.

Hoekema, A. et al., 1983. A binary plant vector strategy based on separation of vir- and T-region of the *Agrobacterium* tumefaciens Ti-plasmid. *Nature*, 303(5913), pp.179-180. Available at: http://dx.doi.org/10.1038/303179a0.

Huckelhoven, R., 2007. Cell Wall – Associated Mechanisms of Disease Resistance and Susceptibility. *Annual Review in phytopathology*, 45, pp.101-127.

Hughes, E. et al., 2004a. Expression of a feedback-resistant anthranilate synthase in *Catharanthus roseus* hairy roots provides evidence for tight regulation of terpenoid indole alkaloid levels. *Biotechnology and Bioengineringeering*, 86, p.718–727.

Hughes, E. et al., 2004b. Metabolic engineering of the indole pathway in *Catharanthus roseus* hairy roots and increased accumulation of tryptamine and serpentine. *Metabolic Engineering*, 6, p.268–276.

Hunter, P.R. et al., 2007. Fluorescent Reporter Proteins for the Tonoplast and the Vacuolar Lumen Identify a Single Vacuolar Compartment in *Arabidopsis* Cells. *Plant Physiology*, 145, pp.1371-1382.

Jolliffe, N.A., Craddock, C P & Frigerio, L, 2005. Pathways for protein transport to seed storage vacuoles. *Biochemical Society Transactions*, 33(5), pp.1016-1018.

Kim, M.J., Baek, K. & Park, C.-M., 2009. Optimization of conditions for transient *Agrobacterium*-mediated gene expression assays in *Arabidopsis*. *Plant Cell Reports*, 28, pp.1159-1167.

Kleizen, B. & Braakman, I., 2004. Protein folding and quality control in the endoplasmic reticulum. *Current Opinion in Cell Biology*, 16, pp.343-349.

La Riva, G. de et al., 1998. *Agrobacterium* tumefaciens: a natural tool for plant transformation. *Journal of Biotechnology*, 1(3), pp.118-133.

Loyola-Vargas, V.M., Galaz-Ávalos, R.M. & Kú-Cauich, R., 2007. Catharanthus biosynthetic enzymes: the road ahead. *Phytochestry Reviews*, 6, pp.307-339.

Matheson, L.A., Hanton, S.L. & Brandizzi, F., 2006. Traffic between the plant endoplasmic reticulum and Golgi apparatus: to the Golgi and beyond. *Current Opinion in Plant Biology*, 9, pp.601-609.

Mathur, J. & Koncz, C., 1998. PEG-Mediated Protoplast Transformation with Naked DNA. *Methods in Molecular Biology*, 82, pp.267-76.

Matsuoka, K., 2000. C-terminal propeptides and vacuolar sorting by BP-80-type proteins: Not all C-terminal propeptides are equal. *The Plant Cell*, 12, pp.181-182.

Matsuoka, K. & Neuhaus, J.-marc, 1999. Cis-elements of protein transport to the plant vacuoles. *Journal of Experimental Botany*, 50(331), pp.165-174.

Mi Jeon, J. et al., 2007. Efficient transient expression and transformation of PEG-mediated gene uptake into mesophyll protoplasts of pepper (Capsicum annuum L.). *Plant Cell Tissue and Organ Culture*, 88, pp.225-232.

Miller, E. & Anderson, M., 1999a. Reply: The role of BP-80 in sorting to the vacuole in stigmas. *The Plant cell*, 11, pp.2071-2073.

Miller, E. & Anderson, M., 1999b. Uncoating the mechanisms of vacuolar protein transport. *Trends in Plant Science*, 4, pp.46-48.

Morikawa, H. & Yamada, Y., 1985. Capillary Microinjection into Protoplasts and Intranuclear Localization of Injected Materials. *Plant Cell Physiology*, 26(2), pp.229-236. Available at: http://pcp.oxfordjournals.org/cgi/content/abstract/26/2/229.

Neuhaus, J.-marc & Rogers, J.C., 1998. Sorting of proteins to vacuoles in plant cells. *Plant Molecular Biology*, 38, pp.127-144.

Newell, C.A., 2000. Plant Transformation Technology: Developments and Applications. *Molecular Biotechnology*, 16, pp.53-65.

Nielsen, K.L. et al., 2001. Differential activity and structure of highly similar peroxidases. Spectroscopic, crystallographic, and enzymatic analyses of lignifying *Arabidopsis* thaliana peroxidase A2 and horseradish peroxidase A2. *Biochemistry*, 40(37), pp.11013-21.

Niwa, Y. et al., 1999. Non-invasive quantitative detection and applications of non-toxic, S65T-type green fluorescent protein in living plants. *The Plant Journal*, 18(4), pp.455-463.

Noble, R.L., 1990. The discovery of the vinca alkaloids-chemotherapeutic agents against cancer. *Biochem. Cell Biol.*, 68, pp.1344-1351.

Okita, T.W., 1996. Compartimentation of proteins in the endomembrane system of plant cells. *Annual Review in Plant Physiology*, 47, pp.327-350.

Otegui, M. et al., 2005. Senescence-associated vacuoles with intense proteolytic activity develop in leaves of *Arabidopsis* and soybean. *The Plant Journal*, 41(6), pp.831-44.

Oudin, A. et al., 2007. The iridoid pathway in *Catharanthus roseus* alkaloid biosynthesis. *Phytochestry Reviews*, 6, pp.259-276.

Palade, G., 1975. Intracellular aspects of the process of protein secretion. In *Physiology or Medicine, Nobel Lecture*. pp. 177-206.

Park, J.H., Oufattole, M. & Rogers, J.C., 2007. Golgi-mediated vacuolar sorting in plant cells: RMR proteins are sorting receptors for the protein aggregation / membrane internalization pathway. *Plant Science*, 172, pp.728-745.

Park, M. et al., 2004. Identification of the Protein Storage Vacuole and Protein Targeting to the Vacuole in Leaf Cells of Three Plant Species. *Plant Physiology*, 134, pp.625-639.

Park, M. et al., 2005. AtRMR1 functions as a cargo receptor for protein trafficking to the protein storage vacuole. *Journal of Cell Biology*, 170(5), p.757–767.

Passardi, F. et al., 2005. Peroxidases have more functions than a Swiss army knife. *Plant Cell Reports*, 24, pp.255-265.

Passardi, F. et al., 2004. The class III peroxidase multigenic family in rice and its evolution in land plants. *Phytochemistry*, 65, pp.1879-1893.

Pelham, H.R., 1990. The retention signal for soluble proteins of the endoplasmic reticulum. *Trends in biochemical sciences*, 15(12), pp.483-6.

Pierre Fabre SA, 2009. CHMP gives positive opinion for vinflunine in Metastatic Treatment of Bladder Cancer in failed treatment cases. *Medical News, Articles, and Blogs*.

Pimpl, P. et al., 2006. Golgi-Mediated Vacuolar Sorting of the Endoplasmic Reticulum Chaperone BiP May Play an Active Role in Quality Control within the Secretory Pathway. *The Plant cell*, 18, pp.198-211.

Potier, P. et al., 1975. Partial Synthesis of Vinblastine-Type Alkaloids. *J.C.S. Chem. Comm*, pp.670-671.

Rao, A.Q. et al., 2009. The myth of plant transformation. *Biotechnology Advances*, 27(6), pp.753-763.

Robinson, D.G., Oliviusson, P. & Hinz, G., 2005. Protein Sorting to the Storage Vacuoles of Plants: A Critical Appraisal. *Traffic*, 6, pp.615-625.

Roytrakul, S. & Verpoorte, R., 2007. Role of vacuolar transporter proteins in plant secondary metabolism: *Catharanthus roseus* cell culture. *Phytochemistry Reviews*, 6, pp.383-396.

Sanderfoot, A.A. & Raikhel, N.V., 1999. The Specificity of Vesicle Trafficking: Coat Proteins and SNAREs. *The Plant cell*, 11, pp.629-641.

Seidah, N.G. & Prat, A., 2002. Precursor convertases in the secretory pathway, cytosol and extracellular milieu. *Essays in biochemistry*, 38, pp.79-94.

Sheen, J., 2001. Update on Signal Transduction Signal Transduction in Maize and *Arabidopsis* Mesophyll Protoplasts. *Plant Physiology. Update on Signal Transduction*, 127, pp.1466-1475.

Singh, S.N. et al., 2001. Effect of an antidiabetic extract of *Catharanthus roseus* on enzymic activities in streptozotocin induced diabetic rats. *Journal of ethnopharmacology*, 76(3), pp.269-77.

Sottomayor, M. et al., 2004. Peroxidase and the biosynthesis of terpenoid indole alkaloids in the medicinal plant *Catharanthus roseus* (L.) G. Don. *Phytochemistry Reviews*, 3, pp.159-171.

Sottomayor, M., Dicosmo, F. & Ros Barceló, A., 1998. Purification and characterization of a-3’,4'-anhydrovinblastine synthase (peroxidase-like) from *Catharanthus roseus* (L.) G. Don. *FEBS Letters*, 428, pp.299-303.

Sottomayor, M. & Ros Barceló, A., 2003. Peroxidase from *Catharanthus roseus* (L.) G. Don and the biosynthesis of alpha-3’,4'-anhydrovinblastine: a specific role for a multifunctional enzyme. *Protoplasma*, 222(1-2), pp.97-105.

Sottomayor, M. & Ros Barceló, A., 2006. The Vinca alkaloids: from biosynthesis and accumulation in plant cells, to uptake, activity and metabolism in animal cells. In *Bioactive Natural Products (Part M). Studies in Natural Products Chemistry. Volume 33, Part 13*. pp. 813-857.

St-Pierre, B., Vazquez-Flota, F. & De Luca, V., 1999. Multicellular compartmentation of *Catharanthus roseus* alkaloid biosynthesis predicts intercellular translocation of a pathway intrmediate. *The Plant cell*, 11(5), pp.887-900.

Takahama, U., 2004. Oxidation of vacuolar and apoplastic phenolic substrates by peroxidase: Physiological significance of the oxidation reactions. *Phytochemistry Reviews*, 3(1/2), pp.207-219.

Tamura, K. et al., 2003. Why green fluorescent fusion proteins have not been observed in the vacuoles of higher plants. *The Plant Journal*, 35, pp.545-555.

Tognolli, M. et al., 2002. Analysis and expression of the class III peroxidase large gene family in *Arabidopsis* thaliana. *Gene*, 288, pp.129-138.

Tu, B.P. & Weissman, J.S., 2004. Oxidative protein folding in eukaryotes. Mechanisms and consequences. *The Journal of cell biology*, 164(3), pp.341-6.

Tzfira, T. & Citovsky, V., 2006. *Agrobacterium*-mediated genetic transformation of plants: biology and biotechnology. *Current Opinion in Biotechnology*, 17, pp.147-154.

Ueki, S. et al., 2009. Functional transient genetic transformation of *Arabidopsis* leaves by biolistic bombardment. *Nature protocols*, 4(1), pp.71-77.

Van Der Heijden, R. et al., 2004. The Catharanthus Alkaloids: Pharmacognosy and Biotechnology. *Current Medicine Chemistry*, 11, pp.607-628.

Verpoorte, R., Lata, B. & Sadowska, A., 2007. *Biology and Biochemistry of Catharanthus roseus (L.) G. Don*,

Vitale, A., Ceriotti, A. & Denecke, J., 1993. The Role of the Endoplasmic Reticulum in Protein Synthesis, Modification and Intracellular Transport. *Journal of Experimental Botany*, 44(9), pp.1417-1444.

Vitale, A. & Denecke, J., 1999. The Endoplasmic Reticulum - Gateway of the Secretory Pathway. *The Plant cell*, 11, pp.615-628.

Vitale, A. & Galili, G., 2001. The Endomembrane System and the Problem of Protein Sorting. *Plant Physiology*, 125, pp.115-118.

Vitale, A. & Hinz, G., 2005. Sorting of proteins to storage vacuoles: how many mechanisms? *Trends in Plant Science*, 10(7), pp.316-323.

Vitale, A. & Raikhel, N.V., 1999. What do proteins need to reach different vacuoles? *Trends in Molecular Medicine*, 4(4), pp.149-155.

Welinder, K.G., 1979. Amino acid sequence studies of horseradish peroxidase. Amino and carboxyl termini, cyanogen bromide and tryptic fragments, the complete sequence, and some structural characteristics of horseradish peroxidase C. *European journal of biochemistry / FEBS*, 96(3), pp.483-502.

Welinder, K.G., 1992. Superfamily of plant, fungal and bacterial peroxidases. *Current Opinion in Structural Biology*, 2(3), pp.388-393.

Welinder, K.G. et al., 2002. Structural diversity and transcription of class III peroxidases from *Arabidopsis* thaliana. *European journal of biochemistry / FEBS*, 269, pp.6063-6081.

Wink, M., 1993. The plant vacuole: a multifuncional compartment. *Journal of Experimental Botany*, 44, pp.231-246.

Wydro, M., Kozubek, E. & Lehmann, P., 2006. Optimization of transient *Agrobacterium*-mediated gene expression system in leaves of Nicotiana benthamiana. *Acta Biochimica Polonica*, 53(2), pp.289-298.

Yoo, S.-D., Cho, Y.-H. & Sheen, J., 2007. *Arabidopsis* mesophyll protoplasts: a versatile cell system for transient gene expression analysis. *Nature protocols*, 2(7), pp.1565-72.

Ziegler, J. & Facchini, P.J., 2008. Alkaloid Biosynthesis : Metabolism and Trafficking. *Annual Review of Plant Biology*, 59, pp.735-769.

Zimmermann, P. et al., 2004. GENEVESTIGATOR. *Arabidopsis* Microarray Database and Analysis Toolbox. *Plant Physiology*, 136, pp.2621-2632.

Zottini, M. et al., 2008. Agroinfiltration of grapevine leaves for fast transient assays of gene expression expression and fro long-term production of stable transformed cells. *Plant Cell Reports*, 27, pp.845-853.

Zouhar, J. & Rojo, E., 2009. Plant vacuoles: where did they come from and where are they heading? *Current Opinion in Plant Biology*, 12, pp.677-684.

Zárate, R. & Verpoorte, R., 2007. Strategies for the genetic modification of the medicinal plant *Catharanthus roseus* (L .) G . Don. *Phytochemistry Reviews*, 6, pp.475-491.